02-1890

ICP-1074
UC-10

INTERIM RESULTS: DEVELOPMENT OF A HEAD-END PROCESS FOR RECOVERING URANIUM AND THORIUM FROM CRUSHED FT. ST. VRAIN FUEL

ALLIED CHEMICAL CORPORATION
IDAHO CHEMICAL PROGRAMS—OPERATIONS OFFICE
IDAHO NATIONAL ENGINEERING LABORATORY
Idaho Falls, Idaho 83401

Allied Chemical

DATE PUBLISHED — OCTOBER 1975

PREPARED FOR THE
UNITED STATES
ENERGY RESEARCH AND DEVELOPMENT ADMINISTRATION
IDAHO OPERATIONS OFFICE
UNDER CONTRACT E (10-1)-1375 S-72-1

Printed in the United States of America
Available from
National Technical Information Service
U. S. Department of Commerce
5285 Port Royal Road
Springfield, Virginia 22161
Price: Printed Copy $5.45; Microfiche $2.25

DISCLAIMER

DISTRIBUTION UNDER CATEGORY:
UC-10
Chemical Separations Processes For
Plutonium and Uranium
TID-4500, R63

ICP-1074

INTERIM RESULTS: DEVELOPMENT OF A HEAD-END PROCESS FOR RECOVERING URANIUM AND THORIUM FROM CRUSHED FT. ST. VRAIN FUEL

by

G. W. Hogg
J. A. Rindfleisch
W. B. Palmer
D. L. Anderson
J. S. Vavruska

ALLIED CHEMICAL CORPORATION
IDAHO CHEMICAL PROGRAMS - OPERATIONS OFFICE
IDAHO NATIONAL ENGINEERING LABORATORY
IDAHO FALLS, IDAHO 83401

Date Published - October 1975

Prepared for the
ENERGY RESEARCH AND DEVELOPMENT ADMINISTRATION
IDAHO OPERATIONS OFFICE
Under Contract E(10-1)-1375 S-72-1

ABSTRACT

Development of processes and equipment for recovering uranium and thorium from crushed Ft. St. Vrain fuel is described. Primary burning, particle classification, particle breaking, secondary burning, and aqueous processing were studied.

SUMMARY

Pilot-plant work of a process for recovering uranium and thorium from Fort. St. Vrain fuel has been performed at the Idaho Chemical Processing Plant (ICPP). The process includes: (1) continuous primary burning of crushed Fort St. Vrain fuel, (2) gas classification of fissile and fertile particles, which comprise the primary burner product, (3) breaking of the silicon carbide coating on the respective fissile and fertile particles to expose pyrolytic carbon and thorium and uranium carbide, (4) batch secondary burning to reduce the carbon content of the ash to less than 2 wt%, (5) dissolution of the secondary burner ash in thorex solution, (6) solids-liquid separation and solids washing, (7) extraction of uranium and thorium from fission products, and (8) removal of volatile fission products to prevent plateout in the process equipment.

Interim pilot-plant results show that: (1) graphite can be burned at the plant equivalent rate of 35 kgC/hr-ft^2 in the primary burner and that fines can be consumed by recycle to the primary burner, (2) separation to greater than 95% pure fissile and 85% pure fertile particles can be effected by a gas classifier, (3) gas jets are capable of breaking silicon carbide coatings at rates compatible with plant requirements; gas utilization efficiencies are sufficiently great that off-gas generated by the jets is less than 5% of the off-gas generated by the process equipment, (4) an artificial inert bed is not required for secondary burning and the carbon content of the bed can easily be reduced to less than 2% in the secondary burner, (5) corrosion rates of thorex solution on 304 L stainless steel are sufficiently low to allow the dissolver to be constructed of 304 L stainless steel, and (6) solids-liquid separation efficiencies using a continuous solid-bowl centrifuge are sufficiently high to process the dissolver product in a pulse-column extractor.

Several other important development areas such as off-gas treatment, non-destructive uranium assay of undissolved solids, and solids transport have not been adequately studied. However, the interium development data show that current HTGR reprocessing concepts are technically sound. The report also contains basic data on the process materials and conditions germane to the safety analysis for the process.

CONTENTS

	PAGE
ABSTRACT	ii
SUMMARY	iii
I. INTRODUCTION	1
II. PROCESS DESCRIPTION AND MATERIALS FLOWSHEET	2
III. PRIMARY BURNING	12
1. HEAT TRANSFER CALCULATIONS	12
2. PRIMARY BURNER OPERABILITY	17
3. CARBON MONOXIDE COMBUSTION TORCH	36
IV. PARTICLE CLASSIFICATION AND PARTICLE BREAKING	47
1. GAS CLASSIFICATION	47
2. PARTICLE BREAKING	53
2.1 Jet Breaking	53
2.2 Roll-Crushing	56
V. SECONDARY BURNING	63
1. HEAT TRANSFER CALCULATIONS	63
2. EXPERIMENTAL PARAMETRIC STUDY	71
VI. AQUEOUS PROCESSING	88
1. DISSOLUTION	88
2. SOLIDS-LIQUID SEPARATION	89
3. FEED ADJUSTMENT	96
4. SOLVENT EXTRACTION	97
VII. OFF-GAS CLEANUP, NON-DESTRUCTIVE ASSAY, AND SOLIDS TRANSPORT	98
VIII. CONCLUSIONS	105
IX. BIBLIOGRAPHY	106

FIGURES

1. Conceptual Ft. St. Vrain Flowsheet. 3
2. Simplified Equipment Flowsheet for Processing Ft. St. Vrain Fuels. 5
3. Effect of Fluidizing Velocity on Combustion Efficiency. 27
4. Effect of Feed Rate on Combustion Efficiency. 28
5. Effect of Bed Temperature on Combustion Efficiency. 29
6. Effect of Bed Weight on Combustion Efficiency. 30
7. Schematic Diagram of Pilot Plant Primary Burner Used For Fines Injection Technique Studies. 32
8. CO Startup Torch for Four-Inch Primary Graphite Burner. 37
9. Startup Temperature Record. 39
10. Number of Torches Required to Heat 16-Inch Burner Based on Results of Pilot-Plant Run P-17. 44
11. Number of Torches Required to Heat 16-Inch Burner Based on Results of Pilot-Plant Run P-26. 45
12. Alpine Multiplex "Zigzag" Classification System. 48
13. Candidate HTGR Gas Classification Pilot-Plant System. 51
14. Gas-Jet Particle Breaker Pilot-Plant. 54
15. Experimental Double-Roll Crusher. 58
16. Required and Calculated Heat Removal Rates for Batch Secondary Burning of Crushed Fertile Particles. 67
17. Required and Calculated Heat Removal Rates for Batch Burning of Crushed Fertile Particles and Unburned Graphite. 68
18. Required and Calculated Heat Removal Rates for Batch Secondary Burning of Crushed Fissile Particles. 69
19. Required and Calculated Heat Removal Rates for Batch Burning of Crushed Fertile Particles, Unburned Graphite, and Graphite Fines. 70
20. Schematic Diagram of Pilot-Plant Secondary Burner. 72
21. Particle Size Distribution of 2-Inch Pilot-Plant Secondary Burner Feed. 80
22. Particle Size Distribution of 2-Inch Pilot-Plant Secondary Burner Product Ash. 81
23. Solid-Bowl Centrifuge Test System. 91
24. Proposed HTGR Centrifuge/Repulp Wash System. 95
25. Equilibrium Diagram: Thorium Nitrate - Nitric Acid - 30% TBP - NPH at 25° C. 103
26. Nitric Acid Distribution Between Aqueous and Organic Phases. 104

TABLES

		PAGE
I.	FISSION PRODUCT INVENTORY PER FT. ST. VRAIN ELEMENT.	8
II.	URANIUM THROUGHPUT PER 24-HOUR PERIOD FOR REPROCESSING FT. ST. VRAIN REACTOR FUEL.	10
III.	FT. ST. VRAIN HEAVY ISOTOPE INVENTORY PER ELEMENT.	11
IV.	SUMMARY OF RESULTS OF HEAT TRANSFER CALCULATIONS FOR BURNING CRUSHED FT. ST. VRAIN FUEL IN A 16-INCH DIAMETER BURNER.	14
V.	RESULTS OF EXPERIMENTALLY DETERMINED BED-TO-WALL HEAT TRANSFER COEFFICIENTS.	16
VI.	SUMMARY OF RUN CONDITIONS FOR IN-VESSEL FILTER TESTING IN THE FOUR-INCH DIAMETER PRIMARY GRAPHITE BURNER.	19
VII.	SUMMARY OF RUN RESULTS FOR IN-VESSEL FILTER TESTING IN THE FOUR-INCH DIAMETER PRIMARY GRAPHTE BURNER.	20
VIII.	SUMMARY OF RUN CONDITIONS FOR EXTERNAL FILTER TESTING IN THE FOUR-INCH DIAMETER PRIMARY GRAPHITE BURNER.	23
IX.	SUMMARY OF RUN RESULTS FOR EXTERNAL FILTER TESTING IN THE FOUR-INCH DIAMETER PRIMARY GRAPHITE BURNER.	24
X.	SUMMARY OF MASS BALANCE CALCULATIONS FOR EXTERNAL FILTER TESTING IN THE FOUR-INCH DIAMETER PRIMARY GRAPHITE BURNER.	25
XI.	SUMMARY OF OPERATING CONDITIONS FOR FINES RECYCLE TESTING IN THE FOUR-INCH DIAMETER PRIMARY GRAPHITE BURNER.	33
XII.	SUMMARY OF RUN RESULTS FOR FINES RECYCLE TESTING IN THE FOUR-INCH DIAMETER PRIMARY GRAPHTE BURNER.	34
XIII.	HEATUP TIME PERIODS FOR CO TORCH TESTING IN THE FOUR-INCH DIAMETER PRIMARY GRAPHITE BURNER.	40
XIV.	HEAT BALANCES FOR RUNS 17 AND 26.	42
XV.	SUMMARY OF RESULTS OF PARAMETRIC "ZIGZAG" CLASSIFICATION STUDIES.	50
XVI.	SUMMARY OF DESIGN FEATURES OF ACPP AND "ZIGZAG" CLASSIFIERS.	52
XVII.	SUMMARY OF PILOT-PLANT JET BREAKER OPERATING CONDITIONS.	55
XVIII.	SUMMARY OF PILOT-PLANT JET GRINDER TEST RESULTS.	57
XIX.	SUMMARY OF RESULTS OF ROLL CRUSHER TESTS.	60
XX.	SUMMARY OF EXPERIMENTS USING SECONDARY BURNER WITH IN-VESSEL FILTERS.	74

		PAGE
XXI.	SUMMARY OF OPERATING DATA RESULTING FROM TWELVE SECONDARY BURNER EXPERIMENTS.	76
XXII.	SUMMARY OF IN-VESSEL FILTER OPERATING DATA RESULTING FROM TWELVE SECONDARY BURNER EXPERIMENTS.	77
XXIII.	DISTRIBUTOR PLATE AND BED ΔP HISTORY	79
XXIV.	MASS MEAN PARTICLE SIZE OF BURNER PRODUCT.	82
XXV.	OFF-GAS ANALYSIS FOR SECONDARY PILOT-PLANT BURNER.	83
XXVI.	FLUIDIZED BED L/D RATIOS BASED ON EXPERIMENTS CONDUCTED USING A GLASS-QUARTZ BURNER.	84
XXVII.	SECONDARY BURNER OPERATING CONDITIONS AND BURN RATES REQUIRED FOR PROCESSING 12 FT. ST. VRAIN FUEL BLOCKS PER DAY.	85
XXVIII.	CORROSION RATES ON 304L STAINLESS STEEL SUBMERGED IN BOILING DISSOLVER SOLUTIONS FOR 96 HOURS.	89
XXIX.	HTGR SOLIDS-LIQUID SEPARATION TESTING USING A 6-INCH CONTINUOUS SOLID BOWL CENTRIFUGE.	93
XXX.	ACID CONCENTRATION OF FT. ST. VRAIN SYNTHETIC EXTRACTION FEED SOLUTIONS AFTER EVAPORATION AND STEAM SHIPPING.	96
XXXI.	EXTRACTION DATA FOR 5% TBP AT 25° C.	99
XXXII.	EXTRACTION DATA FOR 15% TBP IN NPH AT 25° C.	100
XXXIII.	EXTRACTION DATA FOR 30% TBP IN NPH AT 25° C.	101
XXXIV.	EXTRACTION DATA FOR 50% TBP IN NPH AT 25° C.	102

I. INTRODUCTION

A process for recovering uranium from crushed Ft. St. Vrain fuel has been under development at the Idaho Chemical Processing Plant (ICPP). The fuel elements to be reprocessed consist of hexagonal graphite fuels blocks, 31 inches long and 14 inches across the flats. The fuel elements have holes for coolant gases and for insertion of fuel rods. The fuel rods consist of fissile and fertile particles suspended in a graphite matrix; the individual fuel rods are typically 2 inches long and 1/2-inch in diameter. The fissile particles before irradiation contain uranium and thorium carbide "kernels"; the fertile particles contain thorium carbide "kernels". Both fissile and fertile particle "kernels" are coated sequentially by buffer pyrolytic carbon, isotropic pyrolytic carbon, silicon carbide and another coat of isotropic pyrolytic carbon. The particles having the three coating materials are referred to as TRISO particles. Advanced HTGR fuel concepts are based on fertile particles having two carbon coatings and no silicon carbide coating and are referred to as BISO particles. All Ft. St. Vrain fuel particles are TRISO particles.

Reprocessing development of Ft. St. Vrain fuel at ICPP involves work in the following areas:

1. Equipment and material flowsheets
2. Primary fluidized-bed burning
3. Particle classification and breaking
4. Secondary batch burning
5. Aqueous processing
6. Off-Gas cleanup
7. Non-destructive uranium assay
8. Solids transport

The development program is conducted cooperatively with the General Atomic Company (GA) of San Diego and Holifield National Laboratory (HNL) at Oak Ridge, Tennessee.

II. PROCESS DESCRIPTION AND MATERIALS FLOWSHEET

A conceptual materials flowsheet for the head-end processing of Ft. St. Vrain fuel was developed (Figure 1). The materials flowsheet corresponds to the simplified equipment flow diagram shown in Figure 2.

Process Description

The equipment flow diagram (Figure 2) depicts a process in which whole Ft. St. Vrain fuel blocks will be crushed; the crushed product will be transferred pneumatically to a fluidized-bed burner. The bed material, consisting of unburned fuel pieces and fissile and fertile particles, will be fluidized by pure oxygen. Small unburned graphite particles elutriated during combustion will be recycled pneumatically to the burner. The off-gas will be passed through a sophisticated off-gas cleanup system for removing volatile and particulate radioactivity prior to atmospheric release.

Fissile and fertile particles and some unburned graphite will be withdrawn from the burner and charged to a gas classifier. The less dense and smaller fissile particles will be carried in the off-gas leaving the classifier, collected, and stored for subsequent processing. The fertile particles will be continuously withdrawn from the bottom of the classifier and transferred to a fluidized bed containing a gas-jet. The gas-jet will break the silicon carbide coatings and expose the unbroken fuel kernels for further processing. The broken coatings and kernels will be charged batchwise to a secondary fluidized-bed burner where the graphite content of the ash will be reduced to less than 2%.

The secondary burner product ash (uranium and thorium oxides and silicon carbide hulls) will then be dissolved in a 13 $\underline{M}$ HNO_3 - 0.05 $\underline{M}$ HF solution. The solution will dissolve essentially 99.9% of the thorium and uranium. The undissolved solids will be simultaneously separated from the dissolver solution and washed of uranium and thorium in a continuous solid-bowl centrifuge. The uranium- and thorium-bearing solution will then be processed in a tri-butyl-phosphate extraction system to remove fission products and to partition uranium and thorium.

STREAM	1	2	3	4	5	6	7	8	9	10	11	12	13	14	15	16
DESCRIPTION	FUEL CHARGE	PRIMARY CRUSHER PROD	SECONDARY CRUSHER PRODUCT	TERTIARY CRUSHER PROD	PRIMARY BURNER PROD	PRIMARY BURNER OFF – GAS	FISSILE FRACTION FROM CLASSIFIER	FERTILE FRACTION FROM CLASSIFIER	FERTILE CRUSHER PRODUCT	FISSILE CRUSHER PRODUCT	FERTILE SECONDARY BURN PRODUCT	FISSILE SECONDARY BURN PRODUCT	FERTILE SECONDARY BURN OFF – GAS	FISSILE SECONDARY BURN OFF – GAS		
RATE, BLKS/d	12															
C, Kg/d	1152	1152	1152	1152	115 (A)	1037	115	0	16 2	148	0 3 (B)	3 0 (B)	23 6 (C)	187 (C)		
UC_2, Kg/d	63-69	63-69	63-69	63-69	63-69		52-46	12-23	12-23	52-46						
ThC_2, Kg/d	129-118	129-118	129-118	129-118	129-118		51-46	78-72	78-72	51-46						
SiC, Kg/d	54 4	54 4	54 4	54 4	54 4		40 4	14 0	14 0	40 4	14 0	40 4				
CO_2, SCFM						60							1 2	9 2		
O_2, SCFM						4							4 4	35		
Kr, g/d									43-262 (D)	67-173 (D)			173 69	269-105		
H^3 mg/d						39-12			031-24 (D)	067-12 (D)			13-48	26-96		
TOTAL SOLID, Kg/d	1395	1395	1395	1395	358		248	110	110	248	96 7	105				
FERTILE, Kg/d	131	131	131	131	110		0	110	0	0	0	0				
FISSILE, Kg/d	149	149	149	149	133		133	0	0	0	0	0				
SIZE, INCH	142x312	< 6	< 2	< $\frac{3}{16}$	< 028		< 016	< 028	< 010	< 010	< 010	< 010				
B, g/d	176	176	176	176	176		176	0	0	176	0	176				
FISSION PRODUCT, Kg/d	34-14	34-14	34-14	34-14	34-14		21-88	13-52	13-52	21-88	087-35	14-56	041-17 (E)	078-32 (E)		
U, Kg/d	57-63	57-63	57-63	57-63	57-63		47-42	11-21	11-21	47-42	11-21	47-42				
U-233 Kg/d	16-28	16-28	16-28	16-28	16-28		059-11	097-18	097-18	059-11	097-18	059-11				
U_3O_8, Kg/d											13-25	55-50				
ThO_2, Kg/d											806-77	527-48				
Xe, g/d													127-527	196-790		
U-235, Kg/d	33-11	33-11	33-11	33-11	33-11		33-11			33-11		33-11				

(A) 10% C ASSUMED UNBURNED
(B) 2% C ASSUMED UNBURNED
(C) INCLUDED CARBIDES
(D) 20% Kr AND H^3 ASSUMED RELEASED
(E) ALL VOLATILE FISSION PRODUCTS RELEASED INCLUDE Xe, Kr, I, H^3, Ru, Rh, Tc, Te, AND Cr

ACC-A-1618

Figure 1. Conceptual Ft. St. Vrain Flowsheet.

STREAM	15	16	17	18	19	20	21	22	23	24	25	26	27	28	29	30
DESCRIPTION	THOREX DISSOLVENT	FERTILE DISSOLVER PRODUCT	FISSILE DISSOLVER PRODUCT	WATER WASH IN CENTRIFUGE	CENTRIFUGED FERTILE DISSOLVER PRODUCT	CENTRIFUGED FERTILE SOLIDS	CENTRIFUGED FISSILE DISSOLVER PRODUCT	CENTRIFUGED FISSILE SOLIDS	FERTILE FEED EVAPORATED SOL	FISSILE FEED EVAPORATED SOL	FERTILE CONDENSATE	FISSILE CONDENSATE	FERTILE DILUTION WATER	FISSILE DILUTION WATER	FERTILE IAF	FISSILE IAF
FLOW, l/d	347	382 (A)	382 (A)	190	572		572		72	48	500	524	235	157	307	205
FLOW, l/hr	14 5	15 9	15 9	7 9	23 8		23 8		3 0	2 0	20 8	21 8	9 8	6 5	12 8	8 5
C, Kg/d		0 3	3 0		0	0 3	0	3 0								
SiC, Kg/d		14 0	40 4			14 0		40 4								
TOTAL SOLIDS Kg/d		(B) 15-16	(B) 47-46		0 006		0 006									
FISSION PROD, Kg/d		087-35	14-56		(B) 0 43 18	(B) 0 43-18	(B) 07-2 8	(B) 07-2 8	2 43-18	07-2 8					243-18	07-2 8
U, g/l		29-55	12-11		19-37		82-73		5-29	98-88					36-6 8	23-20
Th, g/l		186-177	120-113		124-119		80-75		985-945	953-894	231-219	230-215			231-223	223-209
U-233, g/l		25-47	15-29		17-31		10-19		13-25	12-23					31-59	29-54
B, g/l	10	0 91	1 37		0 61		0 91		4 8	10 8					11	2 5
H M	13	8 7	8 7		5 8		5 8		(D) -0 62	(D) -0 61	6 7	6 4			-0 15	-0 15
NO_2 M	13 3	12 1	12 1		8 1		8 1		15 4	23 1	6 7	6 4			3 6	5 4
Al M	0 10	0 09	0 09		0 06		0 06		0 47	0 72					0 11	0 17
F M	0 05	0 003	0 003		0 002		0 002		0 02	0 02					0 005	0 005
SOLIDS, g/l		39-46	115-120		0 01		0 01		0 08	0 12					0 02	0 03
Th, Kg/d		71-68	46-43		71-68		46-43	0 06 (C)	71-68	46-43					71-68	46-43
U, Kg/d		11-21	17-42		11-21		47-42		11-21	47-42					11-21	47-42
U-233, Kg/d		097-18	057-11		097-18		059-11		097-18	059-11					097-18	059-11
U-235 Kg/d			33-11				33-11			23-11						33-11

(A) 10% INCREASE IN VOLUME FROM SOLIDS
(B) 50% FISSION PRODUCT ASSUMED DISSOLVED
(C) ASSUMES 99 9% RECOVERY
(D) BY STEAM STRIPPING OR EVAPORATION

ACC-A-1619

Figure 1. Conceptual Ft. St. Vrain Flowsheet (Contd.)

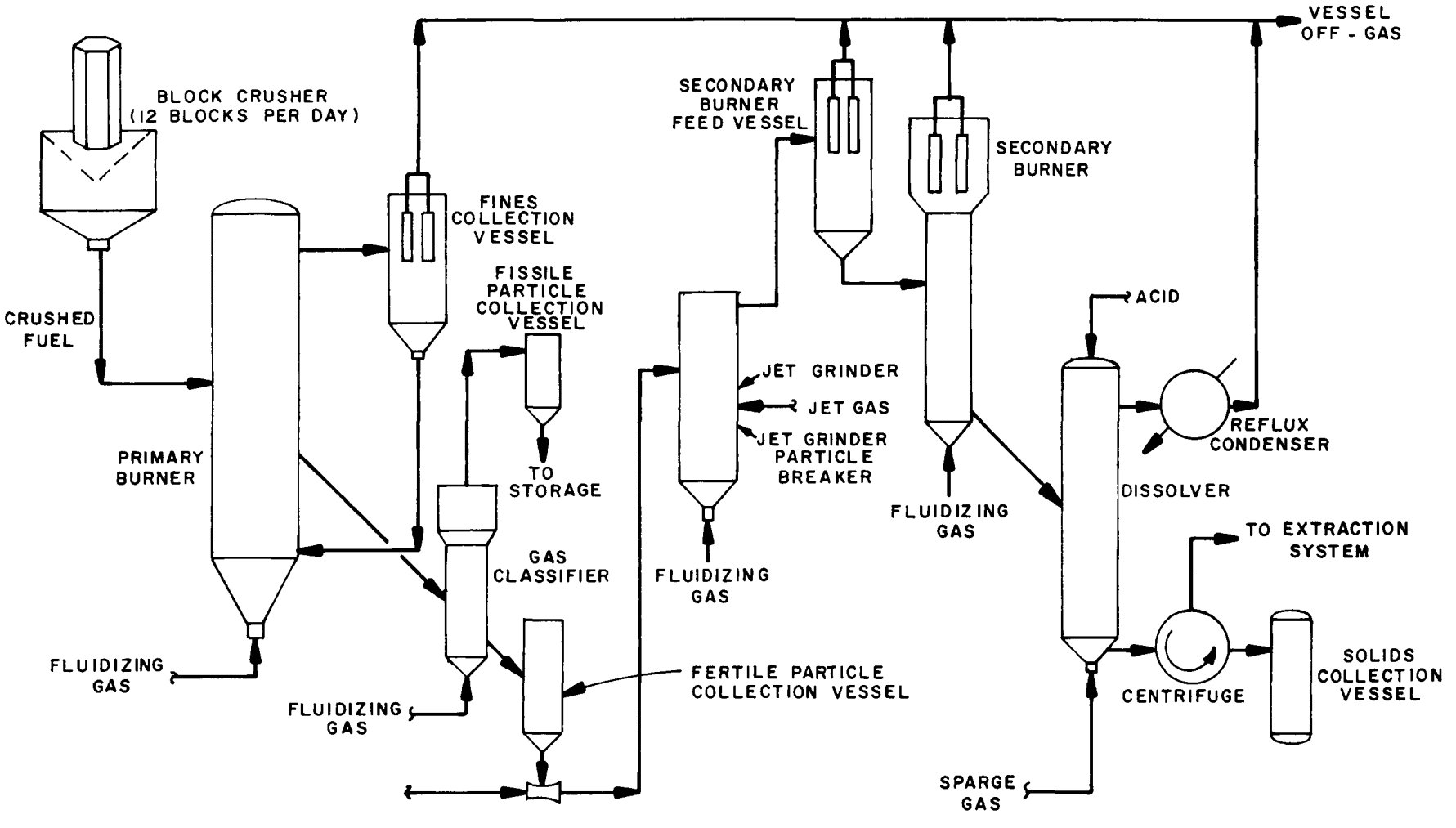

Figure 2. Simplified Equipment for Reprocessing Ft. St. Vrain Fuel

ACC-A-1505

Material Flowsheet Description

The Ft. St. Vrain flowsheet is calculated for two different irradiation periods: one year and six years, with a cooling period of six months. The first value in the flowsheet corresponds to the one-year irradiation time period and the second value to a six-year irradiation period. For example, Stream 1 in Figure 1 shows ThC_2 as 129-118 kg/d. The 129 kg/d is for the one-year irradiation period and the 118 kg/d is for the six-year period.

The material flowsheet shown in Figure 1 is based on processing twelve, 116-kg, Ft. St. Vrain fuel blocks in a 24-hour period. This results in processing 1,395 kg of solids per day and the recovery of 5.7 to 6.3 kg of uranium per day if the fissile and fertile fractions are both processed.

The fuel blocks are fed to a primary crusher that reduces the hexagonal (14 inches across the flats) 31-inch-long blocks to six-inch pieces. A secondary crusher reduces the six-inch pieces to two-inch pieces that are fed into a third crusher. The tertiary crusher completes the fuel crushing step by reducing the two-inch pieces to less than 3/16-inch.

The product from the tertiary crusher is fed to the continuous primary burner where greater than 90% (as high as 99.8%) of the graphite matrix reacts with oxygen to form CO_2 (60 scfm); the CO_2 is exhausted through the off-gas cleanup system (KALC) to the environment. Primary burning results in removal of 75% of the solids as CO_2. It is estimated that about 3.9 to 12.0 mg of tritium per day will be released in the primary burner off-gas with the CO_2. This tritium is contained in the fuel block matrix outside the protective silicon carbide coating of the fuel particles.

The primary burner product is transferred to an air classifier where the fissile and fertile particles are separated. The mass of the fissile fraction, which is 284 kg/day, consists of the fissile particles, unburned carbon, and 176 g of boron, contained in the twelve fuel blocks. The fertile fraction consists of 110 kg/day of essentially all fertile particles.

After separation of the fissile and fertile particles, the coatings of the particles being processed are broken to expose the inner carbon layer and carbide kernels. The resulting crushed product contains carbon and carbides that must be removed by burning (secondary burning) before the ash can be dissolved.

Secondary burning is accomplished by transferring the crushed particles to a batch burner where the carbon content is reduced to 2%. During secondary burning, the volatile fission products such as Xe, H^3, Kr, I, Ru, Rb, Tc, Te, and Cs are assumed to be released into the secondary burner off-gas along with CO_2. Streams 13 and 14 of Figure 1 show the expected composition of the secondary burner off-gas streams for the fertile and fissile fractions, respectively. The predicted amount of each fission product isotope for one and six-year irradiation periods is given in Table I.

The secondary burner ash product is charged to a dissolver where it is contacted with 13 M HNO_3-0.05 M HF - 0.1 M $Al(NO_3)_3$ solution for two hours at a boiling point temperature of approximately 120 °C. The solution dissolves essentially 99.9% of the thorium and uranium and approximately 50% of the fission products from the solids, resulting in 39 to 120 g/ℓ of undissolved solids. The fertile dissolver product is 2.9 and 5.5 g/ℓ uranium and 186 and 178 g/ℓ thorium while the fissile fraction is 12 and 11 g/ℓ uranium and 120 and 113 g/ℓ thorium for one and 6 year irradiation periods, respectively.

The undissolved solids are separated from the dissolver solution by centrifugation and washed to remove any residual uranium and thorium. The wash solution is combined with the dissolver solution, and the solids are dried and analyzed for uranium.

The combined wash and dissolver solution is "feed-adjusted" by evaporation to approximately 3 M thorium and steam stripping to result in a 0.6 M acid deficient solution. The acid deficient solution is then diluted with water to 1 M thorium and 0.15 M acid deficiency in preparation for uranium separation in the extraction columns.

TABLE I

FISSION PRODUCT INVENTORY PER FT. ST. VRAIN ELEMENT (6 Mo. Cooled)

Stable Nuclide	Boiling Point (°C)	Reactor Time (yr)	Fissile (g)	Fertile (g)	Total (g)	Unstable Nuclide	Half-Life
*Kr	-153	1	2.8	1.8	4.6	9 2% Kr^{85}	10.3-Y
		6	10.9	7.2	18.1	7.6% Kr^{85}	
*Rb	700	1	3.4	2.0	5.4	---	
		6	13.9	8.1	22	---	
Sr	1150	1	7.1	3.6	10.7	57% Sr^{90}	28-Y
		6	28.5	14.3	42.8	57% Sr^{90}	
Y	2500	1	3.8	1.9	5.7	3.3% Y^{91}	58-D
		6	15.1	7.5	22.6	0.6% Y^{91}	
Zr	2900	1	27.2	13.6	40.8	0.6% Zr^{95}	65-D
		6	111	55.6	167	0.1% Zr^{95}	
Mo		1	17.2	8.6	25.8	---	
		6	70.6	35.3	105.9	---	
*Tc	200	1	4.7	1.6	6.3	---	
		6	19.4	6.4	25.8	---	
Rh	2500	1	1.9	1.0	2.9	---	
		6	7.8	4.1	11.9	---	
*Ru	108	1	6.4	3.9	10.3	1.5% Ru^{106}	1.01-Y
		6	26.2	15.9	42.1	0.7% Ru^{106}	
Pd	2200	1	1.2	0.5	1.7	---	
		6	5	2	7	---	
*I	185	1	1.5	1.1	2.6	79% I^{129}	1.6 X 10^7-Y
		6	6.1	4.6	10.7	79% I^{129}	
*Te	450	1	2.3	2.1	4.5	---	
		6	7.4	11.2	18.6	---	
*Xe	-107.1	1	16	10.6	26.2	---	
		6	65.8	43.9	109.7		
*Cs	670	1	27.7	11.6	39.3	25% Cs^{137}	30-Y
		6	112.9	47	159.9	24% Cs^{137}	
Ba	2000	1	6.5	3.2	9.77	---	
		6	26.9	13.4	40.3	---	
La	4200	1	5.7	4.8	10.5	---	
		6	23.3	20.0	43.3	---	
Ce	1692	1	13.3	11.5	24.8	15% Ce^{144}	280-D
		6	55.1	47.3	102.4	17% Ce^{144}	
Pr	> 950	1	5.5	5.5	11	---	
		6	22.7	22.7	45.4		
Nd	-	1	18.6	14.8	33.4	---	
		6	76.6	61.6	137.8	---	
Pm	-	1	2	1	3	100% Pm^{147}	2.6-Y
		6	4.9	2.4	7.3	100% Pm^{147}	
Sm	-	1	5.1	2.0	7.1	10% Sm^{151}	93-Y
		6	20.9	8.3	29.2	9% Sm^{151}	
Eu	-	1	0.2	0.1	0.3	---	
		6	0.8	0.3	1.1	---	
Total		1	180 (63%)	107 (37%)	287	---	
		6	732 (63%)	439 (37%)	1171	---	

*Volatile in burner

III. PRIMARY BURNING

Primary burner development was based on processing 12 Ft. St. Vrain fuel blocks per day in a 16-inch diameter burner. The corresponding required steady-state burn rate is 35 kgC/hr-ft^2. The burner operating cycle is semi-continuous: continuous feed and batchwise drawoff. The duration of the anticipated operating cycle is variable and ranges from approximately one to thirty days.

Uranium

The uranium content of the fuel is a function of the time the fuel is in the reactor. For respective one and six-year irradiation periods, the uranium thoughput for fertile particles in Ft. St. Vrain fuel is 1.1 and 2.1 kg/d of which 98% and 90% is U-233, respectively. For processing of the fissile particles, Ft. St. Vrain fuel generates 4.7 and 4.2 kg of uranium per day of which 13% and 26% is U-233, respectively. The U-235 is found only in the fissile fraction and is 3.3 and 1.1 kg/day, which is 70% and 26%, respectively, of the total uranium. The different isotopes of uranium anticipated to be processed for a given irradiation period are shown in Table II.

Fission Products

The quantity of fission products contained within the fuel blocks is also dependent on the time the fuel was in the reactor. The anticipated fission products generated per element from the Ft. St. Vrain reactor core for both one and six-year irradiation periods with a six-month cooling time are shown in Table I. The boiling point of each nuclide in the oxide form is shown to give an idea of which nuclides will be in the off-gas. Any nuclide with a boiling point below 800°C will be expected to volatilize and be included in the off-gas from the secondary burner. These volatile elements include Kr, He, I, ^{3}H , Ru, Rb, Te, Tc, and Cs. Table I also shows the percentage of unstable nuclides present for each element and their half-life. The fissile fraction contains 63% of the fission products while the fertile portion contains only 37%. One-year-irradiated-6-month-cooled fuel contains 287 g of fission products per element while 6 year irradiated-6 month cooled fuel contains 1,171 g per element. A breakdown of the heavy isotope content per element for the different fractions of fuel particles for a six-year irradiation period is shown in Table III.

TABLE II

URANIUM THROUGHPUT PER 24-HOUR PERIOD
FOR REPROCESSING FT. ST. VRAIN REACTOR FUEL
(12 Fuel Blocks)

Reactor Time (year)	Particle Fraction	U-232 (g)	U-233 (kg)	U-234 (kg)	U-235 (kg)	U-236 (kg)	U-238 (kg)	Total U (kg)
1	Fissile	0.044	0.59	0.07	3.3	0.36	0.33	4.65
	Fertile	0.073	0.97	0.11	---	---	---	1.08
	Total	0.117	1.55	0.18	3.3	0.36	0.33	5.72
2	Fissile	0.13	0.94	0.10	2.2	0.58	0.32	4.14
	Fertile	0.21	1.56	0.17	---	---	---	1.73
	Total	0.34	2.50	0.27	2.2	0.58	0.32	5.87
3	Fissile	0.25	3.00	0.15	2.1	0.71	0.31	4.34
	Fertile	0.41	1.13	0.24	---	---	---	2.11
	Total	0.66	1.87	0.39	2.1	0.71	0.31	6.45
4	Fissile	0.42	1.32	0.23	1.9	0.93	0.34	4.72
	Fertile	0.69	2.18	0.37	---	---	---	2.55
	Total	1.11	3.50	0.60	1.9	0.93	0.34	7.27
5	Fissile	0.45	1.43	0.28	1.2	0.98	0.37	4.29
	Fertile	0.75	2.37	0.46	---	---	---	2.84
	Total	1.20	3.80	0.74	1.2	0.98	0.37	7.13
6	Fissile	0.40	1.05	0.22	1.1	1.37	0.43	4.18
	Fertile	0.67	1.75	0.37	---	---	---	2.11
	Total	1.07	2.80	0.59	1.1	1.37	0.43	6.29

TABLE III

FT. ST. VRAIN HEAVY ISOTOPE INVENTORY PER ELEMENT

(6 Year Irradiated-6 Mo. Cooled)

Nuclide	Half-Life[b]	Fissile (g)	Fertile (g)	Total (g)
Th-232	1.4 (10)Y	3(3)	4.5 (3)	7.5 (3)
Pa-233	27.4d	0.1	0.05	0.14
U-232	72Y	0.04	0.06	0.1
U-233	1.6 (5)Y	94	117	211
U-234	2.5 (5)Y	16.1	32.3	48.4
U-235	7.1 (8)Y	100	---	100
U-236	2.4 (7)Y	109	---	109
U-238	4.5 (9)Y	30.3	---	30.3
Np-237	2.1 (6)Y	14.1	---	14.1
Pu-238	89Y	5.9	---	5.9
Pu-239	2.4 (4)Y	1.5	---	1.5
Pu-240	6.8 (3)Y	0.41	---	0.41
Pu-241	13Y	0.44	---	0.44
Pu-242	3.8 (5)Y	0.51	---	0.51
Am-243	7.7 (3)Y	0.21	---	0.21
Cm-244	18.1Y	0.07	---	0.07
Total[a]		372.68	149.4	552.1

(a) Excluding Th^{232}

(b) 1.4 (10)Y = 1.4×10^{10}Y.

Heat transfer calculations were made to determine heat transfer rates through the wall of a shrouded 16-inch diameter primary burner. Burner operability was determined experimentally using in-vessel filters, external filters, or fines recycle to the primary burner. A CO torch was developed for supplying startup and supplemental heat to the primary burner. Bed-to-wall heat transfer coefficients were measured experimentally.

1. Heat Transfer Calculations

Heat transfer calculations were made to determine the vessel configuration necessary to insure the removal of heat equivalent to processing 12 Ft. St. Vrain fuel blocks per day. Calculations were made based on finned and unfinned burner walls surrounded by a cooling air shroud.

Bases of Heat Transfer Calculations

Bases for the heat transfer calculations were:

1) Inside diameter of burner is 16 inches.
2) Fluid-bed heights of 6 ft and 9 ft.
3) Longitudinal and rectangular fins (1-inch high and 1/4-inch wide).
4) Fluid-bed side heat transfer coefficient of 100 Btu/hr-ft^{2}-^{o}F.
5) Bed temperature of 1606^{o}F (875^{o}C).
6) Inlet cooling air temperature of 70^{o}F.
   Outlet cooling air temperature of 300^{o}F.
7) Thermal conductivity of vessel wall of 12 Btu/hr-ft-^{o}F (Hastelloy X).
8) Vessel wall thickness of 0.5 inch.
9) Heat capacities for graphite, off-gases, and product were 0.309, 0.300, and 0.276 Btu/lb-^{o}F, respectively.
10) The volumetric flow rate of the fluidizing gas is 2.5 ft^{3}/min (corresponding to 3 ft/sec superficial velocity).
11) The heat of combustion for graphite was 13,600 Btu/lb.
12) Heat transfer coefficient from bare outside wall to shroud air was 22 Btu/hr-ft^{2}-^{o}F.

Major Assumptions

Major assumptions were:

1) Perfectly mixed fluid bed at a constant temperature.
2) Inside heat transfer coefficients are constant.
3) Outside heat transfer coefficients are constant.
4) Constant metal wall thermal conductivity.
5) Constant temperature, T_{wo}, at base of outside fins.
6) Radiation is neglected.

Calculated Heat Transfer Results

A summary of the results of the heat transfer calculations for specified bed heights and fin conditions is shown in Table IV. The heat that must be removed through the vessel wall (column 1) is based on a 12 block per day processing rate. The calculated heat removal rate for the indicated conditions is shown in column 2. Comparison of the two columns shows that more than the required heat can be removed in all cases except the one in which a 9-ft fluid-bed height is used without fins with fines burning. Extension of these calculated heat removal rates to a 16-inch diameter burner having a fluid-bed height of 9 feet and external fins showed that 20 blocks per day (82 kilograms of carbon per hour) can be processed. Fourteen blocks (57 kilograms of carbon per hour) can be processed in a burner having a 6-ft deep fluidized bed and external fins. The table also shows that when fines are not burned, a fluid-bed height of 6-ft without fins cannot transfer the heat. The calculations showed that internal fins were unnecessary.

The best external fin configuration was fins 1-inch high and 1/4-inch thick with a spacing of 1/4-inch. The fin efficiency was 0.676. The amount of heat removed in the off-gas products, unburned fines, and fissile and fertile particles was 232,000 Btu/hr.

TABLE IV

SUMMARY OF RESULTS OF HEAT TRANSFER CALCULATIONS FOR BURNING CRUSHED FT. ST. VRAIN FUEL IN A 16" DIAMETER PRIMARY BURNER

(1) Heat that must be removed through vessel wall (based on processing 12 blocks per day), Btu/hr	(2) Calculated heat removal rates, Btu/hr	(3) Fluidized bed height, ft.	(4) Fin Specifications
1.24×10^6 (a)	0.955×10^6	9	No fins
1.24×10^6 (a)	2.1×10^6	9	External fins
1.24×10^6 (a)	1.4×10^6	6	External fins
0.794×10^6 (b)	0.635×10^6	6	No fins

(a) Includes fines burning

(b) Does not include fines burning

Primary burner wall temperatures were measured during four pilot-plant burner runs. Three 0.02-inch diameter chromel-alumel thermocouples were installed flush with the outside wall of the 4-inch pilot-plant primary burner. The thermocouples were placed about 0.03 inches inside the wall of the burner and brazing material was applied to hold the thermocouples in place. The brazing material was ground until the original circumference of the burner was obtained. Two of the thermocouples (90^{o} apart) were located 6.75-inches above the distributor plate. The other thermocouple was located 12.75 inches above the distributor plate.

The results of the experimentally based calculations are summarized in Table V. All three runs with a fluidized-bed height of 20 inches resulted in a bed-to-wall heat transfer coefficient value near 100 Btu/hr-ft^2 -^{o}F as expected from previously extrapolated experimental results. Run P-38 yielded the lowest bed-to-wall heat transfer coefficient with a fluidized-bed height of 32 inches. The thermocouple used to measure the shroud cooling air outlet did not provide accurate temperatures. Thus, no outside or overall heat transfer coefficients were calculated for the four runs.

The bed-to-wall heat transfer coefficients were calculated by the following procedure:

1) Heat transfer rates through the burner wall were obtained from an energy balance. The heat transfer rate through the wall was calculated from the total heat generated in the burner (total graphite consumption known) and the heat removed by fines generation, fines recycling, and off-gas.
2) Using the measured outside wall temperatures and calculated heat transfer rate through the wall, the inside wall temperatures were obtained from the heat conductance equation.
3) The bed-to-wall heat transfer coefficients were calculated from the convection equation since the bed-to-wall temperature difference was known. The bed-to-wall heat transfer coefficient is considered a combined radiation and convection heat transfer coefficient.

Two major assumptions were used in the calculations, constant bed temperature and average fines recycle rate.

TABLE V

RESULTS OF EXPERIMENTALLY DETERMINED BED-TO-WALL HEAT TRANSFER COEFFICIENTS

Run Number	Fluidizing Gas Velocity, ft/sec	Bed Temperature, °C	Outside Vessel Wall Temperature, °C	Bed-To-Wall Heat Transfer Coefficient, Btu/hr-ft^2-°F	Fluidized-Bed Height Inches
P-34	1	875	806	91.2	20
P-36	2.5	900	695	114	20
P-38	1	900	837	61.8	32
P-41	1.85	900	799	90.3	20

The shroud-cooling-air-thermocouple problem was subsequently corrected and the overall heat transfer coefficient, U_o, was calculated to be 26.5 Btu/hr-ft^2-^{o}F. The amount of heat removed through the walls of the 16-inch diameter burner using this value of U_o was 1 x 10^6 Btu/hr (6-ft fluid-bed height, external fins only, $(\Delta T)_{lm}$ of 1418^{o}F), and 1.5 x 10^6 Btu/hr (9-ft fluid-bed, external fins $(\Delta T)_{lm}$ of 1418^{o}F). The inside film coefficient obtained using data from the 4-inch diameter primary burner was 138 Btu/hr-ft^2-^{o}F.

Results of the calculations show that:

1. Heat generated by processing 20 Ft. St. Vrain fuel blocks per day in a 16-inch diameter burner can be removed from a 9-ft tall fluid-bed if only external fins are used.
2. Heat generated by processing 14 Ft. St. Vrain fuel blocks per day in a 16-inch diameter burner can be removed from a 6-ft tall fluid-bed if external fins are used.
3. An overall heat transfer coefficient obtained from experimental data indicates heat generated in processing 12 blocks of Ft. St. Vrain fuel per day can be removed from a 6-ft tall fluid-bed burner (externally finned) if fines are not burned. However, if the fluid bed is 9-ft deep and external fins are provided, fines can also be burned.
4. Radiation and heat transfer from the unfluidized section of the burner will also increase the heat tranfer rates.
5. At the anticipated fluidizing gas rates, the bed-to-wall heat transfer coefficient is near 100 Btu/hr-ft^2 -^{o}F.

2. Primary Burner Operability

Ideally, the primary burner should burn all the matrix graphite from the fissile and fertile particles. However whole block crushing generates significant quantities of graphite fines; fines are also generated during burning of the larger graphite pieces. Graphite fines are very light and elutriate rapidly from the fluidized bed.

Two different methods were considered for assuring complete burning of the graphite fines: (1) filters in the primary burner and (2) filters located

in a collection vessel outside the primary burner, with pneumatic fines recycle to the primary burner.

2.1 In-Vessel Filter Testing

Nine runs were made to test the operability of a four-inch diameter primary burner using in-vessel filters. The run conditions are summarized in Table VI and the results in Table VII. The run plan was to test the effect of feed rate, fluidizing velocity, and bed temperature on burning rate and filter performance. Completion of all runs was not possible because of high filter pressure drop, inability to remove heat at the required rate from the burner, and filter burn-through.

The graphite feed rate was controlled at a minimum of 125% of the stoichiometric feed rate to insure a surplus of graphite in the bed. Three fluidizing oxygen velocities (1.0, 1.50, and 2.0 ft/sec) and two bed temperatures, (850°C and 875°C) were tested.

The burner, excluding the in-vessel filters, operated reliably during all nine runs. The CO/O_2 startup torch heated the bed rapidly using either CO or propane as fuel. Except for exhaustion of the CO supply in Run 6, the only operating problems were caused by the in-vessel filter.

All oxygen fluidizing velocities used resulted in good fluidization quality, as evidenced by the bed temperatures always being within a few degrees of one another. At oxygen fluidizing velocities of 1.5 and 2.0 ft/sec, the cooling shroud was not capable of transferring heat at the required rate to maintain the specified bed temperature; as much as 30% air in addition to the oxygen was required to cool the bed. This increased the gas flow rate sufficiently to overload the filter and cause high burner pressure.

The average bed temperature during the runs was 875°C. The first run was attempted at 850°C; any minor disturbance that allowed the temperature to drop sharply caused burning to cease; therefore, Run 1 was terminated. Run 2 was started at an 850°C bed temperature, but unstable burning required increasing the bed temperature to 875°C. Remaining runs were made at a bed temperature of approximately 875°C.

Table VI Summary of Run Conditions for In-Vessel Filter Testing in the Four-Inch Diameter Primary Graphite Burner

Run No.	Startup Bed Weight, Grams	Bed Temperature °C	Oxygen Fluidizing Velocity, ft/sec	Air Fluidizing Velocity [a], ft/sec	Filter Size			Feed Rate Gram/min
					Diam, in.	L, in.	Porosity, μ	
1	3374	850	1.5	0	2	12	35	55
2	3346	850 → 875 [b]	1.5	1	2	12	35	50
3	3220	875	2.0 → 1.5 [c]	2 → 1	2	12	35	61
4	3279	875	2.0	1	2.75	18	5	61
5	3621	875	1.5	1	2.75	18	5	46
6	4122	(d)	1.5	0	2	18	20	46
7	4346	875	1.5	(e)	2	18	20	46
8	4446	875	1.0	(e)	2	18	20	31
9	3072	875	1.0	0	2	12	20	31

(a) Air added to the fluidizing oxygen to cool the bed.

(b) Burning was unstable at 850°C; bed temperature was increased to 875°C.

(c) Fluidizing velocity was reduced because burner pressure was too high.

(d) Bed did not reach operating temperature.

(e) Runs were terminated before this data was recorded.

Table VII Summary of Run Results for In-Vessel Filter Testing in the Four-Inch Diameter Primary Graphite Burner

Run No.	Final Bed Weight, Grams	Combustibles in Final Bed, wt%	Filter ΔP, PSI	Feed Charged to Burner, grams	Duration of Run Min.(c)	Final Weight of Fines on Filter, grams	Comments
1	3607	(a)	3	1110	43	182	Terminated early; unstable burning and high filter ΔP.
2	3300	0.4	4	2574	139	(b)	Completed run; filter ΔP too high.
3	3820	1.2	6	4673	113	132	Completed run at reduced velocity; filter ΔP too high
4	4508	(a)	6	2759	55	1102	Terminated early; high ΔP from fines around filter.
5	3482	5.3	2	4580	120	1090	Completed run; excessive fines around filter.
6	4642	(a)	3	600	13	(b)	Terminated; torch CO supply exhausted.
7	4692	(a)	3	1100	21	0	Terminated; filter burnthrou
8	3758	(a)	2	540	15	0	Terminated; filter burnthrou
9	3840	2.8	2	5725	190	309	Terminated; filter began burning.

(a) This data not recorded; in each case the wt% carbon in the bed was greater than 5% since run was terminated before carbon could be completely burned.

(b) This data not recorded.

(c) Run time is begun when the bed temperature reaches ~ 600°C and feed is started and is ended when the bed temperature drops below 800°C during shutdown.

The amount of graphite left in the bed after a completed run was quite low; the highest value was less than six weight percent. Graphite fines accumulation around the in-vessel filter was significant. During Runs 4 and 5, the entire annular area between the filter and the burner was packed with fines. This may also have been the case during Runs 7, 8, and 9, before the fines ignited and burned the filters.

The blowback system effectively cleaned the filters. After blowback, the filter pressure drop decreased to its "clean" value, but within a few seconds, the pressure drop would increase to its previous value and remain fairly constant until the next blowback pulse. Apparently, the "caked" fines were dislodged from the filter and after dropping into the bed were dispersed and rapidly collected on the filter again.

There was no indication that significant amounts of fines were mixed with the bed or burned during a normal blowback cycle. The most serious problem encountered during the in-vessel filter test was filter burning caused by fines burning around the filters during Runs 7, 8, and 9.

The exact mechanism for fines ignition is unknown. The filters are always a potential area for burning, since an accumulation of finely divided graphite is present, oxygen (usually 2 to 6% in the off-gas) is present, and 300 to 500°C temperatures exist. A spark or an increase in temperature to about 650°C will ignite the fines. However, it is postulated that during blowback, accumulated fines drop from the filter into the top part of the fluidized bed. The lower-bed temperatures and combustion decrease, which results in a surge of oxygen upward through the bed. Simultaneously, the fines are dispersed and heated rapidly. As the surge of oxygen reached the vapor space, the fines ignite and immediately travel to the filter along with the oxygen-rich off-gas. The fines around the filter also ignite, and burning on the surface of the filter takes place.

Based on the results of nine experimental runs, in-vessel filters in the primary burner are not recommended. The test results show that the fines do not mix back into the bed to any significant degree after blowback, even though fines are dislodged from the filter. An expanded top section would allow more effective blowback and lower gas velocities around the filter, but the gas velocity at the top of the bed would not be reduced.

In-vessel filters in the primary burner are subject to burning. Graphite fines, oxygen, and high temperatures in the vicinity of the filter are always possible in the primary burner. The hazard of ignition of graphite fines on the filters could be minimized by increasing the disengaging height, installing a filter cooler, lowering gas velocities, etc., but the reliability of the system would remain questionable.

2.2 External Filter Testing

Fifteen runs were made to test primary burner operability using external filters. The run plan was to test the effect of fluidizing velocity, feed rate, bed temperature, and bed depth on combustion efficiency, fines generation, heat transfer, and general burner operability. Fourteen of the runs were successfully completed; one run at low bed temperature ($\sim 800^{\circ}C$) resulted in the bed being extinguished prematurely. The details of the experimental testing are shown in Reference 1.

The run conditions are summarized in Table VIII and the results of the runs are summarized in Tables IX and X. Run time, weight of fines collected, average off-gas concentrations, and calculated combustion efficiencies are given in Table IX. A mass balance for each run is shown in Table X. The materials charged to the burner were feed, air, and oxygen at controlled rates. The materials exiting the burner were fines and the off-gas, which was analyzed continuously for CO_2, CO, and O_2. The mass balance was made by determining the weight of graphite actually consumed, the weight of graphite which would have produced the amount of CO and CO_2 detected in the off-gas, and the weight of graphite which would have been burned by the amount of oxygen actually consumed during the run. Each of the two theoretical weights were then divided by the actual amount of graphite consumed and multiplied by 100 to obtain the results shown in columns 2 and 3 of Table X.

TABLE VIII

SUMMARY OF RUN CONDITIONS FOR EXTERNAL FILTER TESTING IN THE FOUR-INCH DIAMETER PRIMARY GRAPHITE BURNER

Run No.	Maximum Combustion Rate,[A] kg graphite/ hr-ft^2	Bed Temperature, °C	Fluidizing Velocity,[B] ft/sec	Actual Feed Rate, Grams/min	Stoichiometric Graphite Feed Rate[C] %	Beginning Bed Weight, Grams	Fluidizing Oxygen Rate, scfm
11	15	875	1.5	36	125	2500	1.5
12	20	875	1.8	45	125	2500	2.0
13	25	875	2.3	56	125	2500	2.5
14	30	875	3.1	67	125	2500	3.0
15	35	875	3.6	78	125	2500	3.5
16	25	850	2.2	56	125	2500	2.5
17	25	825	2.2	56	125	2500	2.5
18	25	~ 800	2.2	56	125	2500	2.5
19	25	800	2.1	56	125	2500	2.5
20	25	900	2.3	56	125	2500	2.5
21	25	875	2.2	45	100	2500	2.5
22	25	875	2.2	67	150	2500	2.5
23	25	875	2.2	89	200	2500	2.5
24	25	875	2.2	56	125	3500	2.5
25	25	875	2.2	56	125	4500	2.5

A - Maximum possible combustion rate based on fluidizing oxygen fed to burner.

B - Includes fluidizing oxygen fluidizing air for cooling, and torch purge air.

C - % of stoichiometric rate assuming complete reaction of the fluidizing O_2 with the feed graphite to form CO_2.

TABLE IX

SUMMARY OF RUN RESULTS FOR EXTERNAL FILTER TESTING IN THE FOUR-INCH DIAMETER PRIMARY GRAPHITE BURNER

Run No.	Run Time, Min	Startup-Fines Weight, (B) Grams	Total Fines Weight, Grams	Average Off-Gas Concentration, % CO_2 - % CO - % O_2	Combustion Efficiency, (C) %
11	268	423	2639	45 - 0.8 - 25	64.7
12	198	289	2331	61 - 1.3 - 21	74.8
13	161	191	2344	53 - 2.4 - 17	76.3
14	130	359	2501	44 - 1.4 - 24	65.9
15	108	440	2824	41 - 1.3 - 25	63.3
16	160	300	1619	50 - 2.1 - 25	67.6
17	164	92	1489	48 - 2.1 - 28	64.3
18 (A)	85	175	336	---	---
19	145	285	2047	46 - 2.0 - 35	58.2
20	161	218	2801	51 - 1.7 - 21	72.0
21	194	191	4101	48 - 1.3 - 33	59.9
22	138	196	2020	55 - 3.5 - 16	78.4
23	101	204	2487	55 - 4.7 - 6	91.5
24	157	504	3387	51 - 2.3 - 25	68.1
25	157	81	1805	50 - 2.0 - 24	68.2

A - Run not completed.

B - Fines collected during startup phase of run.

C - Defined as (% CO_2 + % CO) x 100/(% CO_2 + % CO + % O_2).

D - Sudden change in upper bed temperature during final burnout of the bed at the end of the run.

E - Reaction was quenched with N_2 when temperature reached 1060°C.

TABLE X

SUMMARY OF MASS BALANCE CALCULATIONS FOR EXTERNAL FILTER TESTING IN THE FOUR-INCH DIAMETER PRIMARY GRAPHITE BURNER

Run No.	Actual Weight of Graphite Consumed,[A] Grams	Percent Actual Based on CO and CO_2 Production %	Percent Actual Based on Oxygen Consumption, %
11	4051	94	110
12	4359	108	108
13	4346	99	117
14	4189	88	106
15	3866	85	109
16	5071	78	88
17	5204	75	84
18[B]	----	--	---
19	4643	70	73
20	3889	104	124
21	2589	173	180
22	4670	81	94
23	4203	65	88
24	3303	118	132
25	4885	77	91

A - Defined as weight of graphite in feed - weight of graphite in fines.

B - Run 18 not completed.

The fluidizing velocity was varied from 1.45 to 3.58 ft/sec; the graphite feed rate was 100% to 200% of stoichiometric (based on the oxygen flowrate); the bed temperature range was from 800°C to 900°C; the starting bed weights of fissile and fertile particles were 2500, 3500, and 4500 grams.

The results of the combustion efficiency studies are shown in Figures 3 through 6 which gives the average off-gas composition and combustion efficiency as a function of the controlled operating variables. For the purposes of this report, the combustion efficiency is defined as the $(CO + CO_2) \times 100/(CO + CO_2 + O_2)$ ratio. This number is a measure of how efficiently the oxygen is being used by the system. The percent CO_2 in the off-gas would be a good measure of the relative combustion efficiency, except that more nitrogen (torch air, purge air, and fluidizing air) was added in some runs than in others.

Burner operability and temperature control were satisfactory at all run conditions except at bed temperatures below 850°C. At the lower bed temperatures, any transient condition causing the bed temperature to drop would very often extinguish the burning. Run 18 was made specifically to determine the lowest possible bed temperature at which graphite burning was self sustaining in the 4-inch burner. The reaction continued at 770°C, but after the bed temperature was allowed to decrease to 760°C, the temperature continued to drop until all combustion ceased. Burner temperature control was excellent at 900°C.

The following conclusions were reached based on experimental testing in the range of variables studied:

1. Sintered metal filters contained in an external filter pot are satisfactory for separating graphite fines from the primary burner off-gas.
2. The fluidizing velocity in the primary burner should be kept as low as practicable consistent with desired burner throughput rates to increase fines retention in the bed.
3. The feed rate should be controlled so that there is just enough graphite surface area in the bed to burn the oxygen from the fluidizing gas. Too much graphite in the bed will cause increased fines elutriation and poor fluidization.
4. The bed temperature should be maintained above 850°C and preferably near 900°C to increase combustion efficiency and allow smooth burner operation.

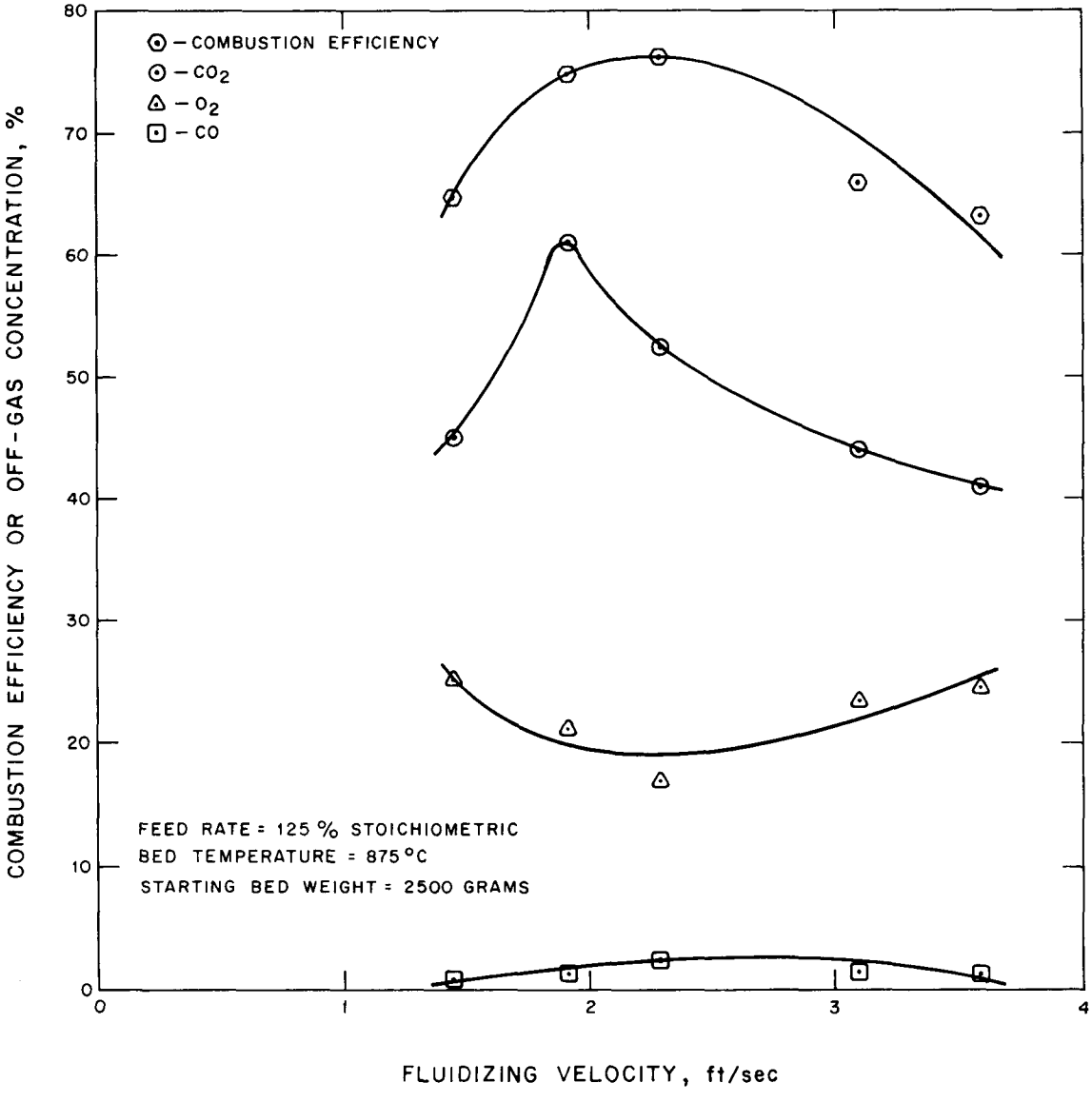

Figure 3. Effect of Fluidizing Velocity on Combustion Efficiency

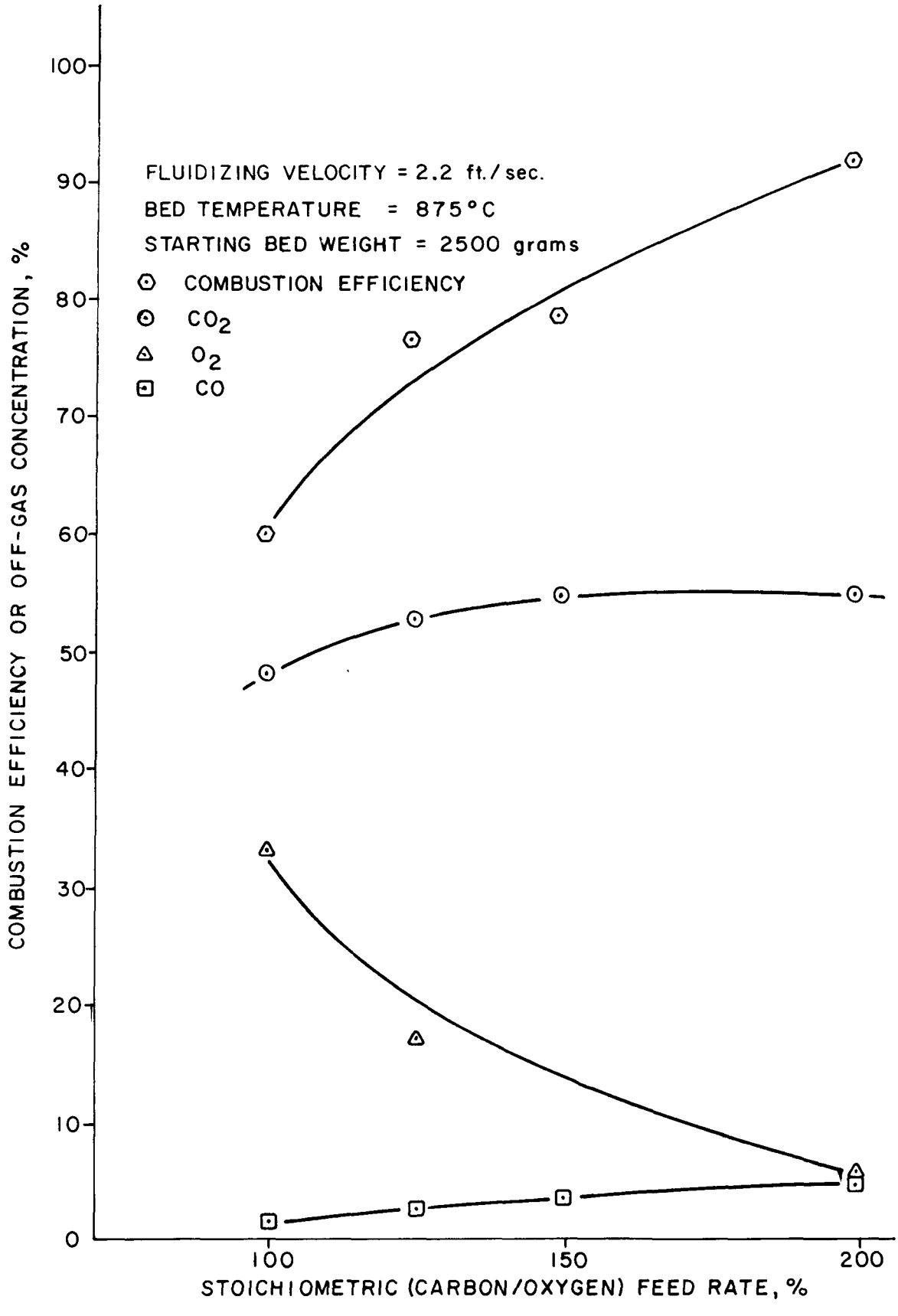

Figure 4. Effect of Feed Rate on Combustion Efficiency

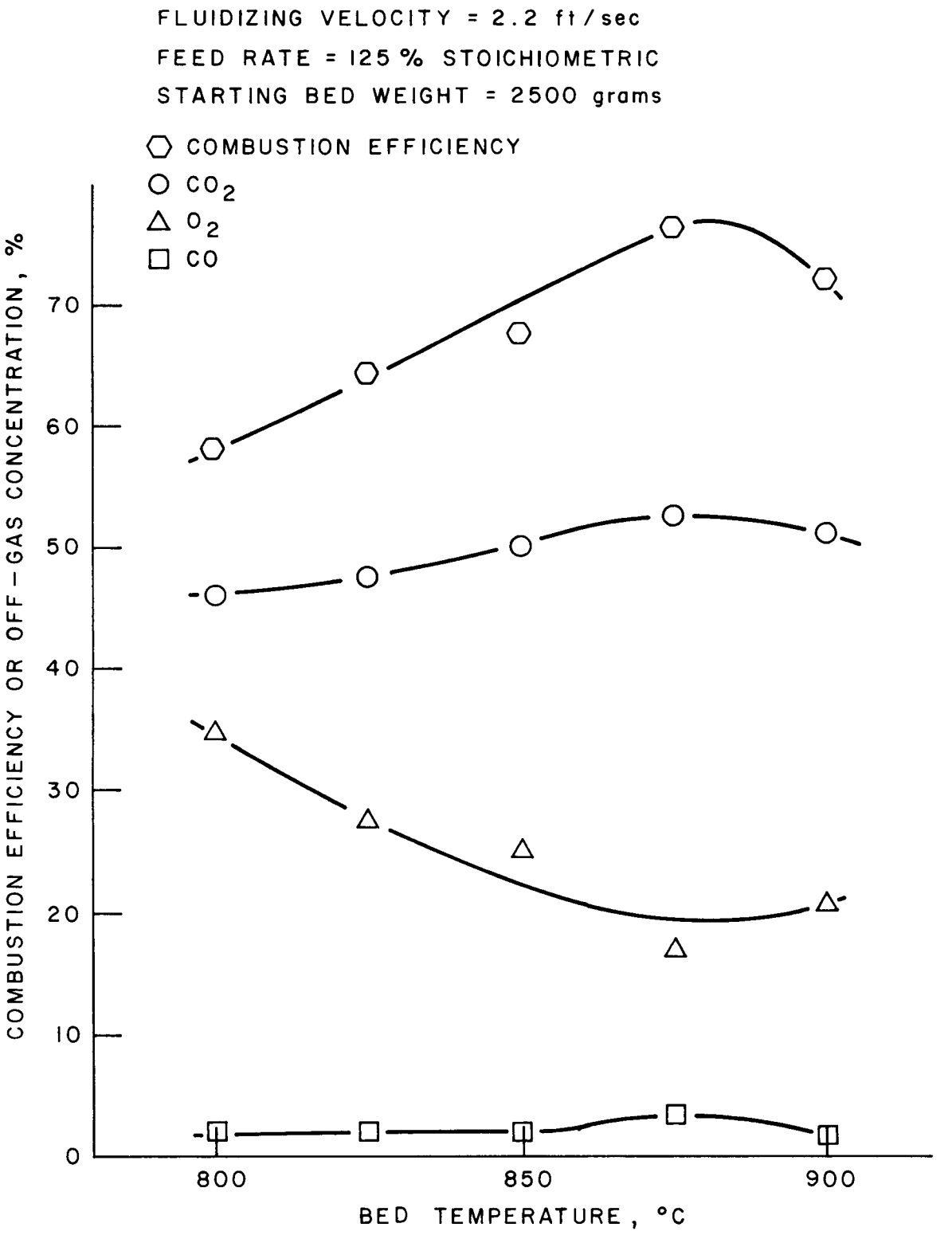

Figure 5. Effect of Bed Temperature on Combustion Efficiency

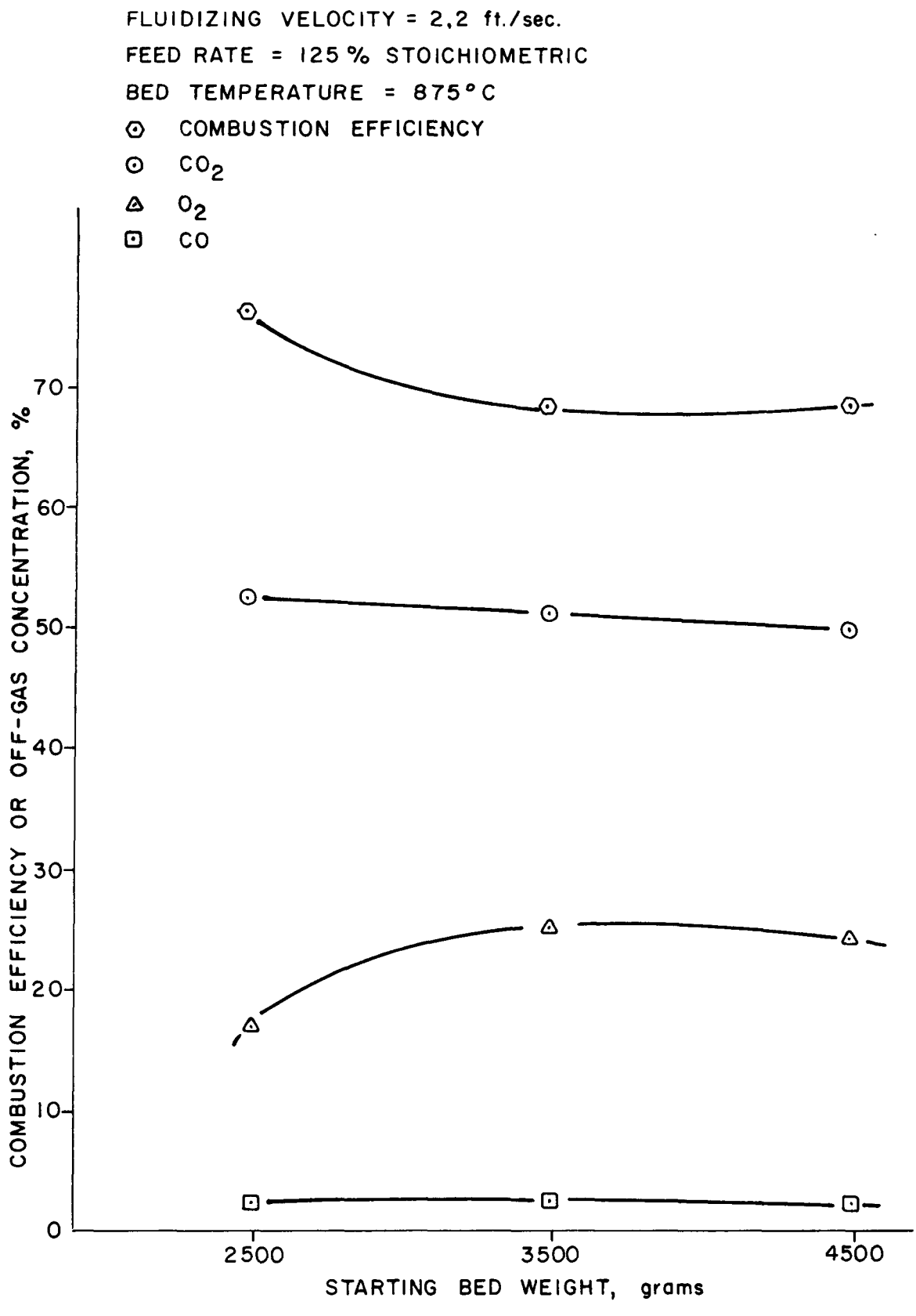

Figure 6. Effect of Bed Weight on Combustion Efficiency

2.3 Fines Recycle Testing

The equipment used for fines burning Runs 31 through 45 was similar to that shown in Figure 7 except no cyclone was provided and the piping in the fines system was smaller. The equipment used for fines burning Runs 46-52 is shown in Figure 7. The equipment consisted of a primary burner vessel, a feed auger system, an off-gas filter system, and a fines recycle system. (Detailed equipment and test descriptions are given in Reference 2.)

Burner startup and supplemental heat was provided by a CO/O_2 combustion torch located in the wall of the fluidized-bed burner. During steady-state operation, the bed temperature was normally controlled by adjusting the fines recycle rate (increasing the fines recycle rate cools the bed).

After the feed supply was exhausted, the graphite was allowed to burn from the bed. The run ended when there was no longer enough graphite in the bed to maintain the burner temperature.

Summaries of the operating conditions and run results for twenty-two fines recycle runs are given in Tables XI and XII, respectively. The first fifteen runs (Runs 31 through 45) were made to test the effect of fluidizing velocity, feed rate, bed temperature, and bed depth on fines burning rate, oxygen utilization, and the general primary burner operability while recycling fines.

Specific values of the independent variables, during the fifteen parametric runs were: graphite feed rate of 100 and 200% of the stoichiometric rate based on the fluidizing oxygen flow rate, bed temperatures of 875 and 900°C, and starting bed weights of 2500 and 4000 grams of fissile and fertile particles. Even though the same amount of feed graphite was metered to the burner in each completed run, the run time varied because of different oxygen fluidizing rates and because different amounts of fines were burned during each run.

The primary burner equipment, the instrumentation, and CO torch performed satisfactorily during the fines recycle runs. The filter chamber and the fines recycle hoppers, however, caused continual fines bridging at burning rates of 35 kg C/hr-ft^2 during the initial series of runs. The fines bridging was due to the lack of an off-gas cyclone to remove the bulk of the entrained fines from the off-gas before they reached the filter pot and a small (1-inch diameter) outlet line at the bottom of the filter pot. However, the fines system worked well at burning rates of 15 and 25 kg C/hr-ft^2, because of the reduced fines loading in the off-gas.

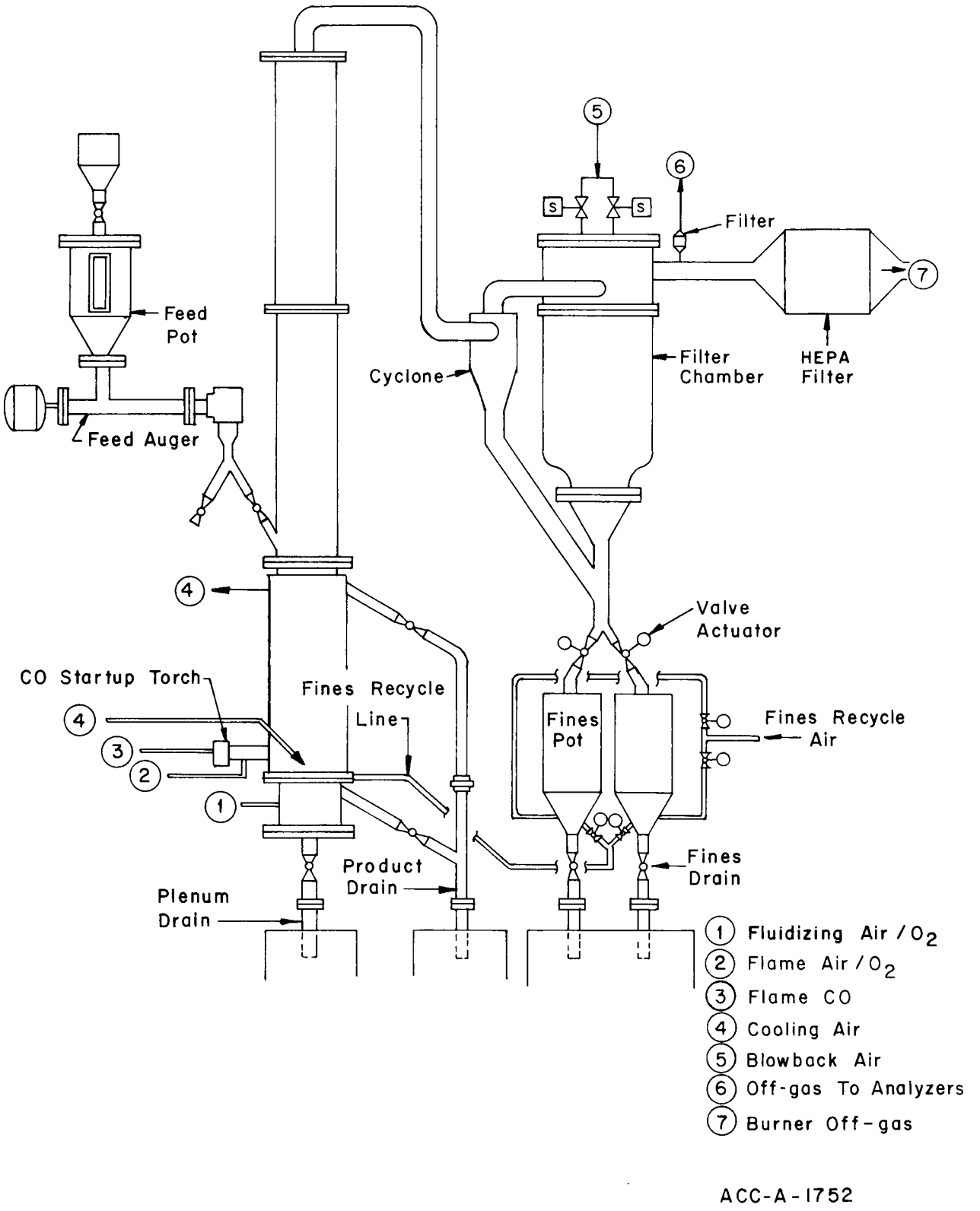

Figure 7. Schematic Diagram of Pilot-Plant Primary Burner Used for Fines Injection Technique Studies (Runs 46 through 52)

TABLE XI

SUMMARY OF OPERATING CONDITIONS FOR FINES RECYCLE TESTING IN THE FOUR-INCH DIAMETER PRIMARY GRAPHITE BURNER

Run No.	Maximum Burning Rate, kg C/hr-ft^2	Oxygen Fluidization Velocity, ft/sec	Feed Rate, grams/min	Stoichiometric Feed Rate, %	Average Bed Temp., ^{o}C	Starting Bed Weight grams	Starting Fines Inventory, grams	Fines Entry Location (a)	Type of Entry (b)
31	35	2.6	125	200	900	4000	3000	3	R
32	35	2.6	125	200	900	4000	3000	3	R
33	15	1.0	27	100	875	2500	3000	3	R
34	15	1.0	27	100	875	2500	3000	3	R
35	15	1.0	54	200	875	4000	3000	3	R
36	35	2.6	62	100	900	2500	3000	3	R
37	35	2.6	62	100	875	4000	3000	3	R
38	15	1.0	27	100	900	4000	3000	3	R
39	35	2.6	125	200	875	2500	3000	3	R
40	15	1.0	54	200	900	2500	3000	3	R
41	25	1.8	45	100	900	2500	3000	3	R
42	15	1.0	0	0	900	4000	3000	3	R
43	25	1.8	89	200	900	4000	3000	3	R
44	25	1.8	45	100	875	4000	3000	3	R
45	25	1.8	89	200	875	2500	3000	3	R
46	35	2.6	62.4	100	900	3111	2500	3	R
47	35	2.6	62.4	100	900	3808	2500	5/16	T
48	35	2.6	62.4	100	900	4000	3000	5/16	T
49	35	2.6	62.4	100	900	4000	3000	5/16	R
50	35	2.6	62.4	100	900	4000	3000	5/16	R
51	35	2.6	62.4	100	900	6000	3000	5/16	R
52	35	2.6	62.4	100	900	4500	3800	5/16	R

(a) Distance above distributor plate in inches

(b) T = Tangential entry, R = Radial entry

TABLE XII

SUMMARY OF RUN RESULTS FOR FINES RECYCLE TESTING IN THE FOUR-INCH DIAMETER PRIMARY GRAPHITE BURNER

Run No.	Final Bed Weight, grams	Final Fines Weight grams	Combustibles In Bed, wt%	Combustibles In Fines, wt%	Total Graphite Burned, grams	Average Off-Gas Concentration O_2, %	CO_2, %	CO, %	Average Filter ΔP, psi	Run Time min	Comments
31(B)	5011	4500	(A)	(A)	5190	6	83	2	2.0	103	Fines bridged in filter pot
32(B)	5160	4531	0.9	92.5	5159	4	82	3	1.6	118	Fines bridged in filter pot
33(C)	--	--	--	--	--	--	--	--	--	--	Early shutdown - fines plug
34	3846	3097	(A)	(A)	6593	5	58	8	0.5	302	Completed run - no fines bridging
35	5260	4322	1.8	93.9	5368	2	63	9	0.6	203	Completed run - no fines bridging
36(B)	3756	4350	(A)	(A)	5340	12	60	4	2.0	136	Fines bridged in filter pot
37(C)	--	--	--	--	--	--	--	--	--	--	Early shutdown - fines plug
38	5064	2064	0.3	90.3	7626	3	60	5	0.7	306	Completed run - no fines bridging
39(C)	--	--	--	--	--	--	--	--	--	--	Early shutdown - fines plug
40	3668	3788	(A)	(A)	5902	3	60	8	0.5	215	Completed run - no fines bridging
41	3787	3001	0.2	90.3	6689	4	62	7	1.3	199	Completed run - no fines bridging
42	3998	2217	(A)	(A)	783	30	45	4	2.0	85	Completed run ~ 11 kg of fines fed-CO torch supplied ~ 50% of process heat
43	4987	4050	0.1	90.6	5640	3	66	8	1.4	148	Completed run - no fines bridging
44	5202	3751	1.5	90.7	5939	9	58	3	2.0	177	Completed run - no fines bridging
45	3600	4377	2.5	89.3	5313	4	60	4	1.7	147	Completed run - no fines bridging
46	3808	2589	(A)	(A)	4171	0.5	67	25	0.7	112	Rubber gasket melted in fines recycle system
47	3835	2835	(A)	(A)	1178	4	64	(A)	0.7	29	Early shutdown - glass fines recycle hopper broke
48	4829	2257	(A)	(A)	7433	0.5	66	14	0.8	141	Completed run - no problems
49	4203	1850	(A)	(A)	6143	0.5	68	14	0.8	61	Early shutdown - Feed system bridged - could not be cleared
50	5696	2229	0.1	72.9	7461	0.5	63	16	0.8	138	Completed run - no problems
51	7429	2228	0.2	70.4	7462	1	69	16	0.8	147	Completed run - no problems
52	3890	1352	0.2	68.7	73,717	1	68	15	1.0	1600	

(A) Data not taken.

(B) Fines bridging occurred in recycle system making the graphite burning data invalid.

(C) Run not completed.

Following the 15 parametric runs, six runs (Runs 46 through 51) were made to test the effect of fines injection technique and a fluidized-bed L/D ratio of 7.5 on fines burning at combustion rates of 35 kg C/hr-ft^2. The burning rate (35 kg C/hr-ft^2), the fluidizing velocity (2.5 ft/sec), the feed rate (62.4 g/min), and the average bed temperature (900^{o}C) were identical for all the runs. Three different fines entries were tested; the first entry tested was radial at a point 3 inches above the distributor plate. The second was a tangential entry 5/16 inch above the plate, and the third was a radial entry 5/16 inch above the plate.

The results of the six fines injection runs demonstrated that the addition of a cyclone and related modifications were successful in eliminating fines plugging and fines bridging in the filter pot or piping at burn rates of 35 kg C/hr-ft^2. The results showed that the entries 5/16 inch above the distributor plate were superior to the entry 3 inches above the distributor for burning fines. Also, the tangential and radial entries were equally effective in burning fines.

The final run (Run 52) was made to test pneumatic fines recycle and general equipment operation during an extended time period. Although previous runs had been made at simulated demonstration plant conditions, none had exceeded a five-hour time period. Additional data were needed to evaluate equipment reliability and steady-state fines inventories.

During the 27-hour run, the bed temperature was controlled between 880 and 920^{o}C except for the brief periods when feed bridging occurred. The burner instrumentation, filter blowback system, off-gas analyzers, and automatic fines hopper switching system all performed with no problems. Occasional fines plugging and feed bridging during product discharging were the only significant problems during the run. No fines plugging whatsoever was detected during previous short-term runs (Runs 45 through 51), but when the valve actuators were installed on the fines-hopper outlet valves, a pipe nipple and coupling (about 4 inches in total length) were added to the fines outlet line to provide enough room for the actuator. About every tenth time the fines pots were switched, a slight plug would form in one of the nipple-coupling sections and momentarily interrupt the fines flow. The plug either immediately cleared itself or was easily cleared by back pressuring the line. The plugs were mostly an inconvenience, because they tended to upset the burner temperature control.

The following conclusions were reached as a result of the fines recycle tests:

1. The primary burner is capable of burning more fines than are generated when operated at a burning rate of 35 kg C/hr-ft^2.

2. The semi-continuous operating mode will consistently produce product with less than 2% combustibles with no supplementary heating and without significantly decreasing the burner throughput.

3. The bed temperature must be maintained as high as material codes and safety will allow to maximize the fines burning rate and oxygen utilization.

4. Fines burning in the vapor space when the oxygen level rises in the off-gas during burner upsets or during the "burnout" period at the end of a cycle is potentially a very serious problem, since the vapor-space burner wall or vessel internals (thermowells, etc.) could be overheated.

3. Carbon Monoxide Combustion Torch

Proposed reprocessing of Ft. St. Vrain fuel calls for burning large quantities of graphite in a fluidized-bed burner. Burner startup and supplemental heat must be provided to bring the burner to operating temperature ($\sim 900^{\circ}$C) and to supply any needed heat during process upsets. The heating method should be safe, rapid, reliable, easy to control and maintain, and operable in any type of bed: hot, cold, deep, shallow, graphite, or fissile and fertile particles.

In-bed combustion of CO gas is potentially a simple and rapid method for startup heating of the HTGR primary graphite burner. All of the heat is transferred directly into the bed; heat losses are minimized, and the bed is always hotter than the burner wall, thus maximizing vessel life. A simple torch was designed and tested during 29 runs in the 4-inch diameter primary graphite burner.

A diagram of the CO combustion torch installed in the primary burner is shown in Figure 8. The torch is made from 1-inch pipe and is six inches long. The flame shroud protrudes less than an inch into the bed. The oxygen is gradually mixed with the CO using a perforated metal cone. The gas mixture is ignited by a spark igniter connected to a 10,000 volt coil.

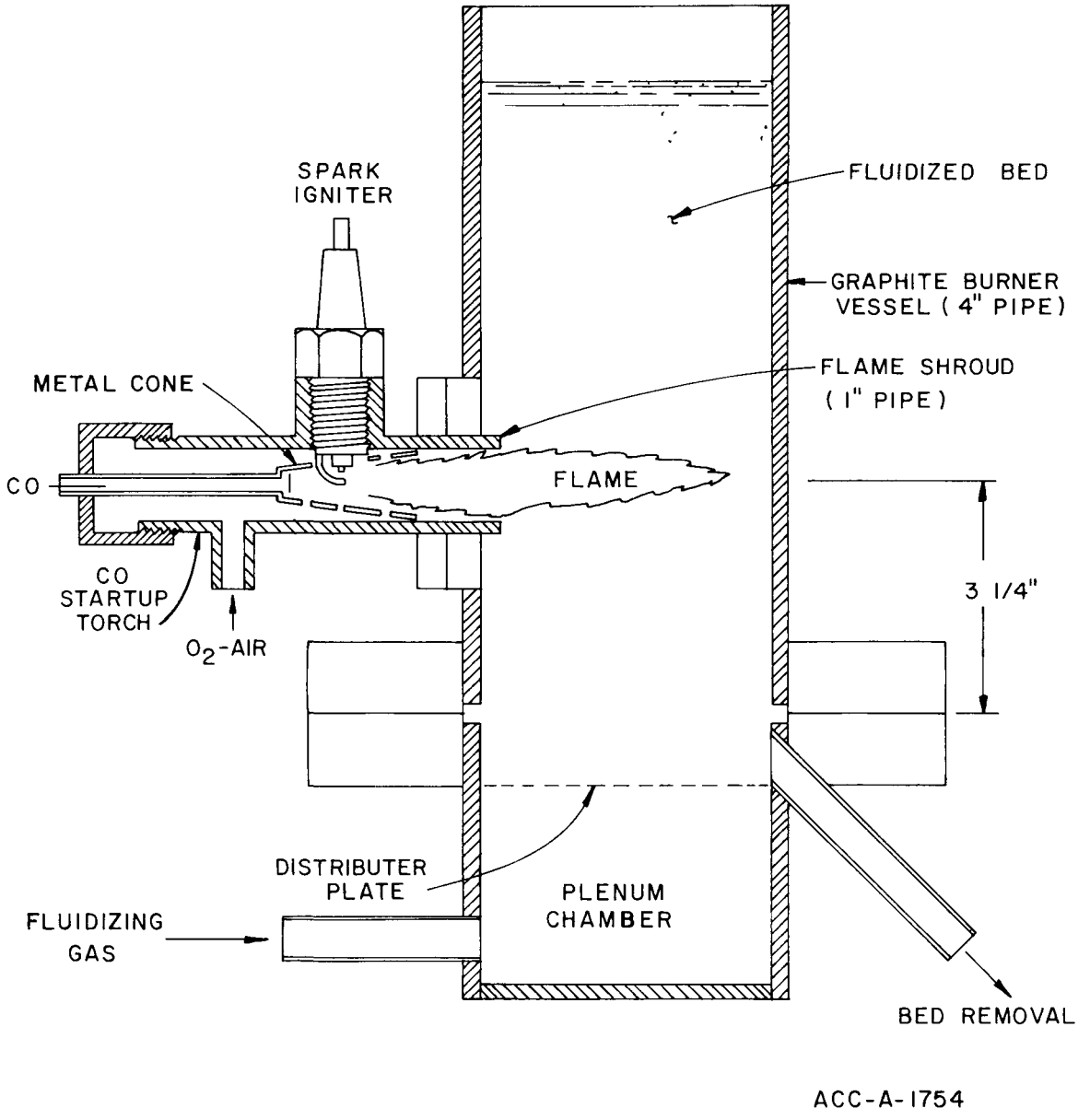

Figure 8. CO Torch Installed in Primary Burner

The startup procedure was similar for all 29 runs. The starting beds for most of the runs were 2500 grams to 4500 grams of fissile and fertile particles. A few of the starting beds contained as much as 25% graphite. A startup temperature record is shown in Figure 9. The bed was fluidized with air at 1 ft/sec. The torch igniter was activated and the CO and O_2 flows were started to the torch at low rates. As soon as the bed temperature indicated torch ignition (usually the bed temperature began rising in less than ten seconds), the gas flows to the torch were increased. The igniter was left in service throughout the startup. Each time the temperature increased 100°C, the fluidizing air rate was decreased to maintain the fluidizing velocity near 1 ft/sec. When the temperature reached 600°C, the fluidizing gas was changed to oxygen and feed was started to the burner. The graphite usually began to burn at approximately 600°C, but the reaction was not self-sustaining in the 4-inch pilot-plant burner until the bed temperature reached 770°C. The burner heatup rate remained constant until the bed temperature reached about 700°C. At this temperature, the graphite combustion became significant and the heating rate increased rapidly. When the bed temperature exceeded 800°C, the torch was gradually deactivated, the shroud cooling air was started, and the shroud cooling air was increased as necessary to control the bed temperature at the desired level. The torch was also used during the runs to reignite the graphite when process upsets extinguished the burning.

The original torch for the 4-inch burner was made entirely from 304L stainless steel, but due to excessive scaling of the shroud and cone material, a torch having an Incoloy 825 shroud and a thicker 304L cone was installed.

The startup heating time periods for 20 primary graphite burner runs are given in Table XIII. Runs 17 and 26 in the 4-inch primary burner were used as bases for calculating the number of torches required in a 16-inch burner. Run 17 provides a heat balance for a long heatup time period and Run 26 for a short heatup time period. Run 26 is used as the example of the most rapid startup heating period.

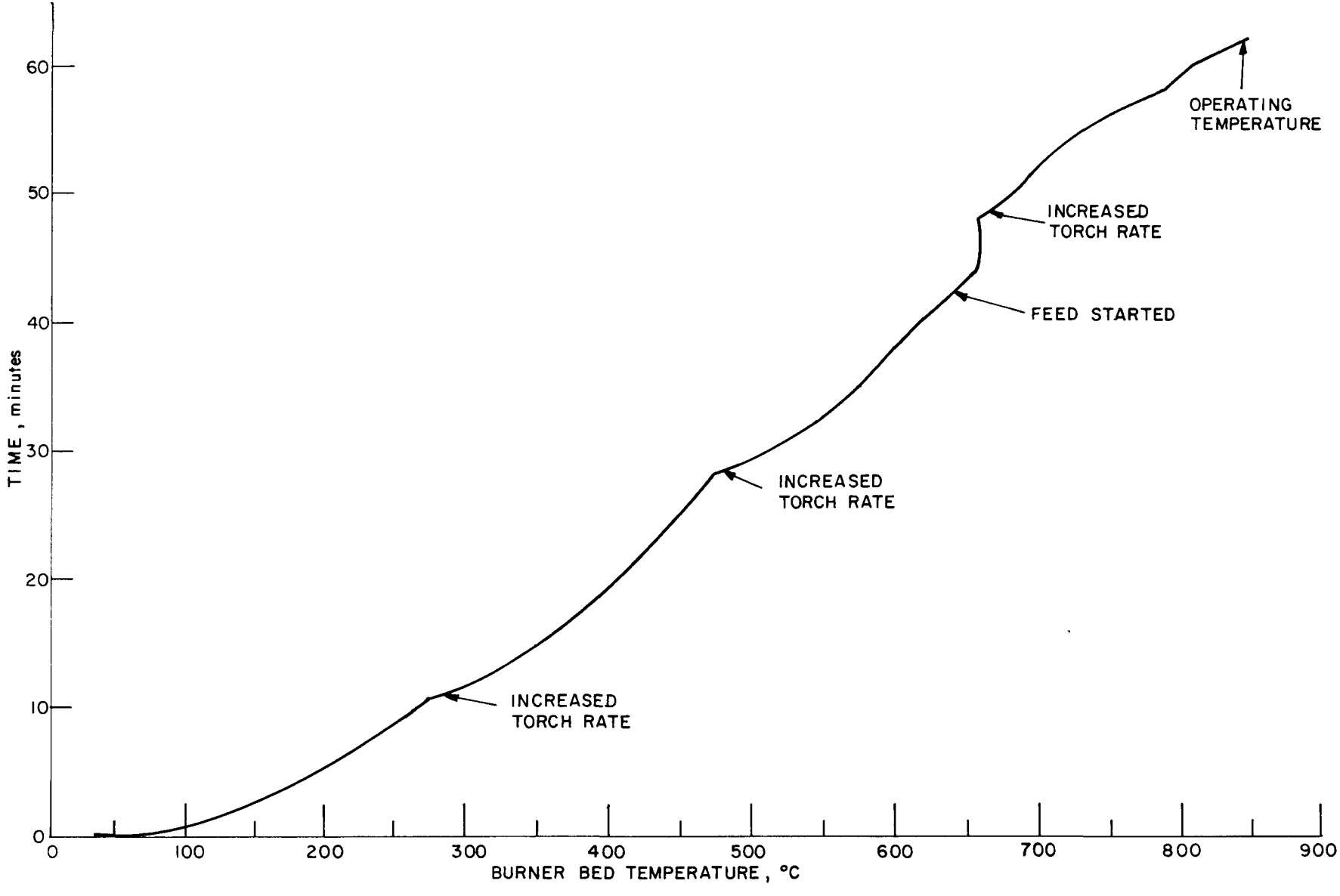

Figure 9. Startup Temperature Record

TABLE XIII

HEATUP TIME PERIODS FOR CO TORCH TESTING IN THE FOUR-INCH DIAMETER PRIMARY GRAPHITE BURNER

Run No.	Starting Bed Weight, Grams	Heatup Time to 600°C, Min.	Heatup Time to 875°C, Min.
10	2743	30	42
11	2500	25	40
12	2577	33	47
13	2500	33	60
14	2500	34	42
15	2500	32	70
16	2500	35	52
17	2500	40	60
18	2500	53	70
19	2500	28	51
20	2500	32	41
21	2500	35	52
22	2500	33	46
23	2500	33	51
24	3500	37	56
25	4500	41	67
26	4000	17	29
27	4000	27	57
28	4000	45	85
29	4000	24	34

Since no melting or sintering occurred during Run 26, the torch may be operated as reliably at much higher heating rates. Table XIV summarizes the heat balances of Runs 17 and 26. The heatup time period from 21°C to 600°C for Run 17 was 40 minutes and for Run 26 was 17 minutes. Table XIV shows that a much lower percentage of the heat was lost to the surroundings or to gas heating in Run 26 than in Run 17. The scaleup based on the Run 17 heat balance will provide the upper limit estimated for the number of torches needed to heat a 16-inch burner, and Run 26 will provide the lower limit estimate.

Bases for Torch Calculations

1. Inside diameter of plant burner is 16 inches, and the vessel wall is 0.5 inches thick.
2. Startup fluidizing velocity is controlled at 1 ft/sec.
3. CO combustion supplies the only process heat; heatup calculations include only the 21°C to 600°C temperature range, where no significant graphite combustion occurs.
4. Gases leave bed at bed temperature.
5. Combustion of CO is 85% complete.
6. Heat supplied by CO combustion is dissipated as follows:
   a. to heat process gases from 21°C to bed temperature.
   b. to heat vessel components in contact with bed from 21°C to 600°C.
   c. to heat bed from 21° to 600°C.
   d. losses from vessel to surroundings.
7. Heat capacities used in calculations (Btu/lb-°F):
   a. vessel - 0.12
   b. fissile and fertile particles - 0.17
   c. air, O_2, CO, N_2 - 0.26
8. Densities used in calculations (lb/scf):
   a. air - 0.07493
   b. O_2 - 0.08281
   c. CO - 0.0725
   d. N_2 - 0.07245
9. CO heat of combustion - 4343.6 Btu/lb at 25°C.
10. The CO flow rate to each of the torches in a 16-inch diameter burner is 2.78 scfm which provides 744 Btu/min at 85% combustion. This represents the highest torch rate which has been tested. Higher torch rates may be acceptable.

TABLE XIV

HEAT BALANCES FOR RUNS 17 and 26

Heat Source or Sink	Run 17		Run 26	
	Btu	Percent of Total Heat	Btu	Percent of Total Heat
Available Heat [a]	10,009.2	100.0	7277.1	100.0
Gas Heating [b]	2405.1	24.0	1275.6	17.5
Vessel Heating (c)	3126.0	31.2	3751.2	51.6
Bed Heating	979.5	9.8	1573.4	21.6
Losses to Surroundings	3498.6	35.0	676.9	9.3

(a) Assumes 85% combustion of CO

(b) Includes heating of fluidizing air and all torch gases from 21°C to bed temperature.

(c) Includes only vessel parts actually in contact with bed.

The scale-up calculations were done by considering each of the four heat sinks separately: (1) gas heating, (2) vessel heating, (3) bed heating, and (4) losses to surroundings.

Gas heating is a function of the torch and fluidizing flow rates. Since the torch setting is constant and the fluidizing velocity is controlled at 1 ft/sec, the heat required for this stream is a function only of the heatup time.

For simplicity, the vessel is divided into two parts: (1) vessel in contact with fluidized bed and (2) vessel in contact with off-gases. Since the heat going to (2) has already been accounted for, the only other vessel heating is from contact with the fluidized bed. Therefore, the amount of heat required to heat the burner from 21°C to 600°C is a function only of the bed depth. Bed heating is also a function of bed depth only.

Since heat losses to the surroundings occur only by radiation, conduction, or convection from the vessel walls, total losses are a function of heatup time period and bed depth. When all of these factors are combined, the resulting equations for the number of torches in a 16-inch burner are:

$$\text{No. torches (based on Run 17)} = 2.78 + \frac{0.30}{t} + \frac{0.677}{t}\,BD$$

$$\text{No. torches (based on Run 26)} = 1.57 + \frac{0.30}{t} + \frac{0.677}{t}\,BD$$

where t = desired heatup time period in hours to raise bed temperature from 21°C to 600°C

BD = bed depth in feet

These two equations are plotted in Figures 10 and 11. The results shown in Table XIII indicate that it takes about 1.5 times as long to heat the burner to 875°C than to 600°C. By using Table XIII and Figures 10 and 11 and knowing the required bed depth and heatup time period, an estimate of the number of torches required to heat a 16-inch burner can be made. If a startup time period of 3 hours (to 875°C) was desired with a bed 6 feet deep, it would take about 2 hours to heat the burner to 600°C. Five torches are required based on Figure 10 and 4 torches based on Figure 11. If longer heatup time periods and/or shallower beds are used, the number of torches decreases accordingly.

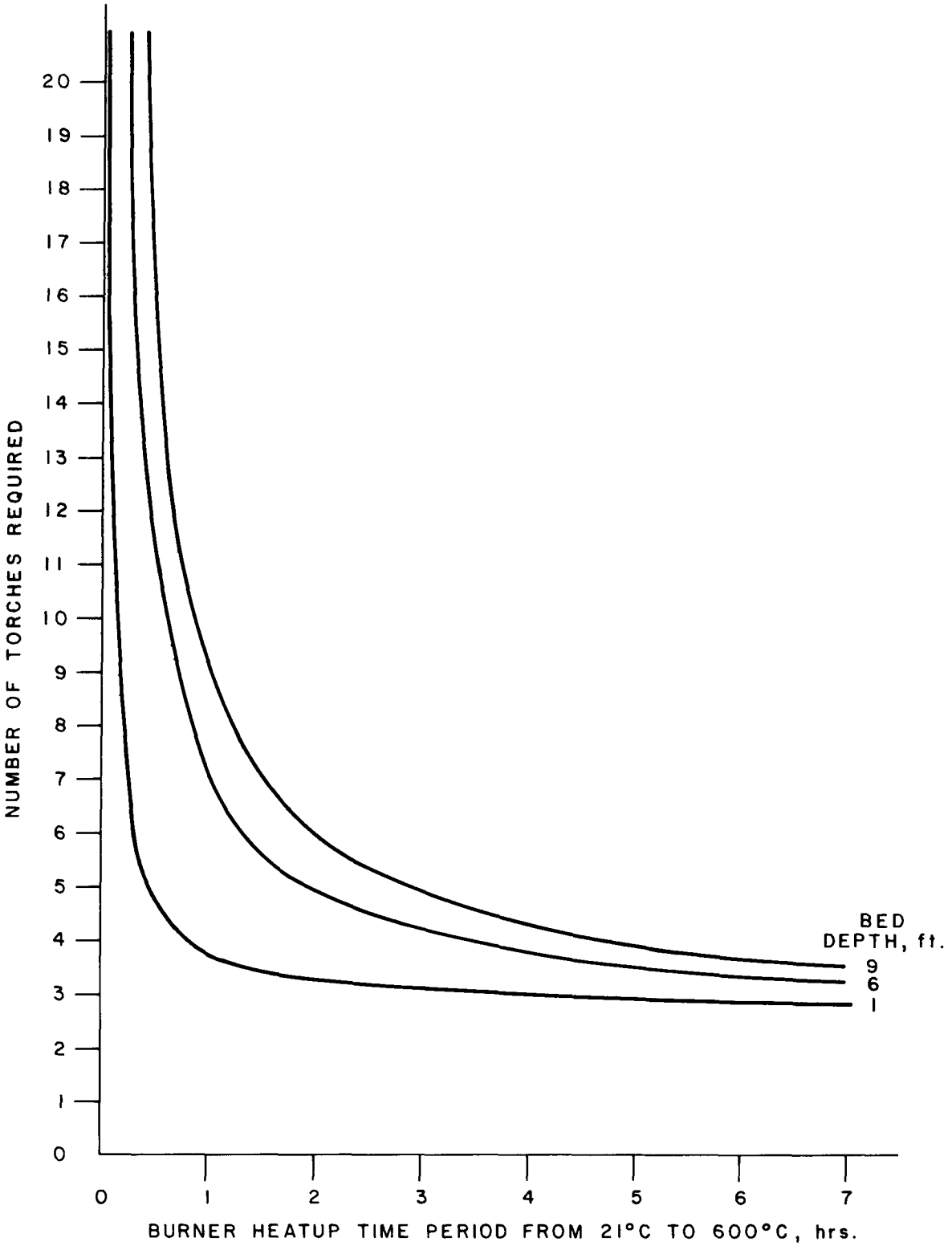

Figure 10. Number of Torches Required to Heat 16-Inch Burner Based on Results of Pilot-Plant Run P17

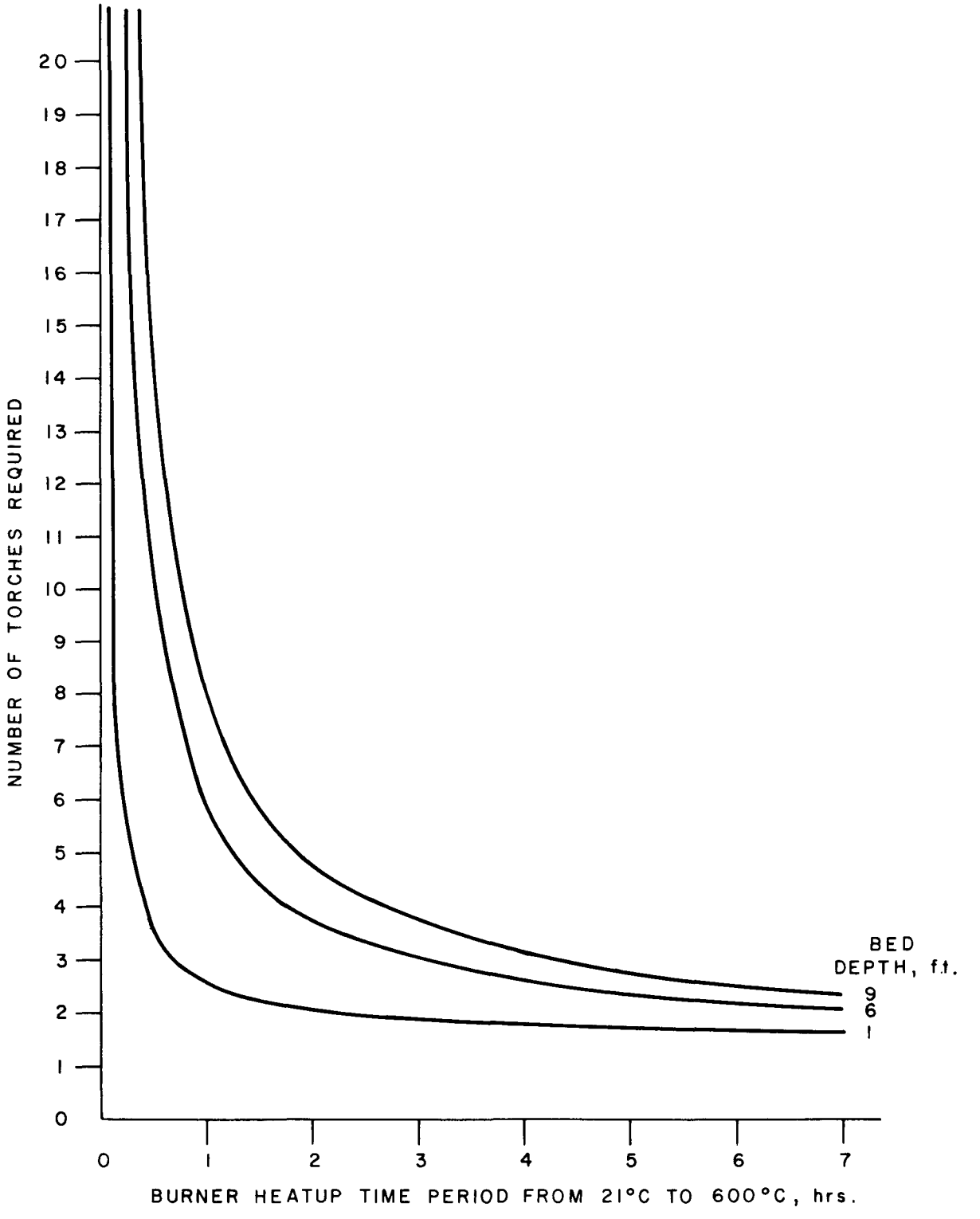

Figure 11. Number of Torches Required to Heat 16-Inch Burner Based on Results of Pilot Plant Run P-26

The following conclusions were reached as a result of the experimental testing:

1. The CO/O_2 combustion torch is a rapid and reliable heating method for the graphite burner.
2. 304L stainless steel is not a suitable construction material for the CO torch, but a material such as Incoloy 825 or Hastelloy-X should be satisfactory.
3. A 16-inch burner will require 3 to 6 torches, depending on bed depth and the specified startup time period.

IV. PARTICLE CLASSIFICATION AND PARTICLE BREAKING

Silicon carbide coated fissile and fertile particles from the primary burner are classified in a gas classifier and the respective particles processed in a particle breaker. Pneumatic classification and particle breaking methods for reprocessing Ft. St. Vrain fuel were conceived and developed by Allied Chemical Corporation - Idaho Chemical Programs (ACC-ICP) personnel.[3,4]

1. Gas Classification

Test results and a description of the pneumatic classifier, conceived and developed at ICPP, are given in Reference 3. Subsequent to initial development of the pneumatic classifier at ICPP a pneumatic classifier, the Alpine "zigzag" classifier, became available commercially. The "zigzag" classifier was purchased for comparison with the unit developed at ICPP.

The Alpine Multiplex "zigzag" classifier, a German-made vertical-displacement air classification system, was tested to determine how effectively the unique "zigzag" design can be used to separate Ft. St. Vrain fissile and fertile particles. Unirradiated Ft. St. Vrain particles--product from the pilot-plant primary burner -- were used for the "zigzag" classifier tests. The primary burner product contained equal concentrations of fissile and fertile particles and about 5 wt% unburned graphite. Goals were to achieve > 85 percent pure fertile particles and > 95% pure fissile particles, simultaneously, using air classification. The results of the tests using the "zigzag" classifier were compared to those obtained using the Air Classifier Pilot Plant (ACPP) developed at ICPP[3].

Experimental Equipment and Procedures

The Alpine Multiplex "zigzag" classification system is shown schematically in Figure 12. The classification column is a 38-inch long "zigzag" vertical column, square in cross-section. The cross-sectional area of the column is 2.5 $in.^2$ and the feed point is located 10 inches below the top of the column. Air is supplied by the vacuum system which induces flow at a constant volumetric rate. Flow through the column is adjusted by a throttling valve which controls the volume of incoming air; make-up air is drawn into the vacuum through a coarse filter.

The operating procedure was similar to that used for the ACPP study: (1) start the vacuum and set the desired air velocity through the column, (2) charge a known weight of feed to the charging pot (about 2500 grams of primary burner product were used in each run), and (3) start and control the flow of feed by opening the feed control valve. As in the ACPP, overhead and bottom product were withdrawn continuously.

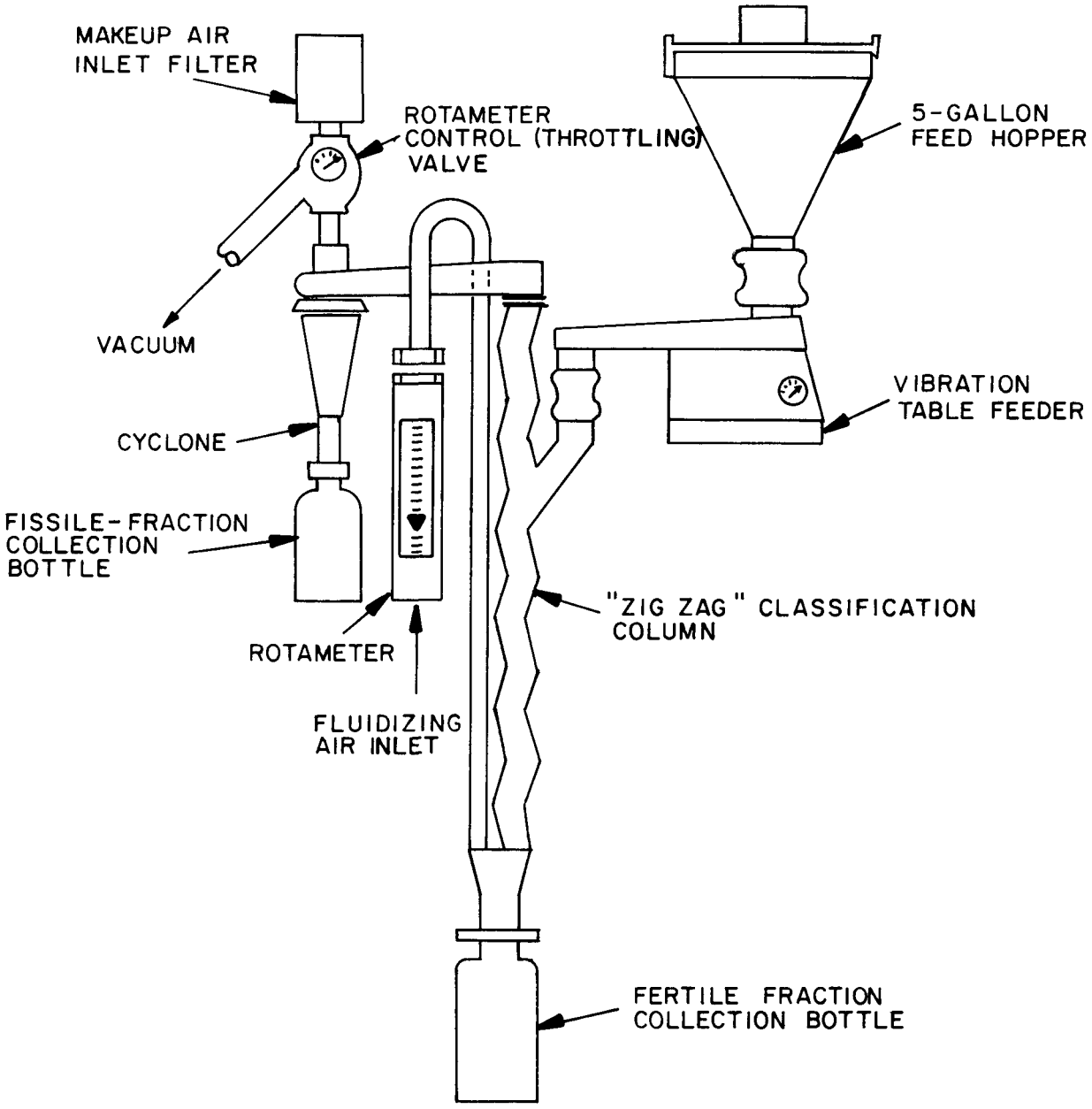

Figure 12. Alpine Multiplex "Zigzag" Classification System

At the completion of each run, both overhead and bottom fractions were weighed, reduced to about 100-gram samples in a sample splitter, and screened through a 35-mesh screen. The purities of each fraction were determined by weighing the quantity of solids left on the screen and comparing that value to the weight of particles which pass through the screen. It was assumed that all particles > 35 mesh (500 mm) are fertile particles and all those < 35 mesh are fissile. Statistical data from the fuel fabricators show, however, that a "cross-over" of particle sizes up to 5 wt% can be expected. Analytical techniques are not sufficiently developed to determine accurately the amount of fissile- or fertile-particle impurities in each classified fraction. After the analyses were completed for each run, the separated fractions were recombined, sampled, and screened for particle breakage data and were re-used as feed in subsequent runs.

Experimental Results

Twelve runs were made using four different air velocities at each of three different particle feed rates. The four air velocities were selected to "bracket" the expected velocity range (based on our experience in the ACPP) to maximize product purities. Similarly, the feed rates were those studied in the ACPP tests. These ranges were 8.3 to 12.2 ft/sec and 75 to 250 grams/min for air velocity and feed rates, respectively.

The results of this parametric study are summarized in Table XV. The most efficient separation occurred at an air velocity of about 10 ft/sec. At this velocity, 98.5 percent pure fissile and 94 percent pure fertile particle fractions were achieved.

Comparison of ACPP and "zigzag" Classifiers

The air classifier pilot plant (ACPP), designed and built at ICPP, and the "zigzag" classification system are both vertical-displacement air classification systems with the same operating principle and approximately the same size. Figure 13 is a schematic representation of both systems showing their approximate sizes and indicating the primary differences in their design. Table XVI is a summary of the major design features of both classifiers.

TABLE XV

SUMMARY OF RESULTS OF PARAMETRIC "ZIGZAG" CLASSIFICATION STUDIES

Run No.	Superficial Fluidizing Air Velocity, ft/sec	Particle Feed Rate, grams/min	Purity of Fissile Particles, wt%	Purity of Fertile Particles, wt%
ZC-1	8.3	161	98.6	76.6
ZC-2	8.3	192	98.8	76.6
ZC-3	8.2	248	98.9	83.8
ZC-4	9.9	145	98.5	89.5
ZC-5	9.9	190	98.5	94.0
ZC-6	9.9	247	98.5	93.6
ZC-7	11.1	118	94.9	94.1
ZC-8	11.1	155	93.6	94.4
ZC-9	11.1	205	96.1	93.5
ZC-10	12.2	95	73.6	95.1
ZC-11	12.2	146	76.0	95.4
ZC-12	12.2	225	82.8	94.8

CANDIDATE VERTICAL CLASSIFIERS

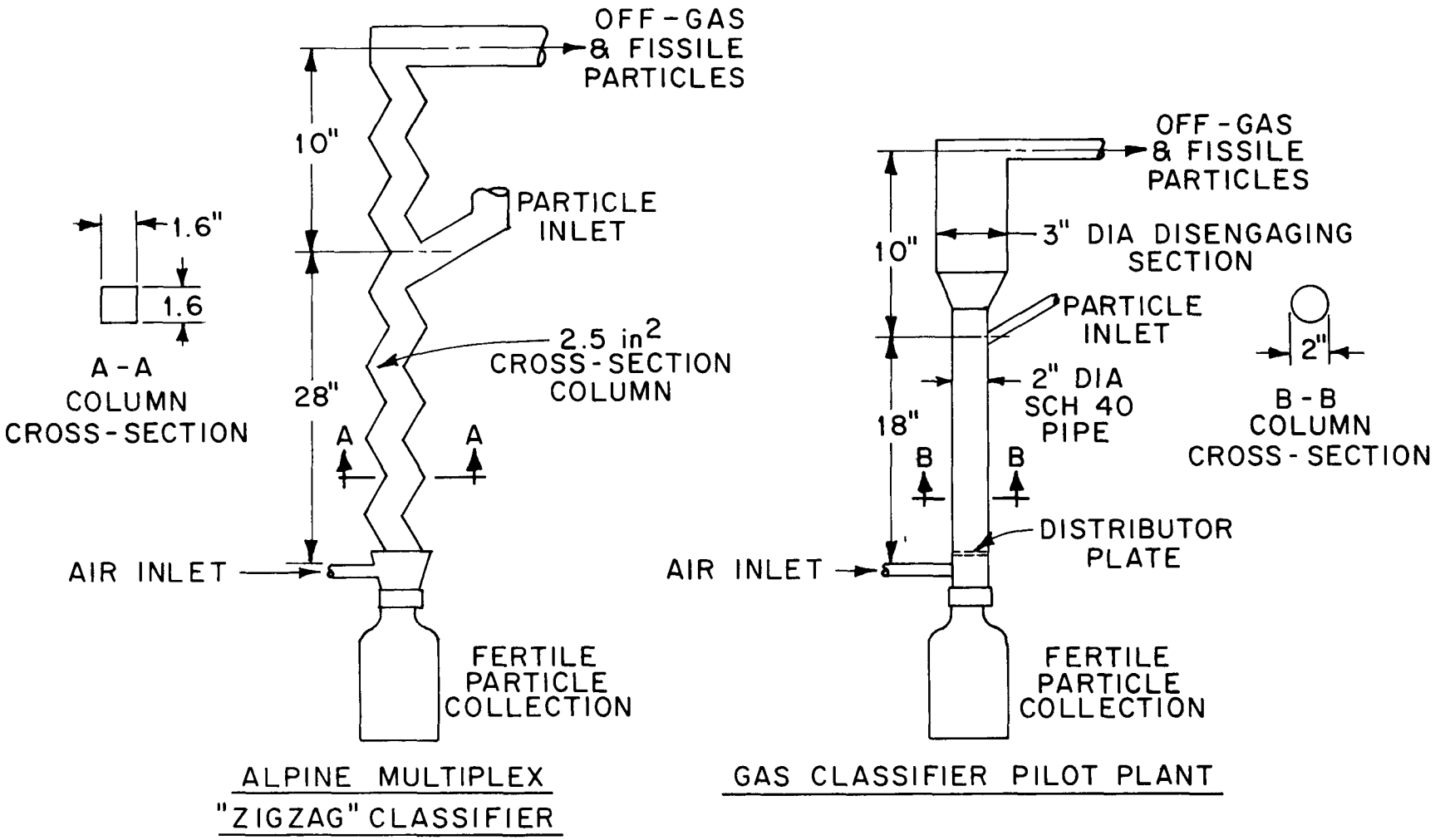

Figure 13. Candidate HTGR Gas Classification Pilot-Plant Systems

ACC-A-1514

TABLE XVI

SUMMARY OF DESIGN FEATURES OF ACPP AND "ZIGZAG" CLASSIFIERS

		"Zigzag"	ACPP
1.	Overall column height, in.	38	28
2.	Height of feed point, in.	28	18
3.	Cross-sectional area, in^2.	2.5	3.4
4.	Shape of cross-section.	Square	Circular

Data show both classifiers were able to achieve 99-percent pure fissile particles and ∿ 95-percent pure fertile particles at their best separation efficiency. This separation efficiency occurred at about 10 ft/sec air velocity in the "zigzag" classifier, whereas 11.5 ft/sec was required in the ACPP. This variance can be attributed to at least two differences: (1) the ACPP has a 3-inch diameter disengaging section, 10 inches long, at the top (the 11.5 ft/sec velocity was based on the cross-sectional area of the 2-inch diameter pipe section). Higher velocities are thus necessary to elutriate fissile particles through this expanded section; (2) the "zigzag" design of the Alpine classifier imparts a vortex motion in each channel compartment. Such motion creates an effective air velocity for elutriation greater than the superficial velocity based on cross-sectional area.

The significant differences in design of the two classifiers and the essentially idential results obtained, indicate the simplicity of the classifier design. Obviously, the only critical parameter is the fluidizing gas velocity.

2. Particle Breaking

Two methods have been considered for breaking silicon carbide coatings on the fertile fuel particles: (1) fluid-bed jet breaking and (2) double-roll crushing. Jet breakers have no moving parts but generate exhaust gases. Roll crushers have the capacity to crush the coatings at the required throughput rates, but the roll tolerances and gap settings require close monitoring.

2.1 Jet Breaking

A two-inch diameter pilot-plant jet particle breaker was tested to determine breaking rates and gas usage requirements for the system. Data were obtained for various jet diameters, jet-to-impact-plate separation distances, and numbers of jets. (Detailed test descriptions are contained in Reference 4).

A diagram of the 2-inch diameter, pilot-plant jet breaker is shown in Figure 14. The unit was made from stainless steel, except for the feed vessel and overhead collection pots, which were glass. The jet tubes were 1/4-inch O. D. stainless steel tubing with one end welded closed and a single small hole drilled through the weld. The impact plates were 304L stainless steel.

The fertile particles used for these tests were obtained by burning the graphite matrix from scrap Ft. St. Vrain fuel compacts in the pilot-plant primary burner and then separating the particles into fissile and fertile fractions.

The operating conditions used for each of the runs are given in Table XVII. The jet sizes tested ranged from 0.0135 to 0.052 inches in diameter. The jet-to-impact-plate separation distance ranged from 0.25 to 2.0 inches. Three jets were used in all runs except Run 37. With the combined flows from the three large jets used in Runs 35 and 36 and the normal fluidizing flow of 1.25 ft/sec, the total velocity in the column was almost 9 ft/sec, which was approaching the elutriation velocity of some of the smaller whole particles. Run 37 was made while operating only one jet and resulted in a total velocity of less than 4 ft/sec, which is much below the elutriation velocity of any whole particle. The first three runs were made to determine the "best" starting bed weight; 750 grams was chosen for the remaining runs.

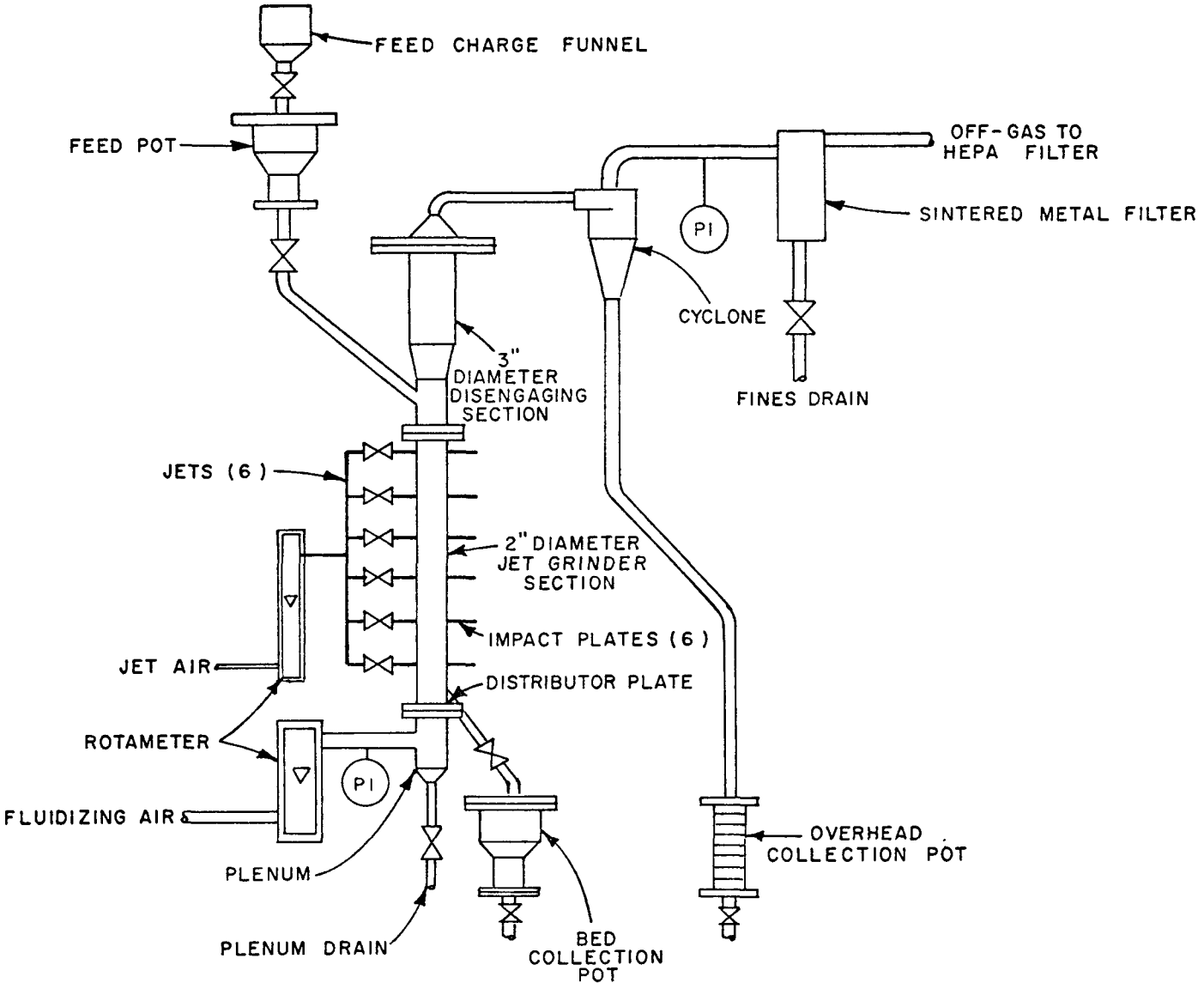

Figure 14. Gas-Jet Particle Breaker Pilot Plant

TABLE XVII

SUMMARY OF PILOT-PLANT JET BREAKER OPERATING CONDITIONS

Run No.	Jet Orifice Diameter, inches	Jet Orifice Area, in^2	Number of jets	Impact Plate Separation, inches	Starting Bed Weight, grams
23	0.021	0.000346	3	0.25	500
24	0.021	0.000346	3	0.25	1000
25	0.021	0.000346	3	0.25	750
26	0.021	0.000346	3	0.50	750
27	0.021	0.000346	3	0.75	750
28	0.021	0.000346	3	1.00	750
29	0.021	0.000346	3	2.00	750
30	0.014	0.000143	3	0.50	750
31	0.028	0.000616	3	0.50	750
32	0.040	0.001257	3	0.50	750
33	0.021	0.000346	3	1.25	750
34	0.035	0.000962	3	0.50	750
35	0.052	0.002124	3	0.50	750
36	0.052	0.002124	3	0.75	750
37	0.052	0.002124	1	0.75	750

The run procedure was to set the fluidizing velocity at 1.25 ft/sec, charge the bed to the column, start the jet air, and after one hour of breaking, shut off the jet air and drain the column. During the run, the overhead volume was recorded as a function of time. After the run the bed and overhead were both weighed and screened to determine the product size distribution.

Fifteen runs were made; the results of the tests are summarized in Table XVIII. The overhead volume collected as a function of time, the effect of jet size on the maximum breaking rate and on the maximum air usage efficiency, and the effect of jet-to-impact plate separation distance on the maximum particle breaking rate per jet were determined.

Fluid-bed jet breaking is an effective method for breaking unirradiated fertile particles. As few as two jets using a total of 5.5 scfm air would be adequate to break particles at the demonstration plant rate of 76 grams per minute. The jet grinder would be simple to operate and maintain in a hot cell, since there are no moving parts or critical tolerances. The impact plates could easily be made remotely replaceable.

2.2 Roll-Crushing

A four-inch diameter pilot-plant double-roll crusher was tested to determine crushing capacity and product particle size and geometry as a function of roll-speed, gap setting, and feed rate. (A detailed description of the test equipment and results of the tests is provided in Reference 5).

The roll crusher used for the experimental testing (Figure 15) utilized two cylindrical rolls, 4 inches in diameter and 1.5 inches long. The clearance between the rolls was adjustable from 0.000 to 0.125 inches. The initial gap adjustment was set by a thickness gauge which puts no load on the rolls; the clearance was checked under a heavy load by running a small piece of lead solder (0.060 inch diameter) between the rolls and measuring the thickness of the solder. The crusher was driven by an electric motor coupled to a worm gear speed reducer. The roll speed was variable from 0 to 200 rpm.

The run procedure was to set the roll clearance and roll speed and then check the roll clearance with solder. The feed was introduced and the crusher allowed to run until all of the particles were crushed. The roll gap was

TABLE XVIII

SUMMARY OF PILOT-PLANT JET GRINDER TEST RESULTS

Run No.	Jet Pressure, psig	Jet Air Consumption, scfm	Maximum Breaking Rate, grams/min	Maximum Air Usage Efficiency, grams/scf air	Bed -35 Mesh, %	Bed MMPD*, inches	Overhead MMPD*, inches
23	96	1.9	7.42	3.89	78.1	0.0165	0.00915
24	95	1.9	12.67	6.63	71.6	0.0171	0.00879
25	94	1.9	10.61	5.55	76.2	0.0168	0.00858
26	95	1.9	17.42	9.12	93.2	0.0149	0.00772
27	94	1.9	17.58	9.20	97.1	0.0142	0.00771
28	94	1.9	17.02	8.91	97.3	0.0140	0.00752
29	94	1.9	8.87	4.64	90.3	0.0166	0.00788
30	96	0.7	2.07	3.05	68.4	0.0175	0.00795
31	92	3.2	41.81	13.19	96.6	0.0140	0.00762
32	94	5.5	97.56	17.61	96.0	0.0151	0.00900
33	95	1.9	15.99	8.37	95.3	0.0147	0.00732
34	85	4.1	60.98	14.98	96.2	0.0138	0.00822
35	95	10.6	292.68	27.72	95.5	0.0148	0.0127
36	95	10.6	395.52	37.46	95.3	0.0147	0.0117
37	93	2.7	67.49	24.63	92.6	0.0151	0.00412

* Mass mean particle diameter.

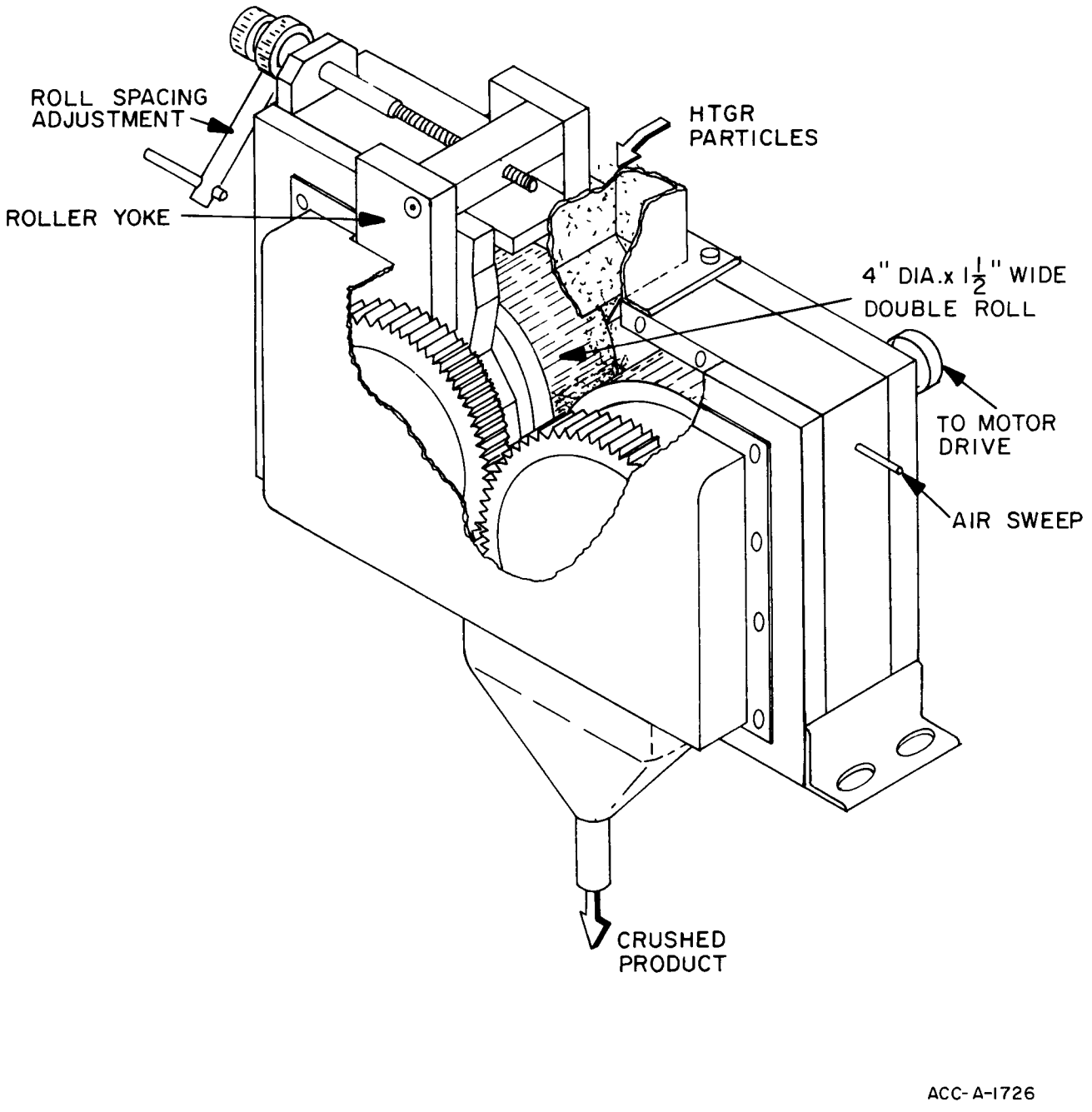

Figure 15. Experimental Double-Roll Crusher

again checked with solder after the run to assure no change had occurred. The crusher product was screened and weighed to determine its mass mean particle diameter (MMPD). To determine the amount of unbroken particles in the crusher product, the material was leached with thorex solution, dried, and air classified to separate the hulls from the whole particles.

The feed material for all of the runs was + 35 U. S. Mesh fertile particles obtained from scrap Ft. St. Vrain fuel rods, and the batch feed size was 50 grams.

Experimental Results

The roll crusher performed satisfactorily during 40 tests; all runs were successfully completed except two. A summary of test results is given in Table XIX. Runs 6 and 23 failed because the crusher stalled as a result of the drive unit not having sufficient power at 20 rpm.

During the first 22 runs, the roll clearance was not measured under a heavy load by passing solder between the rolls nor was the amount of unbroken particles determined. The first five runs tested the effect of roll clearance on product size; Runs 6 through 11 tested various roll speeds, and Runs 12 through 22 tested various feed rates. Runs 23 through 27 were made to determine the crusher capacity as a function of roll speed during flood-feeding. The remaining 12 runs were made to more carefully test the effect of roll clearance on product size and to determine the amount of unbroken particles in the product as a function of roll clearance.

In addition to the 40 parametric runs, tests were made to determine the maximum size of graphite the crusher would accept as a function of roll clearance. All of the graphite pieces which were smaller than 14 U. S. Mesh (0.046 inch) passed through the crusher. The crusher would accept only part of the graphite in the - 12 + 14 U. S. Mesh (0.046 to 0.055 inch) size range. Changing the roll clearance from 0.002 to 0.024 inch did not cause a significant increase in the size of graphite accepted by the crusher.

Conclusions based on results of the study are:

(1) At a roll speed of 40 rpm, the 4-inch diameter roll crusher will crush 2.3 times more material than the required demonstration plant rate of 76 grams per minute.
(2) The roll crusher will produce a satisfactory secondary burner feed with roll clearances between 0.005 and 0.018 inches.

TABLE XIX

SUMMARY OF RESULTS OF ROLL CRUSHER TESTS

	Roll Clearance, in.		Roll	Feed	Product Size		
	Thickness	Crushed(b)	Speed,	Rate,	MMPD,	+ 35 U. S. Mesh,	Unbroken(b),
Run No.	Gauge	Solder	rpm	grams/min	inch	wt%	wt%
1	0.002		100	130	0.00639	0.63	
2	0.008		100	130	0.00813	0.74	
3	0.012		100	130	0.01049	0.37	
4	0.018		100	130	0.01530	14.68	
5	0.024		100	130	0.02054	90.61	
6(a)	0.0012		20	130	---	---	
7	0.0012		40	130	0.01027	0.12	
8	0.0012		80	130	0.00958	0.13	
9	0.0012		120	130	0.00899	0.00	
10	0.0012		140	130	0.00873	0.00	
11	0.0012		180	130	0.00837	0.00	
12	0.0012		100	50	0.00959	0.10	
13	0.0012		100	80	0.00943	0.13	
14	0.0012		100	160	0.00886	0.12	
15	0.0012		100	190	0.00908	0.25	
16	0.0012		100	225	0.00912	0.38	
17	0.0012		100	130	0.00821	0.10	
18	0.0012		100	50	0.00923	0.00	
19	0.0012		100	80	0.00853	0.00	
20	0.0012		100	160	0.00866	0.00	
21	0.0012		100	190	0.00845	0.00	
22	0.0012		100	225	0.01053	0.13	

TABLE XIX (cont.)

SUMMARY OF RESULTS OF ROLL CRUSHER TESTS

Run No.	Roll Clearance, in. Thickness Gauge	Roll Clearance, in. Crushed(b) Solder	Roll Speed, rpm	Feed Rate grams/min	Product Size MMPD, inch	Product Size + 35 U. S. Mesh, wt%	Product Size Unbroken(b) wt%
23(a)	0.011	0.015	20	---	---	---	---
23(a)	0.011	0.015	20	---	---	---	---
24	0.011	0.015	40	176	0.0114	0.34	0.10
25	0.011	0.015	60	375	0.0116	0.20	0.12
26	0.011	0.015	80	546	0.0108	0.20	0.11
27	0.011	0.015	100	625	0.0108	0.24	0.10
28	0.006	0.010	40	74	0.0072	0.10	0.02
29	0.008	0.012	40	75	0.0080	0.10	0.02
30	0.010	0.014	40	78	0.0083	0.10	0.04
31	0.011	0.015	40	75	0.0092	0.10	0.03
32	0.013	0.016	40	76	0.0106	0.16	0.02
33	0.014	0.017	40	73	0.0124	0.40	0.24
34	0.015	0.018	40	74	0.0134	0.51	0.37
35	0.016	0.019	40	77	0.0142	1.42	0.76
36	0.017	0.020	40	75	0.0152	1.83	0.89
38	0.018	0.021	40	77	0.0175	40.54	7.78
39	0.019	0.022	40	71	0.0178	45.51	10.44
40	0.020	0.023	40	73	0.0187	56.62	36.04

(a) The crusher drive did not have sufficient power at 20 rpm and the crusher stalled.

(b) This data not taken for Runs 1-22.

(3) As long as the roll clearance is less than any of the particle diameters, the amount of whole particles in the product is insignificant.

(4) The 4-inch diameter roll crusher will accept particles as large as 0.050 inches in diameter.

(5) The roll speed has only a slight effect on product size.

(6) The feed rate does not appreciably affect the crushed product size.

V. SECONDARY BURNING

Secondary burning studies consisted of heat transfer calculations for the secondary burner and a series of parametric experiments for defining secondary burner operating requirements. In-vessel, above-bed sintered metal filters are acceptable for secondary burning because of the low throughput rates required relative to those for primary burning and the different inherent characteristics of the solids being processed.

1. Heat Transfer Calculations

Heat transfer calculations were made to determine the bed diameter and height required for the secondary burner to insure removal of heat equivalent to processing the following:

1. Fertile particle fraction without unburned graphite (16.2 kilograms per day of pyrolytic carbon, 1.75 kilograms per day of uranium carbide, and 75 kilograms per day of thorium carbide).
2. Fertile particle fraction and graphite consisting of 15% of the combined fissile and fertile particles, (243 kg x .15 = 36 kg/day unburned graphite).
3. Fertile particle fraction, graphite consisting of 15% of the combined fissile and fertile fractions, and primary burner graphite fines (35% of primary burner feed - 400 kg fines).
4. Fissile particles without unburned graphite (33 kilograms per day of pyrolytic carbon, 4.9 kilograms per day of uranium carbide, and 48.5 kilograms per day of thorium carbide).

Bases of Heat Transfer Calculations

Bases of the secondary burner heat transfer calculations were:

1) Inside diameter of burner ranged from 5 inches to 10 inches.
2) Longitudinal and rectangular fins (1-inch high and 1/4-inch wide).
3) Fluid-bed side heat transfer coefficient of 100 Btu/hr-ft^2-^{o}F.
4) Bed temperature of 1606 ^{o}F (875^{o}C).
5) Shroud inlet cooling air temperature of 70^{o}F. Shroud outlet cooling air temperature of 300^{o}F.
6) Thermal conductivity of vessel wall of 12 Btu/hr-ft^2-^{o}F (Hastelloy X).

7) Vessel wall thickness of 0.5-inch.
8) Heat capacity of the off-gas is 0.3 Btu/lb-^{o}F.
9) The superficial velocity of the fluidizing gas is 0.85 ft/sec.
10) The heats of combustion for graphite (including pyrolytic carbon), thorium carbide, and uranium carbide are 13,600, 6870, and 5300 Btu/lb, respectively.
11) Heat transfer coefficients from bare outside walls to shroud air is 22 Btu/hr-ft^{2}-^{o}F.
12) Feed rate to secondary burner previously specified.
13) Mode of operation was batchwise.
14) Bulk density of the solids is 2.11 g/cc.
15) Period of operation per batch was varied from 2 to 6 hours.
16) Density of the off-gas is 0.0303 lb/ft^{3}.

Nomenclature

A_{fo} = Outside finned area, ft^{2}.

A_{m} = Mean area of vessel wall, ft^{2}.

A_{o} = Area of outside wall between fins, ft^{2}.

A_{wi} = Area of inside heat transfer surface, ft^{2}.

A_{wo} = Area of outside bare tube, ft^{2}.

h_{i} = Inside heat transfer coefficient, Btu/hr-ft^{2}-^{o}F.

h_{o} = Outside heat transfer coefficient, Btu/hr-ft^{2}-^{o}F.

H_{o} = Fin height of shroud side fins, inches.

k = Thermal conductivity of metal, Btu/hr-ft-^{o}F.

q = Heat transfer rate, Btu/hr.

T_{a} = Average air temperature in shroud area, ^{o}F.

T_{ai} = Inlet shroud air, ^{o}F.

T_{ae} = Outlet shroud air, ^{o}F.

T_{b} = Temperature of bed, ^{o}F.

T_{wi} = Inside burner wall temperature, ^{o}F.

T_{wo} = Temperature at base of fins, along outside wall, ^{o}F.

$(\Delta T)_{lm}$ = Log mean temperature between fluid bed and shroud cooling air, ^{o}F.

U_o = Overall heat transfer coefficient based on A_{wo}, Btu/hr-ft^2-^{o}F.

X = Burner wall thickness, feet.

y_o = Fin thickness, inches.

ϕ = Fin efficiency, dimensionless.

Major Assumptions

Major assumptions were:

1. Batchwise operation during burning (3 batches per day).
2. Outside heat transfer coefficients are constant.
3. Constant metal wall thermal conductivity.
4. Radiation is neglected.
5. Bulk density is constant.
6. Increase in bed height due to fluidization is 20 percent.

Principal Equations Used in the Calculation

This section describes the equations used to calculate the rate of heat transfer through the secondary burner vessel wall. The equations presented are for a burner wall having external fins.

The inside wall temperature was based on heat transfer by convection from the bed to the inside wall (equation 1). The outside wall temperature was based on conduction through the vessel wall (equation 2). The heat dissipated by convection from the outside finned surface to the shroud air is given in equation (3).

$$T_b - T_{wi} = \frac{q}{A_{wi} h_i} \qquad (1)$$

$$T_{wi} - T_{wo} = \frac{qX}{kA_m} \qquad (2)$$

$$T_{wo} - T_a = \frac{q}{h_o (A_o + A_{fo} \phi)} \qquad (3)$$

The amount of heat dissipated through the vessel wall to the shroud cooling air can be calculated from equation (4) if U_o is known.

$$q = U_o A_{wo} (\Delta T)_{lm} \qquad (4)$$

Equations (1) through (4) were combined to give the overall heat transfer coefficient shown in equation (5),

$$\frac{1}{U_o A_{wo}} = \frac{1}{A_{wi} h_i} + \frac{X}{k A_m} + \frac{1}{h_o (A_o + \phi A_{fo})} \qquad (5)$$

Fin efficiency was obtained from equation (6).

$$\phi = \frac{\text{Tanh } mH_o}{mH_o} \qquad (6)$$

Where $m = \left[\frac{(h_o)}{k \quad yo}\right]^{1/2}$

Results

Figures 16 through 19 show the results of the heat transfer calculations for the secondary burner. Figure 16 shows the results of heat transfer calculations for batch burning of fertile particles without unburned graphite. Figure 16 is based on an inside wall coefficient of 100 Btu/hr-ft^2-^{o}F. The corresponding fluidized-bed height is also shown in the figure for the calculated data points. Figure 17 shows the heat transfer results when graphite (36 kilograms per day) is included in the secondary burner fertile particle feed. Figure 18 shows the burner dimensions required if the crushed fissile particles are burned in the secondary burner. Figure 19 shows the heat transfer requirements if unburned graphite (36 kilograms per day) and primary burner graphite fines

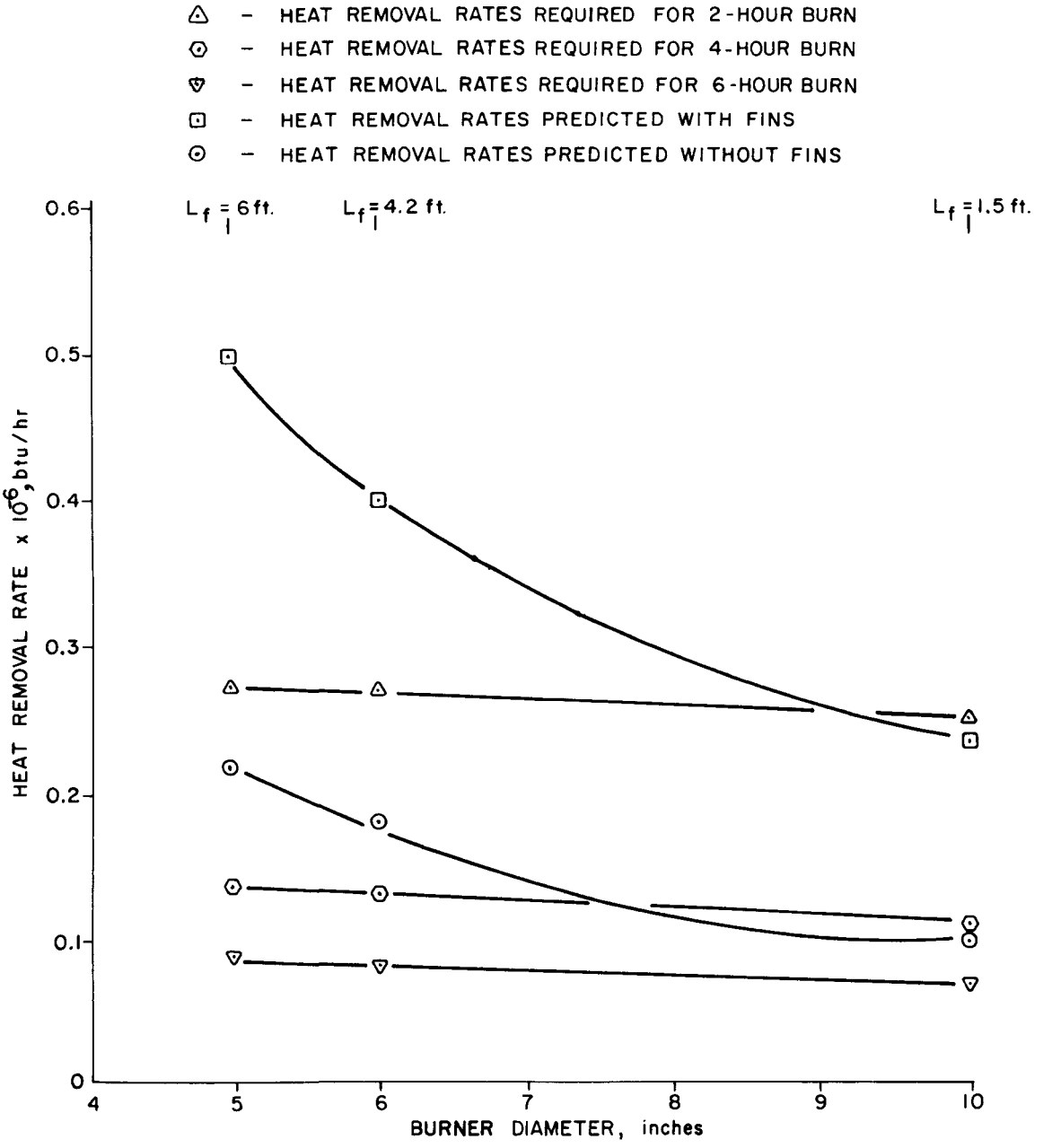

Figure 16. Required and Predicted Heat Removal Rates for Batch Secondary Burning of Crushed Fertile Particles

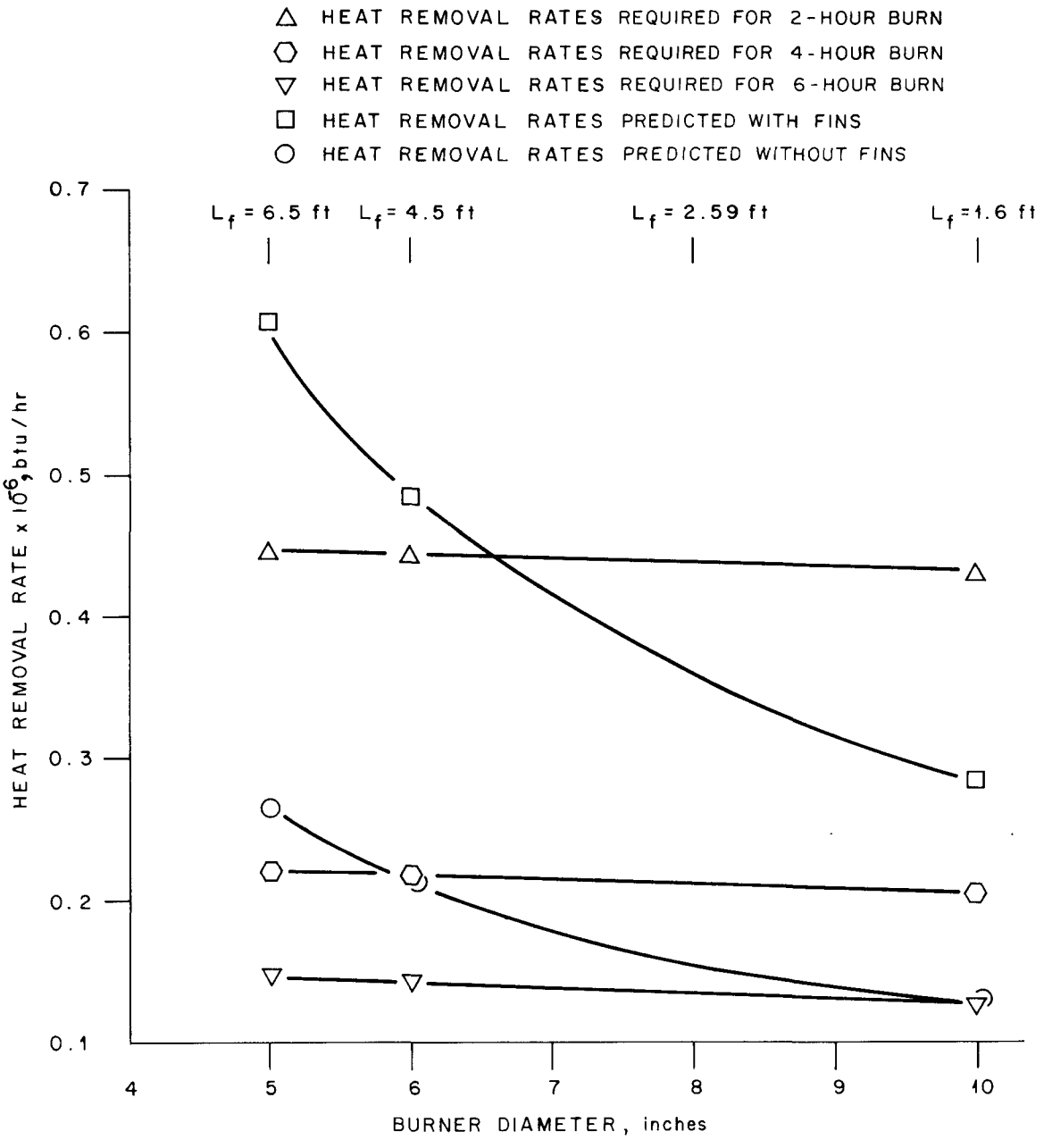

Figure 17. Required and Predicted Heat Removal Rates for Batch Burning of Crushed Fertile Particles and Unburned Graphite

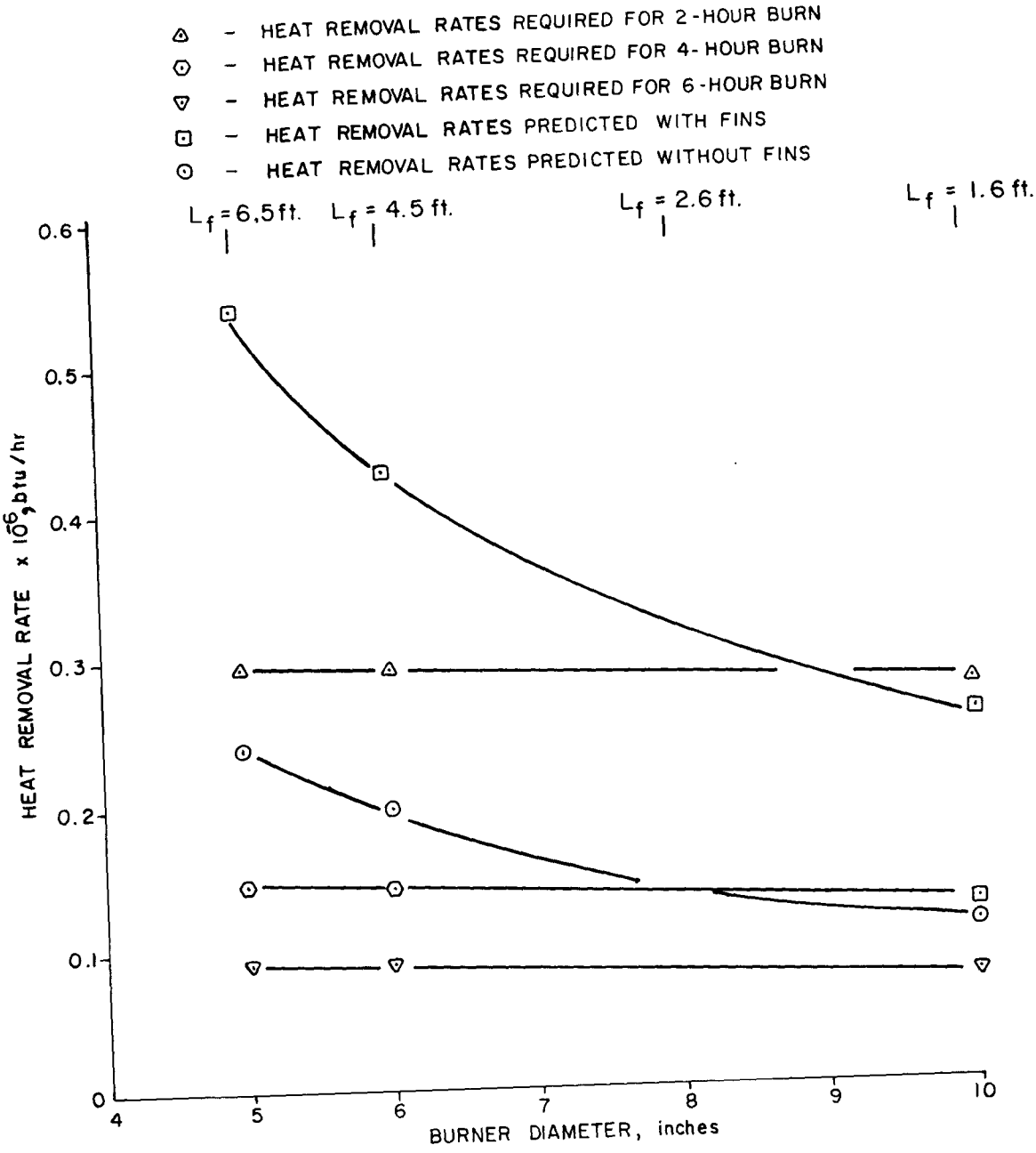

Figure 18. Required and Predicted Heat Removal Rates for Batch Secondary Burning of Crushed Fissile Particles

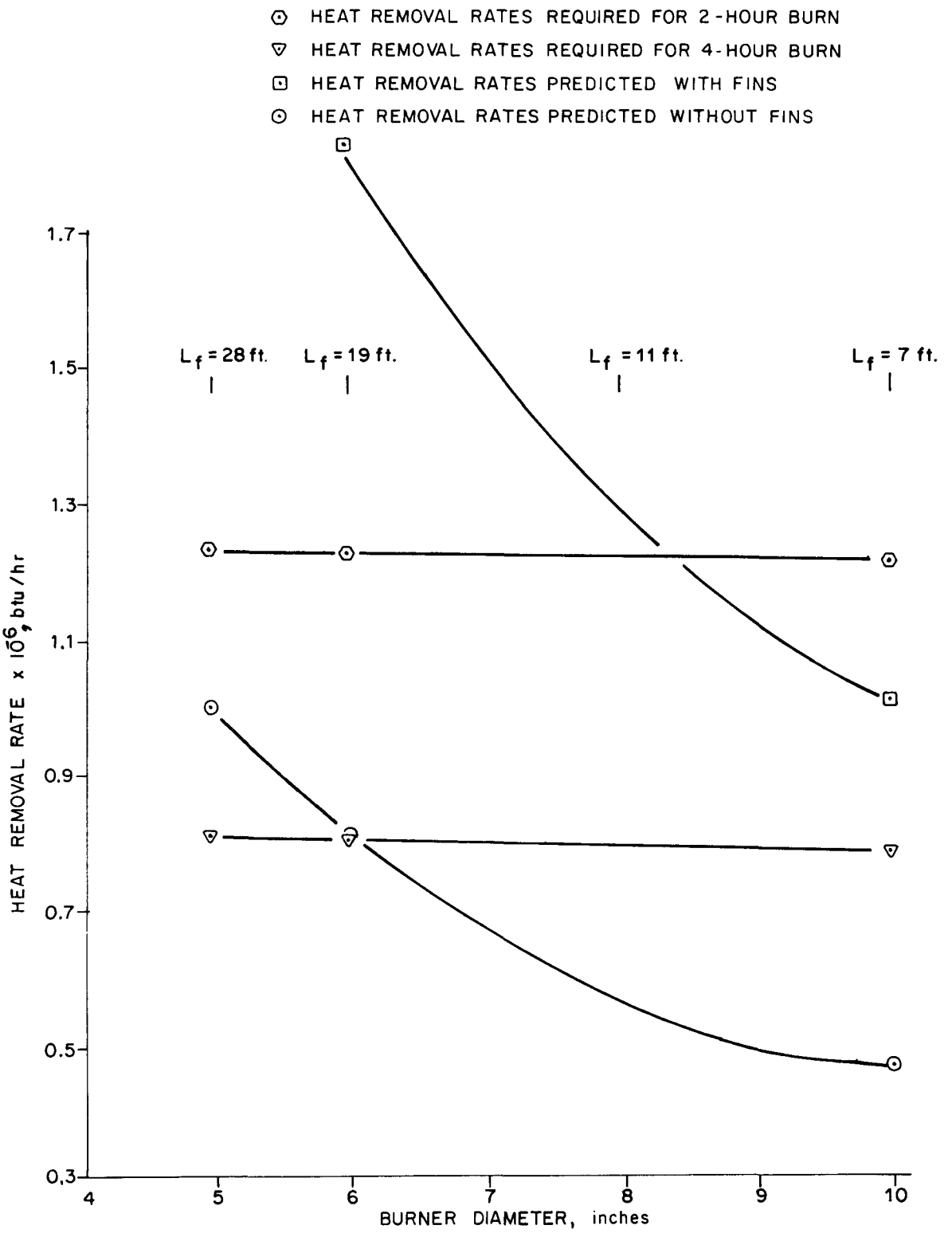

Figure 19. Required and Predicted Heat Removal Rates for Batch Burning of Crushed Fertile Particles, Unburned Graphite, and Graphite Fines

(400 kilograms per day) are included in the fertile particle batch feed to the secondary burner.

The fin efficiency calculated from equation (6) was 0.76 for the fin configuration of 1-inch high and 1/4-inch thick with a spacing of 1/4-inch.

Based on the calculations it was concluded that:

1) External fins are not required if a four-hour combustion period and a six-inch diameter burner are used.
2) A four-hour burn period is adequate for an 8-inch diameter burner having external fins.

2. Experimental Parametric Study

A parametric study consisting of 12 experiments was made in which crushed fertile particles were burned in the 2-inch diameter pilot-plant secondary burner. The objectives of the testing were to determine the operability of the secondary burner for burning crushed fertile particles and to determine the operating conditions that insure burner filter integrity and prevent bed sintering.

Description of Equipment

The secondary burner used to obtain the parametric data is shown schematically in Figure 20. The burner system consisted of a burner vessel, in-vessel filter system, and heating and cooling systems. The burner vessel was 2 inches in diameter, 26-inches high, and constructed of Hastelloy-X, and the 4-inch disengaging section contained an in-vessel sintered metal filter used to remove particles from the off-gas and to provide a means of recycling fines to the bed. A vibrator was provided to assist in dislodging fines from the burner walls and in-vessel filters.

The burner wall was cooled by passing cooling air through a shroud surrounding the burner vessel. Start-up and supplemental heat was provided by eight 2000 watt Calrod heaters located in the annulus surrounding the burner wall. Analyzers were provided for continuously monitoring CO, CO_2, and O_2 in the burner off-gas.

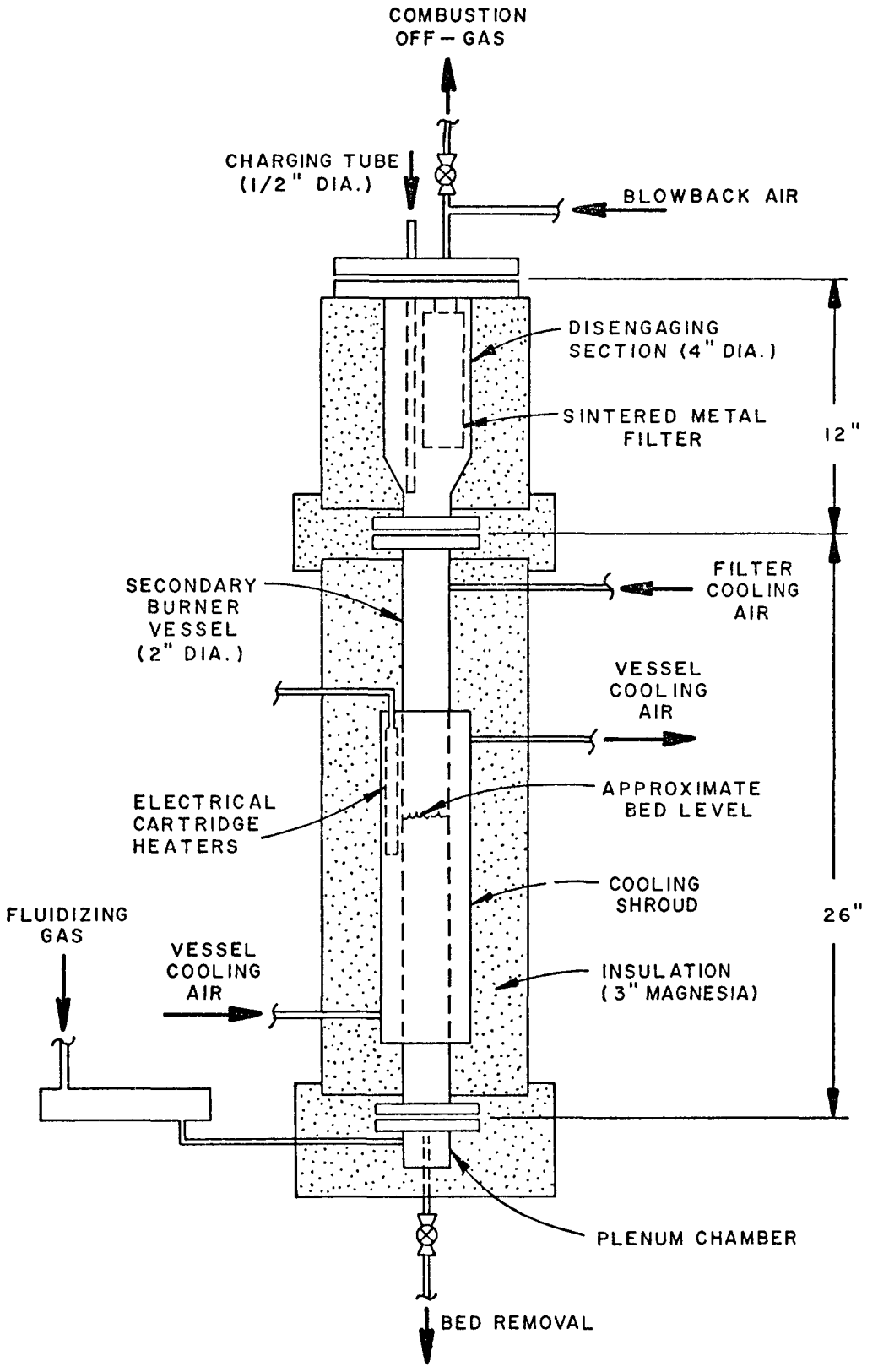

Figure 20. Schematic Diagram of Pilot-Plant Secondary Burner

Specific Test Objectives

The specific test objectives associated with secondary burning of crushed fertile particles were as follows:

1. Reduce dissolver feed to less than 2 percent combustibles at rates equivalent to processing 12 Ft. St. Vrain blocks per day.
2. Establish the fluidizing velocities, oxygen concentrations in the off-gas, bed-to-filter freeboard, bed L/D's and filter face velocities that prevent in-vessel filter failure.
3. Establish the oxygen concentrations in fluidizing gas, fluidizing velocities, bed L/D's and bed temperatures that prevent bed sintering.
4. Determine the required burn rate to process 12 blocks per day with 3 batches per day to prevent bed sintering and filter failure.

Experimental Burner Tests

The operating parameters studied are summarized in Table XX. Fluidizing velocity, bed size, bed temperature, gas compositions, and particles sizes were the principal independent variables studied.

The feed (bed material) used during the testing was product from the 4-inch diameter primary burner that had been air classified and processed in either a roll-crusher or jet breaker. Feed for Runs S-20 through S-25, and S-27 through S-30 was fertile particles crushed at a roll crusher gap setting of 0.014 inch. The fertile particles for Runs S-26 and S-31 were crushed by the roll crusher at gap settings of 0.006-inch and 0.01-inch, respectively. The feed for Run S-32 was processed in a jet breaker.

The filter surface area was 0.23 ft^2 during Runs S-20 through S-23, and for Runs S-24 through S-34 a filter surface area of 0.18 ft^2 was used. Both filters were 5 micron mean pore sizes (grade H).

Two distributor plates were used in the parametric study, one of stainless steel and the other of Incoloy 825. Both plates were 1/16 inches thick with 25 holes, 0.033 inches in diameter.

TABLE XX

SUMMARY OF EXPERIMENTS USING SECONDARY BURNER WITH IN-VESSEL FILTERS.

Run No.	Fluidizing Velocity (ft/sec)	Bed Weight (grams/batch)	Fertile Particles in Feed (%)	Initial Combustibles (%)	Bed Temperature (^{o}C)	Fluidizing Gas Composition Ratios	Feed MMP Mass Mean Particle Diameter)(inches)	L/D Static
S-20	1.5	600	95.9	12.4	800	50 O_2/50 air	0.0096	3.55
S-21	1.5	600	95.9	12.4	750	50 O_2/50 air	0.0096	3.55
S-22	1.5	600	95.9	12.4	900	50 O_2/50 air	0.0096	3.55
S-23	2.5	600	95.9	12.4	900	50 O_2/50 air	0.0096	3.55
S-24	1.5	600	95.9	18.05	900	50 O_2/50 air	0.0097	3.55
S-25	1.5	600	95.9	18.95	900	70 O_2/30 air	0.0097	3.55
S-26	1.5	600	95.9	16.3	900	50 O_2/50 air	0.0075	3.5
S-27,S-28	1.5	600	88.4	16.6 to 16.9	900	80 O_2/20 air	0.010	3.4
S-29	1.5	600	88.4	16.1	900	Pine O_2	0.010	3.4
S-30	1.5	1000	88.4	18.35	900	50 O_2/50 air	0.010	5.7
S-31	1.5	600	88.4	-	900	50 O_2/50 air	0.008	3.5
S-32	1.5	600	88.4	18.0	900	50 O_2/50 air	0.010	2.8

Experimental Results

Operating data resulting from the 12 parametric secondary burner tests are summarized in Table XXI. Nineteen burner "checkout" runs were made previous to the parametric study to test the operability of the burner and to provide a basis for selecting operating levels of variables for the parametric study.

Data were obtained regarding burn rates, combustible content of product ash, filter integrity, bed sintering tendencies, distributor plate integrity, particle size distribution, and off-gas composition.

Burn Rates

The calculated burn rates attained during the main combustion period based on off-gas analysis (CO and CO_2, and O_2) are shown in Table XXI. Burn rates increased with increasing oxygen concentrations in the fluidizing gas and with increasing fluidizing velocities. The burn rates based on oxygen concentrations reported include oxygen in the purge air. The purge gases accounted for approximately 15% of the total fluidizing gas.

Combustible Content of the Burner Feed and Ash

The combustible content of the burner feed ranged from 12 to 19 percent and averaged 16 percent (Table XXI). The combustible content was based on results obtained when two samples of feed were held at $900^{o}C$ in a furnace for 24-hours.

The maximum filter temperature, pressure drop, and face velocities across the in-vessel filter during the main combustion period are shown in Table XXII. The filter temperature was measured by a thermocouple placed in contact with the outside wall of the in-vessel filter, 2.75 inches above the bottom of the filter.

TABLE XXI

SUMMARY OF OPERATING DATA RESULTING FROM TWELVE SECONDARY BURNER EXPERIMENTS

Run No.	Main Combustion Period (min)	Initial Percent Combustibles	Percent Combustibles Left in Bed	Fluidizing Gas velocity (ft/sec)	Burn Rate Based on CO and CO_2 (kg C/hr-ft^2)	Burn Rate Based on Inlet O_2 (kg C/hr-ft^2)
S-20	13.1	12.4	1.94	1.5	11.8	13.6
S-21	14.1	-	2.21	1.5	12.9	13.9
S-22	12.9	12.4	1.67	1.5	12.4	12.3
S-23	9.4	12.4	1.54	2.5	17.5	18.9
S-24[a]	18	18.1	1.5	1.5	13.1	11.5
S-25[b]	11.1	19.0	1.04	1.5	15.9	15.9
S-26	13.1	16.3	6.38	1.5	14.4	13.1
S-27	-	16.6	-	1.5	-	-
S-28[c]	11.3	16.9	0.74	1.5	15.5	17.0
S-29[d]	-	16.1	-	1.5	-	-
S-30	15.0	18.4	4.38	1.5	13.1	12.8
S-31	15.2	17.5	0.635	1.5	13.1	12.1
S-32	10.1	18.0	0.98	1.5	12.3	12.8

a. Longer "burn-out" period used (1 hour instead of 30 min.), and smaller in-vessel filter used (filter area is 0.18 sq. ft.).

b. Vibrator added to bottom of burner to aid in recycling fines to bed during "burn-out" period.

c. Filter plugged as a result of adding fluidizing nitrogen to quench above bed burning.

d. Bed sintered, and distributor plate was damaged.

TABLE XXII

SUMMARY OF IN-VESSEL FILTER OPERATING DATA RESULTING FROM TWELVE SECONDARY BURNER EXPERIMENTS

Run No.	Maximum Filter Temperature (^{o}C)	Filter ΔP During Main Burn (psig)	Face Velocity During Main Burn (scfm/ft^{2})
S-20	345	0.5	4.47 to 6.10
S-21	264	1.7 to 2.3	5.59 to 4.72
S-22	474	0.9 to 1.2	4.09 to 6.79
S-23	615	1.1	5.4 to 10.7 to 19.6
S-24	276	0.8 to 1.5	4.92 to 6.38
S-25	315	1.2 to 1.8	5.27 to 7.11
S-26	275	1.1 to 1.7	5.13 to 6.58
S-27	258	Filter Plugged	--
S-28	359	0.5 to 1.0	5.68 to 7.60
S-29	170	--	--
S-30	330	1.2 to 2.2	5.03 to 7.22
S-31	393	0.8 to 1.3	5.47 to 7.97
S-32	260	1.2 to 1.3	6.38

In all cases in which nitrogen cooling was used the oxygen concentration in the off-gas was allowed to reach 23% or greater before the fluidizing velocity was reduced to 0.5 ft/sec. Nitrogen cooling gas was used only if the filter temperature exceeded 500°C.

Particle size distribution of the crushed fertile feed did not appear to affect the pressure drop across the in-vessel filters. Particulates removed from the filter after Runs S-28 through S-32 were placed in a furnace at 900°C for 24 hours. The resulting average weight change per filter was nine percent.

Bed Sintering

Significant bed sintering occurred during Runs S-29 and S-30. During Run S-29 the bed was fluidized at about 1.5 ft/sec and the oxygen concentration entering the burner through the distributor plate was 92 percent (includes 7.4 percent nitrogen entering with the purge air). After burning at this gas concentration and fluidizing velocity for about 6 minutes, the bed temperature suddenly increased to 1070°C before the bed could be cooled with fluidizing nitrogen. Removal of the burner lower plenum disclosed extensive bed sintering and damage to the Incoloy distributor plate.

Run S-30 was conducted using a 1000 gram bed and the burner was fluidized at 1.5 ft/sec during the combustion period. The maximum temperature (950°C) in the bed was reached after the fluidizing velocity was reduced. After the run, several agglomerates were recovered from the final bed.

The operating conditions used during Runs S-29 and S-30 are indicative of conditions that must be avoided during plant operations to prevent bed sintering. They also partially define limits of allowable operating ranges.

Distributor Plate Performance

The pressure drop performance of the distributor plates is summarized in Table XXIII. The pressure differentials provide a basis for scaling distributor plate design.

Particle Size Distribution

The particle size distributions for crushed-fertile-particle burner feed and fertile particle ash are shown in Figures 21 and 22, respectively. All feed was burned to less than 2 percent combustibles, except for burner feed crushed at a gap setting of 0.006. The resulting mass mean particle diameter of all burner product batches is shown in Table XXIV. The particle size distribution data provide a basis for defining particle size distributions acceptable for processing in a larger scale secondary burner.

TABLE XXIII

DISTRIBUTOR PLATE AND BED ΔP HISTORY

Run No.	ΔP-Startup (inches of H_2O	ΔP-Preburn (inches of H_2O)	ΔP-Main Burn (inches of H_2O)	ΔP-Burn Out (inches of H_2O)
S-20	25 to 30	20 to 25	31	8
S-21	35 to 21	18 to 21	27	12
S-22	23 to 18	18	23	10
S-23	24 to 20	18	28 to 26.5	12
S-24	18 to 13	14	17 to 13	9 to 8
S-25	16 to 12	14	15 to 12	6
S-26	16 to 12	14	16 to 13	6
S-28	17 to 12	15	15 to 14	10 to 8
S-29[a]	16 to 10	14	13	-
S-30[b]	20 to 23	20 to 21	25 to 22	11 to 10
S-31	13 to 11	-	12 to 15 to 11	7 to 8
S-32	12	-	10	-

a. Bed sintered with damage distributor plate.

b. New distributor plate.

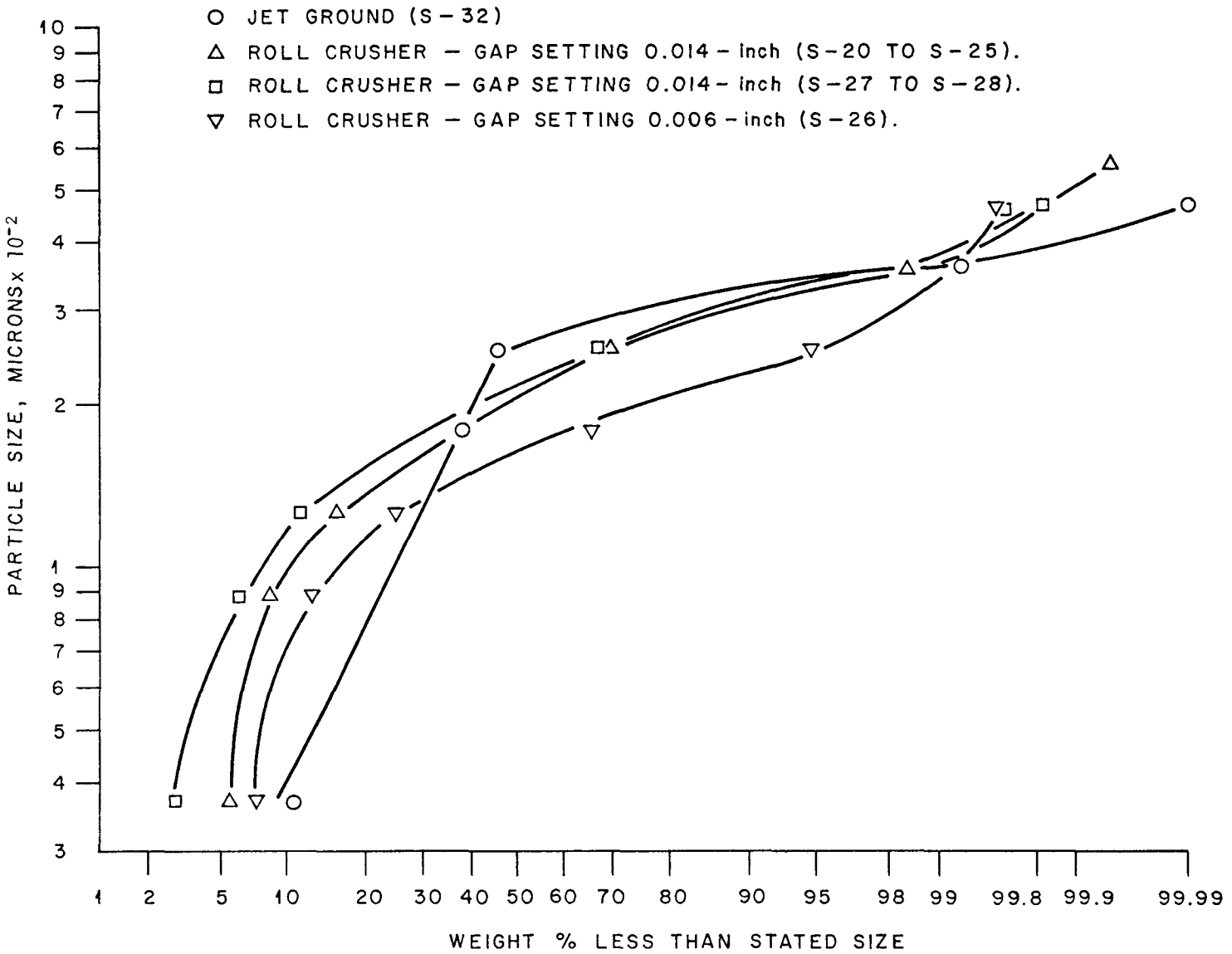

Figure 21. Particle Size Distribution of 2-Inch Pilot Plant Secondary Burner Feed

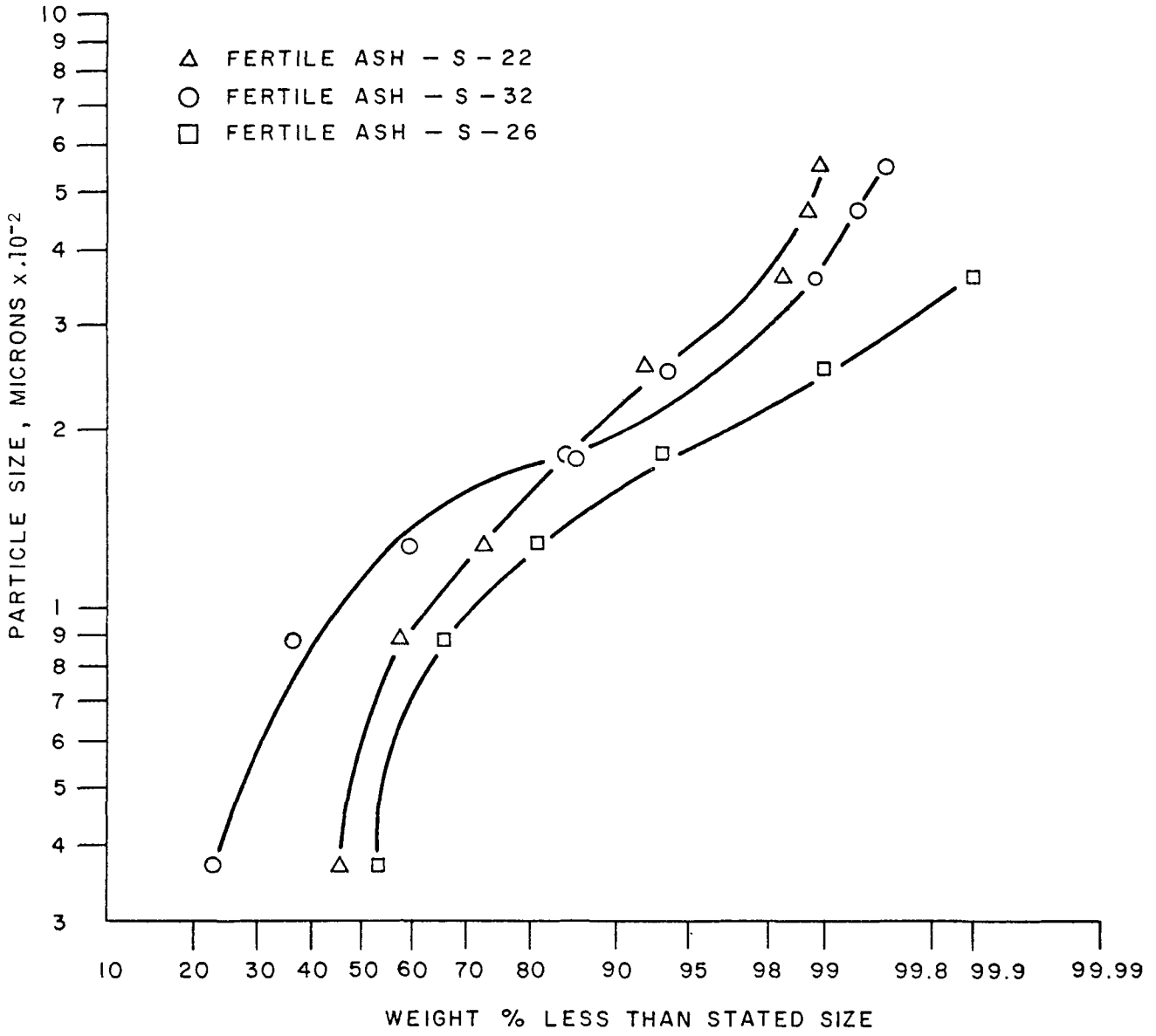

Figure 22. Particle Size Distribution of 2-Inch Pilot Plant Secondary Burner Product Ash

TABLE XXIV

MASS MEAN PARTICLE SIZE OF BURNER PRODUCT

Run No.	Mass Mean Particle Size (microns)
S-20	0.0047
S-21	0.0061
S-22	0.0051
S-23	0.0054
S-24	0.0055
S-25	0.0052
S-26	0.0042
S-28	0.0059
S-30	-
S-31	-
S-32	0.0059

Off-Gas Analysis

The off-gas analyses for the secondary burner tests are summarized in Table XXV. The average oxygen, carbon monoxide, carbon dioxide, and calculated nitrogen concentrations are shown. The ranges of the gas concentrations in the off-gas during the combustion and burn-out periods are also given in the Table. The data provides a basis for designing and operating a scaled-up burner.

Fluidized Bed L/D Ratios

The results of tests showing the effect of fluidizing velocity on bed L/D ratios for crushed fertile particles are given in Table XXVI. The L/D ratio doubled when the fluidizing velocity was increased from static conditions to 1.5 ft/sec. Based on these results the calculated filter-to-bed freeboard for a 600 gram-bed at 1.5 ft/sec and 1000 grams-bed at 1.5 ft/sec would be about 1.3 and 0.6 ft., respectively. For a fluidizing velocity of 2.5 ft/sec, the fluidized L/D for a 600 gram bed gives a filter-to-bed freeboard of about 0.4 ft.

Burner Operating Conditions and Burn Rates

The burner operating conditions that will produce a given experimentally verified burn rate are summarized in Table XXVII. Data are provided for both 6- and 8-inch diameter burners and for 2 and 3 batch cycles per day. The required burn rate based on a three-batch per day processing cycle for an 8-inch diameter burner using a 4-hour combustion period is 14.2 kgC/hr-ft^2. This appears to be the most likely operating conditon for the plant burner. The burn rates reported are based on processing 12 Ft. St. Vrain fuel blocks per day.

TABLE XXVI

FLUIDIZED BED L/D RATIOS BASED ON EXPERIMENTS CONDUCTED USING A Quartz-Glass BURNER

Bed Weight (grams)	Static L/D Ratio	Fluidizing Velocity (ft/sec)	Fluidized L/D Ratio
1400	4.35	1	6.09
1400	4.35	1.5	9.14

TABLE XXV

OFF-GAS ANALYSIS FOR SECONDARY PILOT PLANT BURNER

Run No.	Average % During Main Combustion				Percent Total	Percent Range During Main Combustion		Percent Range During Burn Out		
	CO	CO_2	O_2	N_2		CO	CO_2	CO	CO_2	O_2
S-20	5.1	43.84	1.0	45.9	95.44	8.2 to 2.75	36 to 43	2.8 to 0.1	63 to 0	3 to 82
S-21	4.1	46.77	0	45.2	96.08	8.2 to 0.5	42 to 49	1.0 to 0.1	65 to 1	2 to 78
S-22	6.79	47.94	0	44.5	99.23	8.0 to 6.5 to 9.3	45 to 50	10< to 0	51.1 to 0	2 to 81
S-23	8.8	44.9	0	42.0	95.7	9.05 to 10<	46.5 to 31	8.5 to 0	20 to 0	5 to 77
S-24	5.16	51.5	0.5	44.5	101.7	7.6 to 0.6	48 to 53.25	1.2 to 9	63.75 to 60	5 to 76
S-25	6.89	59.29	1.1	32.5	99.78	9.5 to 0.2	54 to 62.25	1.2 to 0	65 to 0	5 to 80
S-26	6.51	52.50	1.0	45.47	105.43	10 to 0.2	43.5 to 52.5	0.2 to 0	60 to 2	5 to 81
S-27	6.22	60.0	1.0	26.23	93.45	9.5 to 0.5	58 to 61	0.5 to 0	0.5 to 0	64to0to8
S-30	7.54	46.95	1.5	45.4	101.39	8.8 to 5.34	45 to 51	10< to 0	58to63to0	5 to 79
S-31	4.92	50.68	3.0	45.4	104.0	9.58 to 0.28	45 to 54	0.28 to 0	64 to 0	-
S-32	4.05	48.64	2.0	45.4	100.09	10< to 0.6	41.5 to 53.25	1.2 to 0	64 to 0	-

TABLE XXVII

SECONDARY BURNER OPERATING CONDITIONS AND BURN RATES REQUIRED FOR PROCESSING 12 FT. ST. VRAIN FUEL BLOCKS PER DAY

Experimental Burn Rate ($kgC/hr-ft^2$)	Fluidizing Velocity (ft/sec)	Oxygen Concentration in Total Gas Entering Burner (%)	O_2 Concentration In Fluidizing Gas(%)	Required Combustion period(hr)	Burner Diameter (inches)
Three batches per day:					
13.1	1.5	55.5	62.5	4.3	8
15.9	1.5	67.7	77	6.6	6
15.9	1.5	67.7	77	3.6	8
17.0	1.5	73.8	85	5.9	6
17.0	1.5	59	85	3.3	8
18.9	2.5	59	62.5	5.3	6
18.9	2.5	59	62.5	3.0	8
23.5	3.0[a]	58	62.5	4.3	6
23.5	3.0[a]	58	62.5	2.4	8
Two batches per day:					
18.9	2.5	59	62.5	6.0	8
23.5	3.0[a]	58	62.5	8.6	6
23.5	3.0[a]	58	62.5	4.8	8

a - Based on burner "check-out" runs.

Experimental Procedure

The following experimental procedure was used:

1. Fluidization was initiated at 1.0 to 1.5 ft/sec, and power to the Calrod heaters was activated.

2. When the bed temperature reached 400°C, the fluidizing gas was switched from air to oxygen.

3. The power to the Calrod heaters was switched off when the bed temperature reached 700 to 800°C.

4. When the bed temperature was within 50° of the desired operating temperature for the main combustion period, the fluidizing gas was switched from oxygen to the pre-designated oxygen-air mixture.

5. At the end of the main combustion period (determined by bed temperature dropping and oxygen concentration in the off-gas increasing) pure oxygen was reintroduced as the fluidizing gas and the fluidizing velocity was reduced to 0.5 ft/sec to maintain high burn rates.

6. During the "burn-out" period (residual carbon is burned from the bed), the bed temperature was held at 900°C by the Calrod heaters for 30 minutes or until the burn rate was about 0.04 gram of carbon per minute. The Calrod heaters were always used when the pure oxygen fluidizing gas could not maintain 750 to 820°C bed temperature and a 900°C temperature immediately above the bed.

Conclusions

1. Either a six or an eight-inch diameter burner has the required capacity for processing secondary burner feed corresponding to 12 Ft. St. Vrain fuel blocks per day.

2. Filter failure occurs at certain combinations of fluidizing velocity, oxygen concentration in the off-gas, bed-to-filter free-board, filter operating temperature, filter pressure drop, and bed particle size.

Based on the experimental data, filter failure in the 2-inch diameter pilot-plant burner will not occur during the "combustion" period if, simultaneously, the fluidizing velocity does not exceed 1.5 ft/sec., the oxygen concentration in the off-gas does not exceed 20%, the filter operating temperature does not exceed

500°C, a minimum of 1.3 feet of bed-to-filter freeboard is provided, the filter face velocity does not exceed 7 ft/min, and the filter pressure drop does not exceed 2 psig.

Filter failure during the "burnout" period will not occur if, simultaneously, the fluidizing velocity is 0.5 ft/sec, the filter operating temperature does not exceed 500°C, two feet of bed-to-filter freeboard is provided, the maximum filter face velocity does not exceed 7 ft/min., and the maximum filter ΔP does not exceed 2 psi.

Filter failure due to ignition of carbon on the filter occurred during the "combustion" period when, simultaneously, the fluidizing velocity was 2.5 ft/sec, 0_2 concentration in the off-gas was greater than 15%, the filter operating temperature was 700°C, and filter-to-bed freeboard was 0.4 ft.

3. Bed sintering occurs at certain combinations of fluidizing velocity, oxygen concentration in the fluidizing gas, bed L/D ratios and mean bed temperature. Based on the experimental data, bed sintering will not occur in the 2-inch diameter burner if, simultaneously, the fluidizing velocity is $\geq$ 1.5 ft/sec, oxygen concentration in the fluidizing gas is less than 80%, the fluidized bed L/D ratio is $7 \leq L/D \leq 8$, and the mean bed temperature is < 900°C.

Bed sintering occurred when, simultaneously, the fluidizing velocity was < 1.5 ft/sec, the oxygen concentration in the fluidizing gas was > 87%, the bed L/D ratio was 14, and the mean bed temperature was 900°C.

4. Recommended normal operating conditions for processing 12 Ft. St. Vrain fuel blocks per day in an 8-inch diameter burner on a 3-batch-per-day basis are:

RECOMMENDED NORMAL OPERATING CONDITIONS

	"Combustion" Period	"Burnout" Period
Fluidizing velocity, ft/sec.	1.5	0.5
0_2 concentration in off-gas, %	$\leq$ 15	$\leq$ 87%
Max, filter temperature, °C	500	500
Bed-to-Filter freeboard, ft	$\geq$ 2	$\geq$ 2
L/D Ratio (fluidized)	7	-
0_2 concentration in fluidizing gas %	$\leq$ 75	$\leq$ 87
Bed temperature, °C	875	875
Filter face velocity, ft/min.	$\leq$ 7	$\leq$ 7
Filter ΔP, psi	$\leq$ 1.5	$\leq$ 1.5

VI. AQUEOUS PROCESSING

Aqueous processing in support of Ft. St. Vrain reprocessing consists of laboratory development and pilot-plant testing of dissolution, solids-liquid separation, extraction feed adjustment, and solvent extraction techniques.

1. Dissolution

Laboratory scale tests were conducted to establish the corrosion rate of 304L stainless steel in contact with thorex solution (13 M HNO_3 - 0.05 M HF - 0.1 M $Al(NO_3)_3$). The results of the tests are summarized in Table XXVIII. As shown in the table, the amount of aluminum, boron, and fluoride was varied.

Results of the tests showed that the only solution less corrosive than the thorex solution was thorex solution with boron. All other combinations showed corrosion rates higher than for thorex solution, and in some cases, the corrosion rates were unacceptable ($\geq$ 5 mils/month).

TABLE XXVIII

CORROSION RATES ON 304L STAINLESS STEEL
SUBMERGED IN BOILING DISSOLVER SOLUTIONS FOR 96 HOURS

Solution	Corrosion Rate, mil/mo.
13 M HNO_3 - 0.05 M HF - 0.1 M Al $(NO_3)_3$ (Normal thorex solution)	1.55
13 M HNO_3 - 0.05 M HF	32.6
13 M HNO_3 - 0.05 M HF - 3.0 g/ℓB	2.81
13 M HNO_3 - 0.1 M HF - 3.0 g/ℓB	3.53
13 M HNO_3 - 0.05 M HF - 0.1 $Al(NO_3)_3$ - 1 g/ℓB	0.87
13 M HNO_3 - 0.0125 M HBF_4	9.3
13 M HNO_3 - 0.025 M HBF_4	20.5
13 M HNO_3 - 0.05 M HF 1 g/ℓB	4.44

2. Solids-Liquid Separation

Pilot-plant studies were made to determine the solids-liquid separation and subsequent solids washing efficiencies for processing simulated Ft. St. Vrain dissolver effluent in a continuous solid-bowl centrifuge. The studies were undertaken to provide a basis for acceptance of the continuous solid-bowl centrifuge as a method of solids-liquid separation and solids washing in the Ft. St. Vrain process.

Solid Bowl Centrifuge System Description

The continuous solid bowl centrifuge test system consisted of the following primary components (Figure 23): 1) a centrifuge complete with slurry feed inlet, in-bowl nozzles, in-bowl decontamination wash nozzles, solid and liquid effluent outlets, 2) a slurry feed tank equipped with provisions for air sparging to promote solid suspension, and 3) a feed line for slurry transport by gravity from the slurry feed tank to the centrifuge feed inlet.

The centrifuge used for the experimental testing was a 6-inch diameter continuous solid bowl centrifuge manufactured by Bird Machine Company. The bowl contour was a cylinder - 10^{o} cone combination having an inside diameter of 6 inches (at large end); the bowl was 12 inches long. The conveyor trunnion contained compartments for introducing feed and for dual wash. Wash nozzles distributed water on the inside surface of the bowl. Feed ports were used to distribute feed at the approximate junction of the cylinder and the 10^{o} cone.

Five decontamination wash nozzles were provided at the top of the bowl cover for rinsing the outside of the bowl. Solids were discharged vertically downward. All materials not coated with chromium oxide that were in contact with the dissolver effluent were constructed of 304 ELC, stainless steel. The centrifuge was driven by a 5 HP, 3460 RPM motor having a V-belt pulley drive.

The slurry feed tank was a 12-inch diameter cylinder having a 60^{o} conical bottom and 25 liter capacity. Sparge air at 100 psig was metered through the apex of the cone to maintain adequate solids suspension. A 3/4 inch ball valve located 2-1/2 inches below the air sparge line regulated feed addition to the centrifuge. A 90^{o}, 3/4 inch elbow located below the ball valve resulted in no solids plugging problems during slurry transport. A short length of 3/4 inch, 304 SS flexible metal hose served as the slurry feed line to the centrifuge. The apex of the slurry feed tank cone was approximately 15 inches above the centrifuge bowl centerline.

Simulated Ft. St. Vrain Feed Slurry and Sample Analysis

Ft. St. Vrain simulated feed slurry for solids-liquid separation testing consisted of pre-leached, silicon carbide, fertile-fuel-particle hulls suspended in 9.5 M nitric acid.

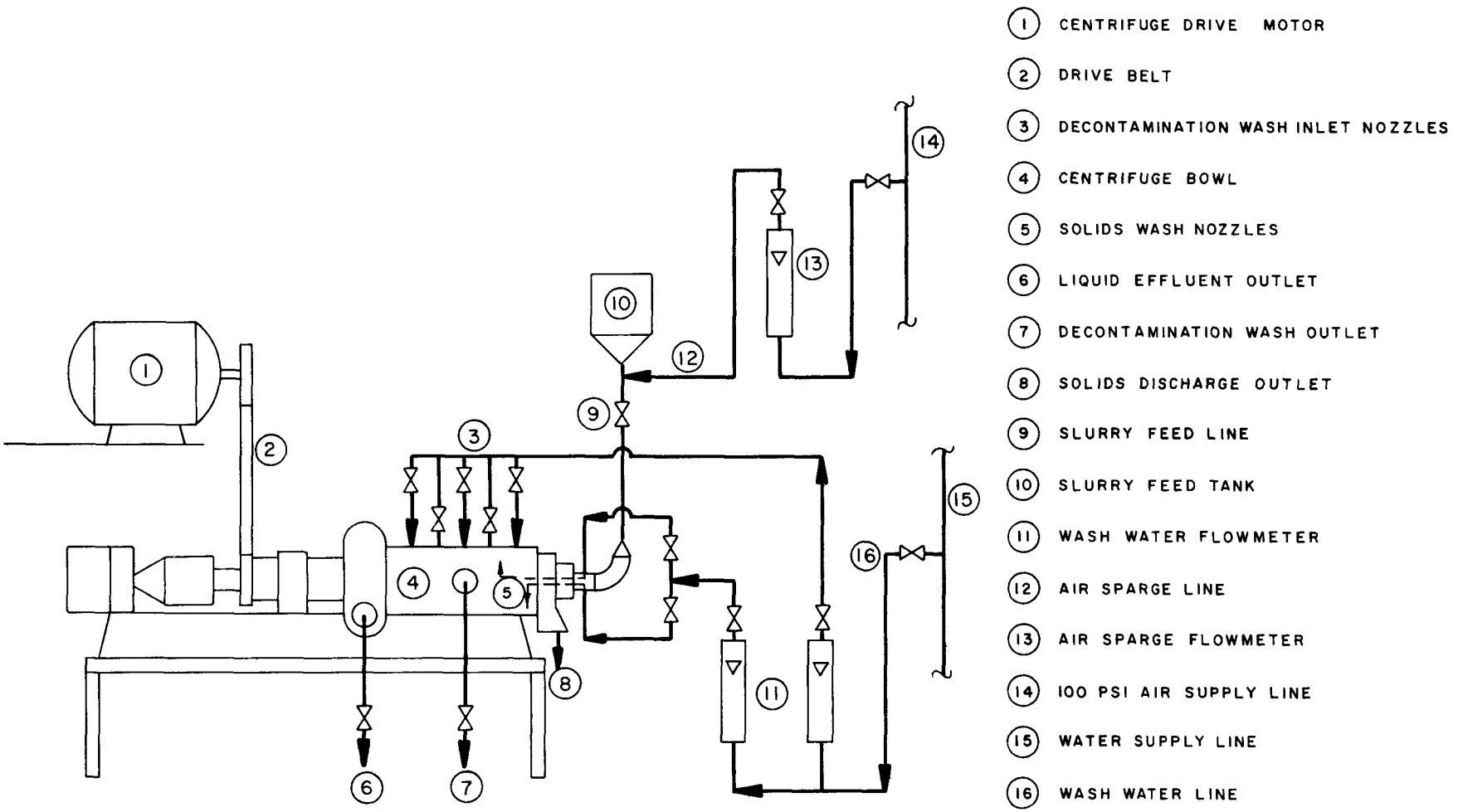

Figure 23. Solid Bowl Centrifuge Test System

Moisture analysis of the discharged solids involved drying and determining the loss in weight due to evaportion of occluded nitric acid.

Liquid effluent clarity was determined by filtration and collection of the undissolved solids in the supernate on a 10 μ type LC millipore filter.

Experimental Procedures

All experimental runs using the continuous centrifuge were batchwise. The specific feed was mixed in the slurry feed tank at an air sparge rate of 2.7 scfm/ ft^2 of cross-sectional area of solids suspension.

The centrifuge rotation rate was fixed by selection of the motor drive sheave diameter. The slurry feed rate was controlled by adjusting the ball valve opening at the base of the feed tank. Two supernate samples were analysed for undissolved solids content after a steady-state feed rate was reached.

Flowrate measurements were taken based on the change in liquid level of the slurry feed with time. Discharged solids were collected in a polyethylene bag attached to the solids discharge flange of the centrifuge. After an entire batch of slurry had been fed, the centrifuge was shut down. The hold-up volume of the bowl was 750 ml. and consisted of a solids-rich liquor which would discharge from the liquid effluent outlet when rotation ceased. The undissolved solids concentration of this effluent was approximately twice that of the feed slurry. Discharge of this hold-up volume should present no problem in plant operation provided the downstream diverter valve is positioned to direct the liquor to the repulp tank.

Results and Discussion

A. Solids-Liquid Separation

The centrifuge was operated at two rotation rates, 2400 and 4200 rpm, corresponding to 500 and 1475 g's, respectively. At each rotation rate, a slurry solids loading and slurry feed rate was chosen. Run conditions appear in Table XXIX.

TABLE XXIX

HTGR SOLIDS-LIQUID SEPARATION TESTING USING 6-INCH CONTINUOUS SOLID BOWL CENTRIFUGE

Run No.	Rotation Rate, RPM	Slurry Feed Rate, ℓ-min^{-1}	Solids Conc. in Feed wt%
C-1	2400	0.5	2.0
C-2	4200	0.5	2.0
C-3	2400	4.0	2.0
C-4	4200	4.0	2.0
C-5	2400	0.5	8.0
C-6	4200	0.5	8.0
C-7	2400	4.0	8.0
C-8	4200	4.0	8.0

The separation efficiency, SE, is defined as:

$$SE = 1 - \frac{C_e}{C_f}$$

Where C_e = Concentration of undissolved solids in the liquid effluent, grams/liter.

C_f = Concentration of suspended solids in the feed slurry, grams/liter.

The percent solids recovery is 100 x SE.

Results of the solids-liquid separation testing indicate that the moisture content of discharged solids increases with increasing slurry feed rate, increasing slurry solids loading, and decreasing centrifugal force. The moisture content ranged from 1.85% by weight for Run C-2 to 12.0 % for Run C-7.

In general, liquid effluent clarity and, thus separation efficiency, increased with increasing slurry solids loading, decreasing slurry feed rate, and decreasing centrifugal force. Solids recoveries ranged from 87.0% to 99.8% with undissolved solids contents in the liquid effluent ranging from .084 g/ℓ to 3.5 g/ℓ. Although no precise data are available, extraction columns at ICPP have tolerated suspended solids concentrations of 0.5 g/ℓ. Thus, the range of operating conditions for use in a commercial plant has been examined.

In-Bowl and Repulp Washing of Solids

Although no data are presently available on the effect of in-bowl and repulp washing of solids, in-bowl washing is expected to remove a negligable quantity of thorium and uranium from the solids and repulping will be necessary. A flow diagram of a possible repulp wash system coupled to the continuous solid-bowl centrifuge is shown in Figure 24. Studies on in-bowl and repulp washing of solids are in progress.

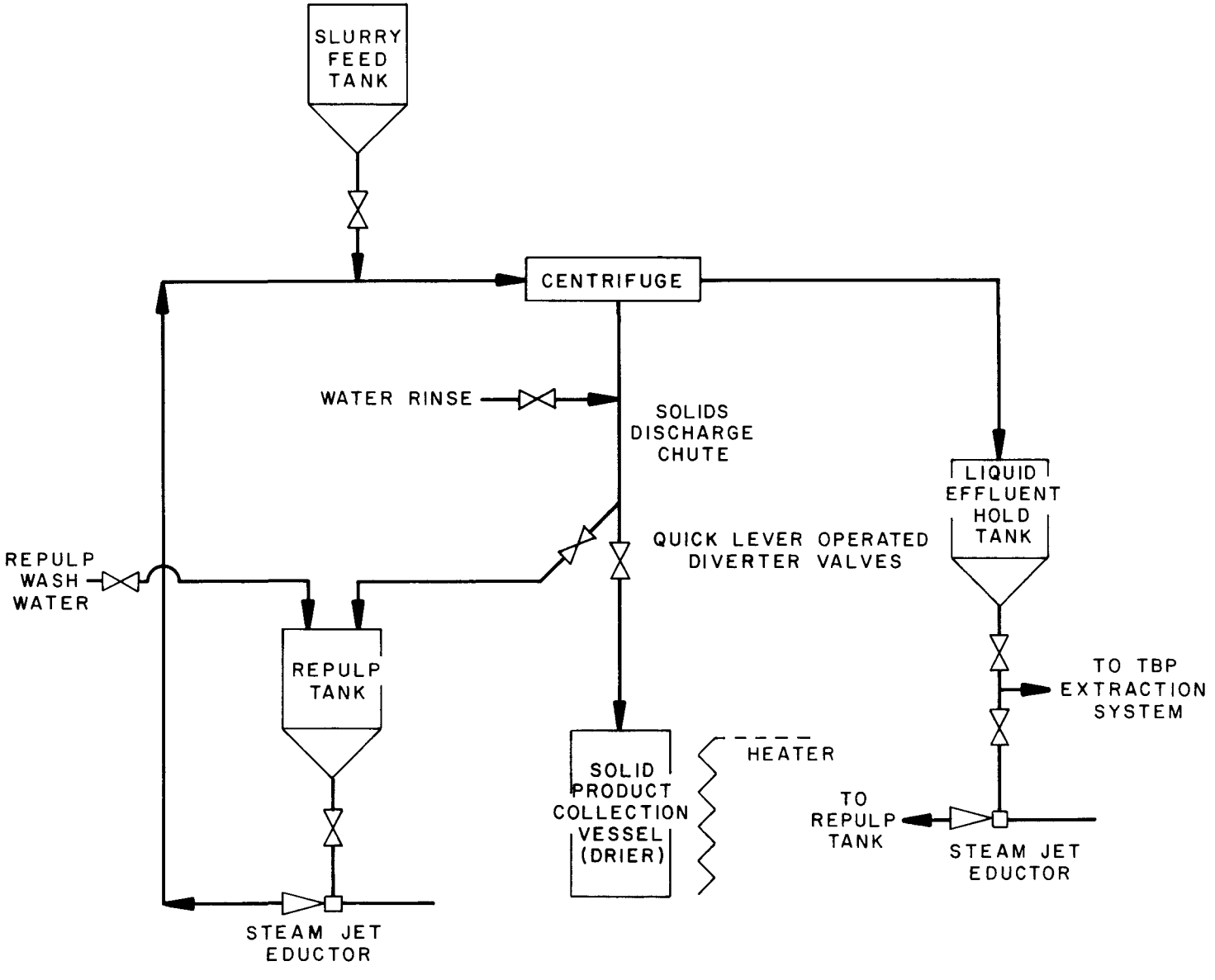

Figure 24. Proposed HTGR Centrifuge/Repulp Wash System

3. Feed Adjustment

In order to obtain the desired acid concentration in feed used for extraction studies, steam stripping studies using synthetic feed were made. The feed was stripped to acid deficiency and then adjusted to the desired acid, thorium, and uranium concentration before contacting with the organic solvent.

The results of steam stripping seven different solutions are shown in Table XXX. Obtaining an acid deficient feed is not difficult. As high as a 1.37 N^b acid deficiency was obtained in 3 hours for a 0.5 ℓ solution. The exact conditions for achieving a desired high acid, low acid, neutral, or acid deficient sample were not determined.

TABLE XXX

ACID CONCENTRATION OF FT. ST. VRAIN SYNTHETIC EXTRACTION FEED SOLUTIONS AFTER EVAPORATION AND STEAM STRIPPING

Run	Resulting Th, M	Heating & Stripping Time, min.	Initial Vol. / Final Vol.	Acid Concentration
1	-	-	3	0.67 N^a
2	-	180	5	1.37 N^b
3	3.97[(a)]	-	5	0.57 N^b
4	2.31	137	4	0.16 N^b
5	2.28	102	6	0.84 N^b
6	1.97	96	5	0.52 N^b

(a) Starting concentration was 1.5 M; all the others were 1.0M.

4. Solvent Extraction

Acid, thorium, and uranium equilibrium data in support of the HTGR solvent extraction process have been generated experimentally. The data were obtained using 5, 15, 30 and 50% tributylphosphate (TBP) in normal paraffin hydrocarbon (NPH) for different acid concentrations in the aqueous feed*.

Experimental Procedure

The laboratory work was conducted using separatory funnels. The feed was synthesized by dissolving ThO_2 and U_3O_8 in acid thorex to simulate dissolver effluent of approximately 1 M thorium and 14 g/liter uranium. The aqueous solution was contacted with organic for 5 min with a separation time of approximately 5 min. Each phase was then analyzed for acid, uranium and thorium. All tests were conducted at room temperature. From these data, equilibrium coefficients (E_a^o) were determined.

Four different concentrations of TBP in NPH were used: 5, 15, 30, and 50% by volume. The solvent was washed successively with 0.04 M HNO_3, 0.05 M Na_2CO_3, and 0.04 M HNO_3 prior to extraction to remove any degradation products that would interfere with the extraction process.

Stripping-distribution and dispersion-coalescence studies were not conducted. However, experiments were conducted to obtain further data on third phase formation. This was done with the same equipment used for obtaining the equilibrium data. Concentrations of the various constituents were varied to give the operating conditions for formation of the second organic phase. The data on the third phase formation is incomplete and will be transmitted in a later report.

---

* The uranium analysis data for solutions having thorium to uranium concentration ratios greater than 500,000 were possibly in error due to thorium interference in the analytical procedures used. The concentration values given in the Tables were corrected for the interference of thorium and are believed to be well within 10% of the correct values. The interference problem has been resolved.

Experimental Results

Data were obtained for uranium, thorium and acid for 5, 15, 30 and 50% TBP in NPH; the data are shown in Tables XXXI through XXXIV, respectively. All concentrations are in terms of molarity.

Correlations can be obtained from the available data such as the one shown in Figure 25. The figure shows the distribution of thorium in 30% TBP at various aqueous-phase acid concentrations. It is shown that an increase in acid concentration gives better extraction coefficients; this is generally true for the concentrations of TBP studied. Similar correlations can be obtained for uranium.

Figure 26 shows the distribution of nitric acid in the aqueous and organic phases as a function of TBP concentrations; more acid is contained in the organic phase at higher TBP concentrations.

The highest distribution coefficient value found for thorium was 2 for an aqueous acid concentration of 1.4 N acid and a TBP concentration of 50%. The highest distribution coefficient value using 30% TBP and 1.9 N acid was 0.97; at 15% and 5% TBP concentrations, the respective distribution coefficients were 0.37 and 0.06.

Acid deficient feed shows poor extraction coefficients for both thorium and uranium.

VII. OFF-GAS CLEANUP, NON-DESTRUCTIVE ASSAY, AND SOLIDS TRANSPORT

Equipment is being installed and tested for evaluating the flow path of volatile fission products, non-destructive uranium assay of undissolved Ft. St. Vrain solids, and solids transport studies. Graphite spiked with Cs, Ru, Te, and Tc is being burned in a 2.3-inch diameter glass "quartz" burner, simulating primary and secondary burning. The objective of the tests,which are in progress, is to define the temperature and types of surfaces where plate-out of the volatile fission products will occur; equipment for removal of the volatile fission products will then be designed and tested as required.

TABLE XXXI

EXTRACTION DATA FOR 5% TBP IN NPH AT 25°C

Ha*	Ho**	H-E_a^o	Tha ($\times 10^{-2}$)	Tho ($\times 10^{-2}$)	Th-E_a^o	Ua ($\times 10^{-5}$)	Uo ($\times 10^{-5}$)	U-E_a^o
0.18N[b]	0.02N[b]	0.11	53.9	1.12	0.02	3.02	5.04	1.7
0.17N[b]	0.01N[b]	0.06	57.8	1.39	0.02	28.9	50.4	1.7
0.16N[b]	0.02N[b]	0.12	61.6	1.79	0.03	286	326	1.1
0.16N[b]	0.01N[b]	0.06	51.3	0.94	0.02	14.2	23.5	1.7
0.16N[b]	0.01N[b]	0.06	44.5	0.60	0.01	0.80	1.34	1.7
0.14N[b]	.01N[b]	0.07	59.1	1.50	0.03	286	185	0.7
0.01N[b]	0.005N[b]	0.50	73.7	18.6	0.25	744	1193	1.6
0.06	0.002	0.03	35.9	0.67	0.02	0.34	0.46	1.4
0.08	0.003	0.04	43.1	1.13	0.03	2.4	5.5	2.2
0.09	0.003	0.03	53.0	1.79	0.03	7.1	11.3	1.6
0.09	0.002	0.02	46.6	1.38	0.03	0.92	2.5	2.7
0.10	0.005	0.05	52.2	1.84	0.03	37.4	126	3.4
0.11	0.006	0.05	58.6	2.24	0.04	58.8	238	4.0
0.14	0	0	70.3	2.28	0.03	655	1218	1.9
0.93	0.04	0.04	90.1	2.80	0.03	782	2121	2.7
1.52	0.06	0.04	11.5	0.67	0.06	1.13	3.15	2.8
1.63	0.06	0.03	12.8	0.81	0.06	5.50	17.6	3.2
1.63	0.05	0.03	13.4	0.81	0.06	6.3	15.1	2.4
1.69	0.06	0.04	14.0	0.79	0.06	18.1	75.6	4.2
1.71	0.06	0.04	14.4	0.81	0.06	23.1	159	6.9
1.77	0.06	0.03	14.8	0.81	0.05	79.8	251	3.1

* Ha - Acid concentration in aqueous phase.

** Ho - Acid concentration in organic phase.

TABLE XXXII

EXTRACTION DATA FOR 15% TBP IN NPH AT 25°C

Ha	Ho	H-E^o_a	Tha ($\times 10^{-2}$)	Tho ($\times 10^{-2}$)	Th-E^o_a	Ua ($\times 10^{-5}$)	Uo ($\times 10^{-5}$)	U-E^o_a
0.20N[b]	0.02N[b]	0.10	27.6	1.3	0.05	0.88	1.89	2.1
0.19N[b]	0	0	33.7	2.7	0.08	9.6	28	2.9
0.18N[b]	0.02N[b]	0.11	44.8	6.1	0.14	150	336	2.2
0.18N[b]	0	0	26.1	1.2	0.05	2.7	3.9	1.4
0.18N[b]	0.02N[b]	0.11	20.9	0.54	0.03	0.11	0.21	1.9
0.16N[b]	0.02N[b]	0.12	36.5	4.1	0.11	41.6	180	4.3
0.01N[b]	0.02	-	66.8	6.3	0.09	361	1584	4.4
0.02	0.002	0.10	13.9	0.52	0.04	0.088	0.17	1.9
0.03	0.004	0.13	18.4	1.1	0.06	1.18	2.5	2.1
0.03	0.005	0.17	19.1	1.4	0.07	0.21	0.71	3.4
0.06	0.007	0.12	26.4	2.9	0.11	1.89	8.8	4.7
0.07	0.014	0.20	30.9	4.0	0.13	21.4	121	5.6
0.09	0.02	0.20	40.1	6.6	0.16	29.0	253	8.7
0.12	0.005	0.04	61.2	6.8	0.11	218	1387	6.4
1.09	0.12	0.11	3.72	0.91	0.24	0.11	0.71	6.6
1.33	0.14	0.11	5.78	1.80	0.31	1.18	8.40	7.1
1.43	0.13	0.09	7.16	2.23	0.31	0.73	3.32	4.5
1.57	0.14	0.09	9.14	2.98	0.33	4.74	26.3	5.5
1.57	0.16	0.10	9.05	3.39	0.37	9.24	178	19.3
1.69	0.15	0.09	12.2	3.96	0.32	30.2	334	11.1
1.96	0.16	0.08	14.4	4.8	0.33	125	886	7.1

TABLE XXXIII

EXTRACTION DATA FOR 30% TBP IN NPH AT 25°C

Ha	Ho	$H-E^{o}_{a}$	$Tha_{(x\ 10^{-2})}$	$Tho_{(x\ 10^{-2})}$	$Th-E^{o}_{a}$	$Ua_{(x\ 10^{-5})}$	$Uo_{(x\ 10^{-5})}$	$U-E^{o}_{a}$
0.20N[b]	0	-	17.2	1.00	0.34	0.34	0.79	2.3
0.19N[b]	0	-	21.3	2.45	0.19	4.7	12.6	2.7
0.19N[b]	0.05N[b]	0.6	32.8	8.71	0.77	67.6	350	5.2
0.18N[b]	0.02N[b]	0.11	26.0	5.26	0.65	34.7	189	5.4
0.18N[b]	0	-	17.6	1.03	0.06	0.55	1.6	2.9
0.18N[b]	0	-	14.3	0.39	0.03	0.025	0.076	3.0
0.14N[b]	0.07N[b]	0.5	56.9	23.4	0.41	240	1660	6.9
0.01	0.01	1	10.1	0.98	0.10	0.55	1.47	2.7
0.01	0.008	0.8	6.55	0.52	0.08	0.080	0.071	0.89
0.02	0.01	0.5	9.70	0.88	0.09	0.046	0.19	4.1
0.05	0.03	0.6	14.0	2.46	0.18	0.92	3.90	4.2
0.05	0.05	1.0	18.5	4.74	0.26	14.3	137	9.6
0.06	0.04	0.67	25.6	10.0	0.39	19.3	202	10.5
0.16	0.02	0.13	1.59	0.033	0.02	0.021	0.034	1.6
0.29	0.04	0.14	2.09	0.14	0.07	0.13	0.55	4.2
0.29	0.06	0.21	6.51	1.22	0.18	0.21	1.26	6.0
0.30	0.08	0.27	19.3	8.06	0.42	25.2	276	11.0
0.30	0.06	0.20	2.99	0.25	0.08	0.088	0.034	0.39
0.33	0.06	0.18	1.79	0.11	0.06	< 0.021	< 0.021	-
0.34	0.07	0.21	1.10	0.06	0.05	< 0.021	< 0.021	-
0.66	0.14	0.21	1.70	0.45	0.26	0.071	0.39	5.4
0.66	0.14	0.21	3.55	1.28	0.36	3.23	16.8	5.2
0.92	0.21	0.23	2.66	1.52	0.57	0.50	5.04	10.1
1.05	0.24	0.23	2.69	2.25	0.84	0.12	1.64	13.7
1.32	0.28	0.21	4.35	3.99	0.92	1.43	19.7	13.8
1.33	0.25	0.19	5.65	5.17	0.92	5.46	177	32.4
1.57	0.34	0.22	8.19	7.41	0.90	17.2	439	25.5
1.92	0.33	0.17	11.9	11.6	0.97	76	983	12.9

TABLE XXXIV

EXTRACTION DATA FOR 50% TBP IN NPH AT 25°C

Ha	Ho	$H\text{-}E^{o}_{a}$	$Tha_{(x\ 10^{-2})}$	$Tho_{(x\ 10^{-2})}$	$Th\text{-}E^{o}_{a}$	$Ua_{(x10^{-5})}$	$Uo_{(x\ 10^{-5})}$	$U\text{-}E^{o}_{a}$
0.35	0.11	0.31	1.28	0.23	0.18	0.029	0.23	7.9
0.62	0.23	0.37	1.81	1.00	0.55	0.34	2.60	7.6
0.72	0.30	0.42	1.44	0.91	0.63	0.05	0.84	16.8
0.96	0.40	0.42	2.30	2.92	1.3	0.55	8.82	16.0
1.08	0.43	0.40	3.80	5.91	1.6	4.62	184	39.8
1.44	0.51	0.35	5.30	10.5	2.0	12.2	343	28.1

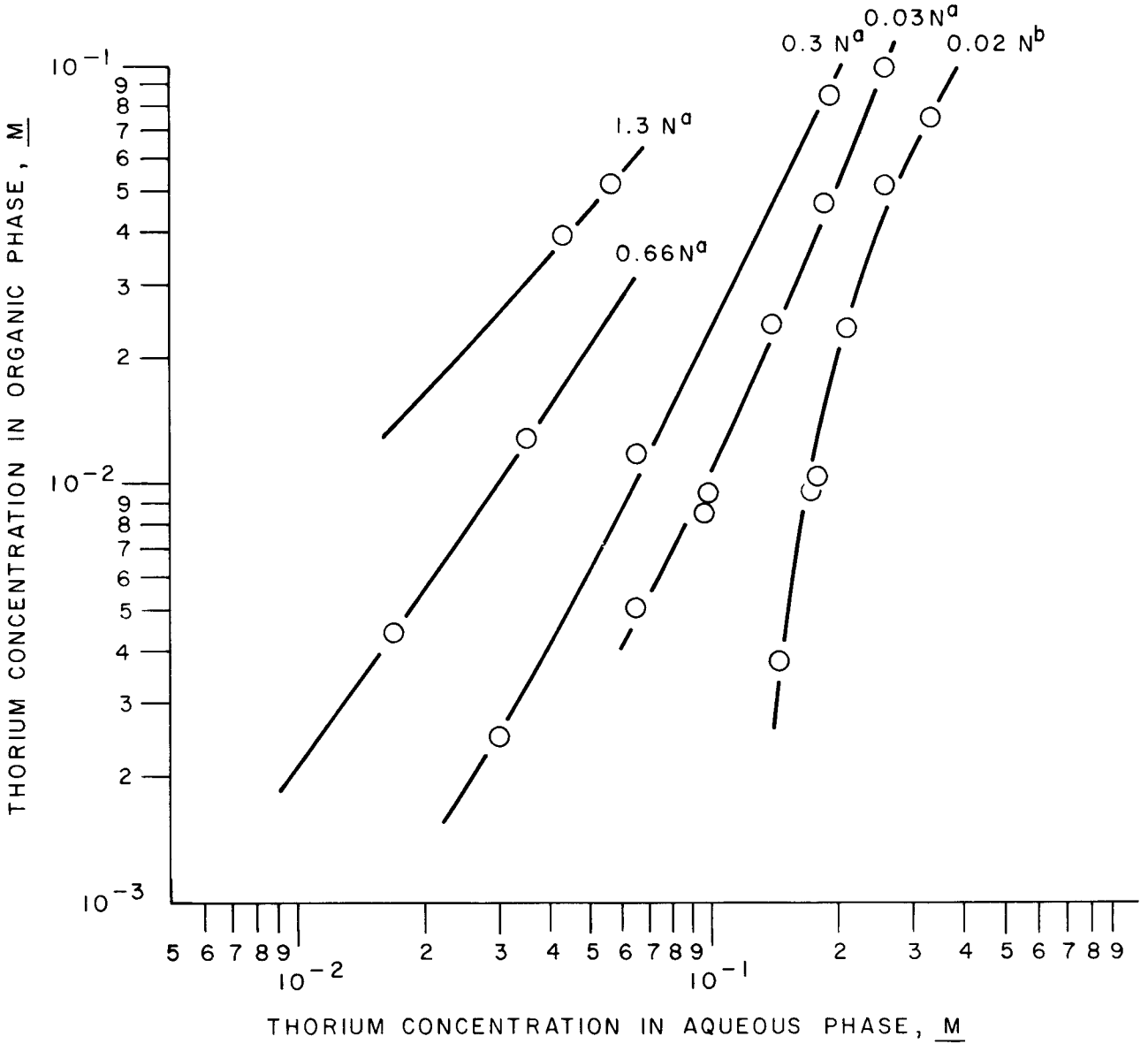

Figure 25. Equilibrium Diagram: Thorium Nitrate-Nitric Acid-30% TBP-NPH at 25°C

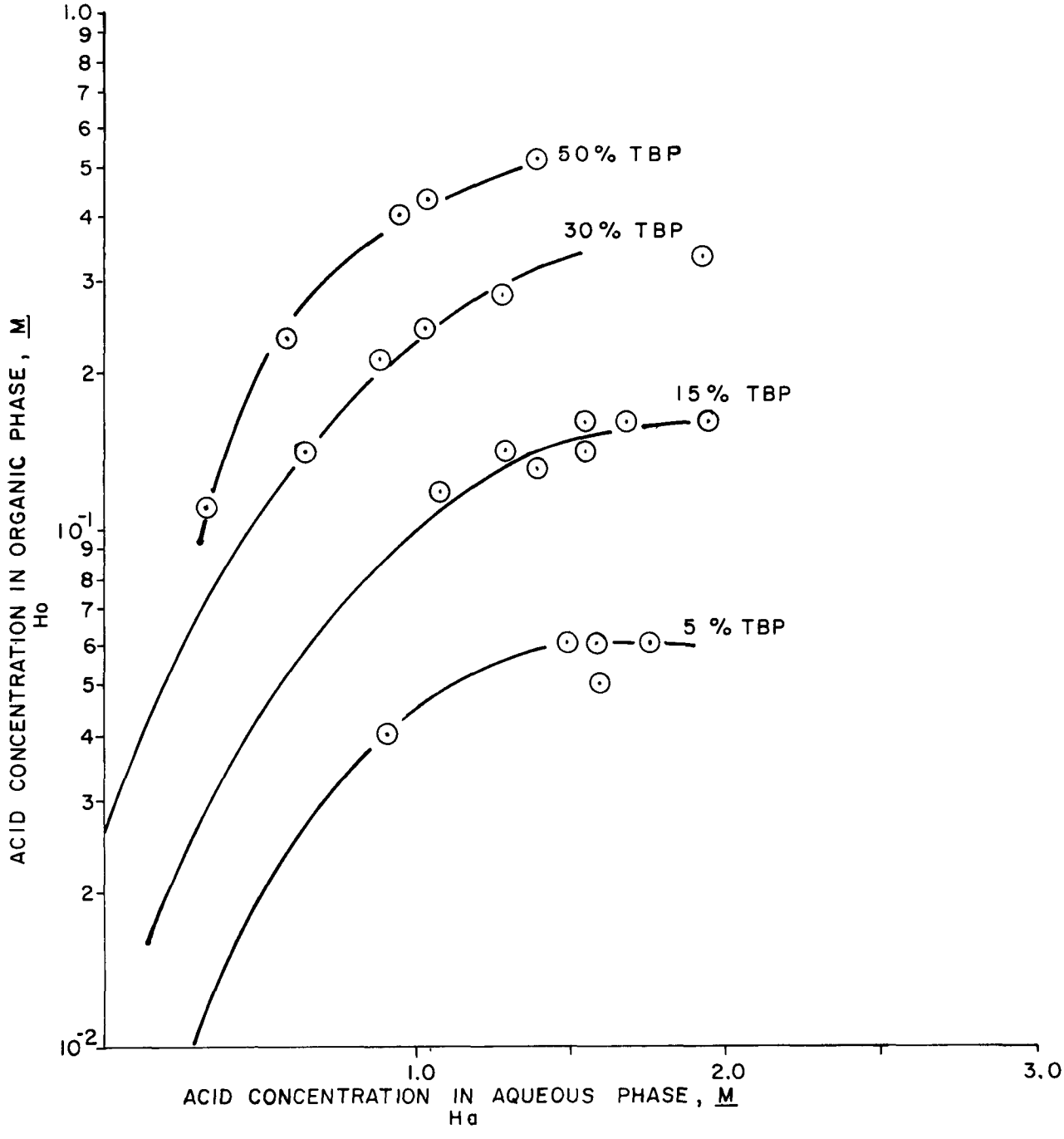

Figure 26. Nitric Acid Distribution Between Aqueous and Organic Phases

A neutron interrogation device, manufactured by National Nuclear Corp., is being installed; the device will be tested for monitoring uranium in undissolved centrifuged solids. The neutron interrogator detects fast neutrons resulting from bombardment of uranium by thermal neutrons. Preliminary feasibility tests indicate the device is uniquely insensitive to gamma radiation.

Equipment is also being assembled for demonstrating solids transport from hoppers by gravity flow and gas jets.

VIII. CONCLUSIONS

Interim pilot-plant results and calculations show that head-end processing of crushed Ft. St. Vrain fuel can be accomplished using practical processing methods. Specific conclusion regarding the process (based on processing twelve fuel blocks per day) are:

1. Heat transfer calculations and experimental burn rates show that a 6-inch diameter primary burner has sufficient capacity to process twelve fuel blocks per day. Graphite fines generated during fuel crushing and burning can be recycled and burned in the primary burner. The primary burner operating cycle should be as long as practical. Fines burning has not been tested in high-carbon content ($\geq$ 40%) beds. Such tests are significant only if the burner operating cycle is less than two days.

2. The primary burner product can be classified into 95% pure fissile particles and 85% pure fertile particles in a 2-inch diameter gas classifier using acceptable gas rates.

3. The fertile particle fraction can be processed in either a jet breaker or roll-crusher to separate the silicon carbide hulls from the fuel kernel. Wear rates were not determined for either roll-crushers or jet breakers. Fissile particle processing in either a roll-crusher or jet breaker has not been tested.

4. The carbon content of crushed fertile particles can be reduced to less than 2 wt% in a batch secondary burner equipped with in-vessel filters. Inert bed material is not required to prevent bed sintering. Safe operating conditions

were defined for both the "combustion" and "burn-out" period. Conditions were defined for which bed sintering and filter burn-through are potentially high. An 8-inch diameter secondary burner is adequate for processing feed at rates corresponding to processing 12 Ft. St. Vrain fuel blocks per day.

5. A dissolver constructed of 304L stainless steel has sufficient corrosion resistance for dissolving secondary burner ash in boiling thorex solution.

6. A continuous solid-bowl centrifuge appears suitable for solids-liquid separation. In-bowl washing of solids does not appear promising. Re-pulp washing of solids is being tested to define uranium and thorium recovery efficiencies.

7. Equilibrium data are available for design of solvent extraction equipment for processing Ft. St. Vrain centrifuge supernate.

8. Off-gas cleanup, non-destructive uranium assay, and solids transport are important development areas that have not been adequately studied to date.

IX BIBLIOGRAPHY

1. W. B. Palmer, Interim Experimental Results: Primary Graphite Burner Testing Without Fines Recycle, ICP-1068, April 1975.

2. W. B. Palmer, Interim Experimental Results: Fines Recycle Testing Using the Primary Graphite Burner, ICP-1069, April 1975.

3. M. K. Valentine, Separation of Unirradiated Ft. St. Vrain Fissile and Fertile Particles by Gas Classification, ICP-1051, April 1974.

4. W. B. Palmer, Interim Experimental Results: Breaking Silicon Carbide Coatings on Ft. St. Vrain Fertile Particles Using a Gas Jet, ICP-1062, March 1975.

5. W. B. Palmer, Experimental Testing of the Double Roll Crusher for Breaking Silicon Carbide Coatings on Unirradiated Ft. St. Vrain Fuel Particles, ICP-1070 March 1975.

DISTRIBUTION RECORD FOR ICP-1074

External

110 - UC-10, Chemical Separations Processes for Plutonium and Uranium
TID-4500,R63

Internal

1 - Chicago Patent Group - ERDA
9800 South Cass Avenue
Argonne, Illinois 60439

3 - A. T. Morphew, Classification and Technical Information Branch
ERDA-ID
Idaho Falls, Idaho 83401

18 - Special Internal Distribution - B. R. Wheeler, ACC

11 - INEL Technical Library

65 - Authors

Total Copies Printed - 208